**ISTANBUL TECHNICAL UNIVERSITY ★ GRADUATE SCHOOL OF SCIENCE ENGINEERING AND TECHNOLOGY**

# FRAGILITY EVALUATION OF STEEL TRUSS RAILWAY BRIDGES IN TURKEY

**M.Sc. THESIS**

**Seda KONOR**

**Department of Civil Engineering**

**Structure Engineering Programme**

**JUNE 2017**

**ISTANBUL TECHNICAL UNIVERSITY ★ GRADUATE SCHOOL OF SCIENCE ENGINEERING AND TECHNOLOGY**

# FRAGILITY EVALUATION OF STEEL TRUSS RAILWAY BRIDGES IN TURKEY

**M.Sc. THESIS**

**Seda KONOR**
**(501141035)**

**Department of Civil Engineering**

**Structure Engineering Programme**

**Thesis Advisor: Assoc. Prof. Dr. Kadir ÖZAKGÜL**

**JUNE 2017**

**ISTANBUL TEKNİK ÜNİVERSİTESİ ★ FEN BİLİMLERİ ENSTİTÜSÜ**

# TÜRKİYE'DEKİ ÇELİK KAFES DEMİRYOLU KÖPRÜLERİNİN HASAR GÖREBİLİRLİK EĞRİLERİNİN ELDE EDİLMESİ

**YÜKSEK LİSANS TEZİ**

**Seda KONOR**
**(501141035)**

**İnşaat Mühendisliği Anabilim Dalı**

**Yapı Mühendisliği Programı**

**Tez Danışmanı: Doç. Dr. Kadir ÖZAKGÜL**

**HAZİRAN 2017**

Seda Konor, a M.Sc. student of İTU Graduate School of Science Engineering and Technology student ID 501141035, successfully defended the thesis/dissertation entitled "FRAGILITY EVALUATION OF STEEL TRUSS RAILWAY BRIDGES IN TURKEY", which she prepared after fulfilling the requirements specified in the associated legislations, before the jury whose signatures are below.

| | | |
|---|---|---|
| **Thesis Advisor :** | **Assoc. Prof. Dr. Kadir ÖZAKGÜL**<br>Istanbul Technical University | ..... |
| **Jury Members :** | **Assoc. Prof. Dr. Filiz PİROĞLU**<br>Istanbul Technical University | ..... |
| | **Asst. Prof. Dr. Devrim ÖZHENDEKÇİ**<br>Yıldız Technical University | ..... |

**Date of Submission : 05 May 2017**
**Date of Defense : 13 June 2017**

***To my lovely family,***

**FOREWORD**

I would like to thank my supervisor, Dr. Kadir Özakgül who made this dissertation possible with his knowledge, support and helpful suggestions in discussion.

I would also like to thank Dr. Barlas Özden Çağlayan and Mehmet Fatih Yılmaz for their guidance, advice, criticism and insight throughout the study.

I would like to thank the staff of General Directorate of Turkish State Railways for providing bridge data used for the case studies.

Last but not least, I would like to thank my parents and my sister who have supported me in my whole life. I owe a grateful thank to my fiance Mümin Çentez for his all effort for keeping me focus in and my family-in-law for their encouraging support.

May 2017

Seda KONOR
Civil Engineer

**TABLE OF CONTENTS**

**Page**

**FOREWORD** ..... **ix**
**TABLE OF CONTENTS** ..... **xi**
**ABBREVIATIONS** ..... **xiii**
**SYMBOLS** ..... **xv**
**LIST OF TABLES** ..... **xvii**
**LIST OF FIGURES** ..... **xix**
**SUMMARY** ..... **xxiii**
**ÖZET** ..... **xxv**
**1. INTRODUCTION** ..... **1**
**2. LITERATURE REVIEW** ..... **3**
2.1 Scope of Literature Review ..... 3
2.2 Review of Steel Truss Bridges ..... 3
2.2.1 History of truss bridges ..... 4
2.2.2 Types of trusses ..... 7
2.3 Review of Fragility Curve Development Methods ..... 11
2.3.1 Expert-base fragility curves ..... 11
2.3.2 Empirical fragility curves ..... 12
2.3.3 Analytical fragility curves ..... 14
2.3.3.1 Elastic spectral analysis ..... 14
2.3.3.2 Nonlinear static analysis ..... 15
2.3.3.3 Nonlinear dynamic analysis ..... 17
2.3.3.4 Incremental dynamic analysis ..... 19
2.3.4 Hybrid fragility curves ..... 19
**3. DEVELOPMENT OF ANALYTICAL FRAGILITY CURVES** ..... **23**
3.1 Selection of Ground Motion Records ..... 23
3.2 Nonlinear Time History Analysis ..... 26
3.3 Modal Updating ..... 31
3.4 Fragility Curve Development Methodology ..... 31
**4. CASE STUDIES** ..... **33**
4.1 Case Study 1: Karaçam Bridge ..... 33
4.1.1 General ..... 33
4.1.2 Experimental results ..... 34
4.1.3 Analytical results ..... 34
4.1.3.1 Original bridge model ..... 34
4.1.3.2 Fragility curves of original bridge model ..... 34
4.1.3.3 Modal updating of bridge model ..... 37
4.1.3.4 Fragility curves of updated bridge model ..... 37
4.1.3.5 Comparison of fragility curves ..... 39
4.2 Case Study 2: Cambazkaya Bridge ..... 39
4.2.1 General ..... 39
4.2.2 Experimental results ..... 40
4.2.3 Analytical results ..... 40

4.2.3.1 Original bridge model ..... 40
4.2.3.2 Fragility curves of original bridge model ..... 41
4.2.3.3 Modal updating of bridge model ..... 42
4.2.3.4 Fragility curves of updated bridge model ..... 43
4.2.3.5 Comparison of fragility curves ..... 44
4.3 Case Study 3: Ceyhan Bridge ..... 45
4.3.1 General ..... 45
4.3.2 Experimental results ..... 45
4.3.3 Analytical results ..... 47
4.3.3.1 Original bridge model ..... 47
4.3.3.2 Fragility curves of original bridge model ..... 47
4.3.3.3 Modal updating of bridge model ..... 48
4.3.3.4 Fragility curves of updated bridge model ..... 49
4.3.3.5 Comparison of fragility curves ..... 51
**5. CONCLUSIONS AND RECOMMENDATIONS ..... 53**
**REFERENCES ..... 55**
**APPENDICES ..... 61**
**CURRICULUM VITAE ..... 99**

## ABBREVIATIONS

**CSM** **:** Capacity Spectrum Method
**MSC** **:** Multispan Continuous
**NDA** **:** Nonlinear Dynamic Analysis
**PGA** **:** Peak Ground Acceleration
**SS** **:** Simply Supported
**TCDD** **:** Turkish State Railways Administration

**SYMBOLS**

**g** **:** Gravitational acceleration
**D** **:** Demand
**C** **:** Capacity
**IM** **:** Intensity measure
**P** **:** Probability
$\boldsymbol{\Phi}$ **:** Standard normal distribution
***X*** **:** Lognormal distributed response displacement
**λ** **:** Mean
**ζ** **:** Standard deviation
**s** **:** Standard normal variable

## LIST OF TABLES

**Page**

**Table 2.1 :** Truss typologies (Pipinato and De Miranda, 2016). ..... 8
**Table 2.2 :** Categorization of vulnerability curve (Kwon and Elnashi, 2006). ..... 21
**Table 3.1 :** Site class definitions (FEMA 450, 2003). ..... 24
**Table 3.2 :** Selected ground motion records for soil class A. ..... 28
**Table 3.3 :** Selected ground motion records for soil class B. ..... 29
**Table 3.4 :** Selected ground motion records for soil class C. ..... 30
**Table 4.1 :** Analytical and experimental frequencies before and after model calibration of Karacam Railway Bridge. ..... 37
**Table 4.2 :** Analytical and experimental frequencies before and after model calibration of Cambazkaya Railway Bridge. ..... 43
**Table 4.3 :** Analytical and experimental frequencies before and after model calibration of Ceyhan Railway Bridge. ..... 50

**LIST OF FIGURES**

**Page**

**Figure 2.1 :** Truss main components (Pipinato and De Miranda, 2016). ..... 5
**Figure 2.2 :** King-post truss (Dufour, 1909). ..... 6
**Figure 2.3 :** King-post truss bridge stiffened by arch (Dufour, 1909). ..... 6
**Figure 2.4 :** Burr truss bridge, arched (Dufour, 1909). ..... 6
**Figure 2.5 :** St. Louis bridge over Mississippi river, United States (Troyano, 2003). 6
**Figure 2.6 :** Queensboro bridge over East River, United States (www. nyc.gov). ..... 7
**Figure 2.7 :** An example of continuous truss bridge (Gosh, 2006). ..... 7
**Figure 2.8 :** Intersection of capacity-demand acceleration-displacement spectra (Mander, 1999). ..... 16
**Figure 2.9 :** Schematic representation of the NDA procedure to develop fragility curves (Billah, 2015). ..... 17
**Figure 3.1 :** Flow chart for presented approach. ..... 24
**Figure 3.2 :** Earthquake zoning map of Turkey (www.deprem.gov.tr, 2016). ..... 25
**Figure 3.3 :** Response spectra of selected 20 ground motions of soil class A. ..... 25
**Figure 3.4 :** Response spectra of selected 20 ground motions of soil class B. ..... 25
**Figure 3.5 :** Response spectra of selected 20 ground motions of soil class C. ..... 26
**Figure 3.6 :** Response spectra of selected 60 ground motions of soil class A-B-C. . 26
**Figure 3.7 :** Maximum seismic response of different damage parameters (Avşar, 2009). ..... 27
**Figure 4.1 :** General view of Karaçam Railway Bridge (Uzgider et al., 1996a). ..... 34
**Figure 4.2 :** Experimental mode shapes and corresponding frequencies of Karaçam Railway Bridge (Uzgider et al., 1996a). ..... 35
**Figure 4.3 :** Analytical frequencies of original Karaçam bridge model. ..... 36
**Figure 4.4 :** Analytical frequencies of updated Karaçam bridge model. ..... 38
**Figure 4.5** : General view of Cambazkaya Railway Bridge (Uzgider et al., 1996b). 40
**Figure 4.6 :** Experimental mode shapes and corresponding frequencies of Cambazkaya Railway Bridge (Uzgider et al., 1996b). ..... 41
**Figure 4.7 :** Analytical frequencies of original Cambazkaya bridge model. ..... 42
**Figure 4.8 :** Analytical frequencies of updated Cambazkaya bridge model. ..... 44
**Figure 4.9 :** General view of Ceyhan Railway Bridge. ..... 46
**Figure 4.10 :** An example bi-axial accelerometer unit. ..... 46
**Figure 4.11 :** 16-channel data acquisition system. ..... 46
**Figure 4.12 :** Locations of accelerometers on Ceyhan Railway Bridge. ..... 47
**Figure 4.13 :** Experimental mode shapes and corresponding frequencies of Ceyhan Railway Bridge. ..... 48
**Figure 4.14 :** Analytical frequencies of the original Ceyhan bridge model. ..... 49
**Figure 4.15 :** Analytical frequencies of updated Ceyhan bridge model. ..... 50
**Figure A.1 :** Fragility curves of original Karaçam bridge model for soil class A. ... 62
**Figure A.2 :** Fragility curves of original Karaçam bridge model for soil class B. .... 63
**Figure A.3 :** Fragility curves of original Karaçam bridge model for soil class C. .... 64
**Figure A.4 :** Fragility curves of original Karaçam bridge model for soil class A-B-C. ..... 65

**Figure A.5 :** Fragility curves of updated Karaçam bridge model for soil class A. ... 66
**Figure A.6 :** Fragility curves of updated Karaçam bridge model for soil class B..... 67
**Figure A.7 :** Fragility curves of updated Karaçam bridge model for soil class C..... 68
**Figure A.8 :** Fragility curves of updated Karaçam bridge model for soil class A-B-C. ..... 69
**Figure A.9 :** Comparison fragility curves of original and updated Karaçam bridge model for soil class A. ..... 70
**Figure A.10 :** Comparison fragility curves of original and updated Karaçam bridge model for soil class B. ..... 71
**Figure A.11 :** Comparison fragility curves of original and updated Karaçam bridge model for soil class C. ..... 72
**Figure A.12 :** Comparison fragility curves of original and updated Karaçam bridge model for soil class A-B-C. ..... 73
**Figure B.1 :** Fragility curves of original Cambazkaya bridge model for soil class A. ..... 74
**Figure B.2 :** Fragility curves of original Cambazkaya bridge model for soil class B. ..... 75
**Figure B.3 :** Fragility curves of original Cambazkaya bridge model for soil class C. ..... 76
**Figure B.4 :** Fragility curves of original Cambazkaya bridge model for soil class A-B-C. ..... 77
**Figure B.5 :** Fragility curves of updated Cambazkaya bridge model for soil class A. ..... 78
**Figure B.6 :** Fragility curves of updated Cambazkaya bridge model for soil class B. ..... 79
**Figure B.7 :** Fragility curves of updated Cambazkaya bridge model for soil class C. ..... 80
**Figure B.8 :** Fragility curves of updated Cambazkaya bridge model for soil class A-B-C. ..... 81
**Figure B.9 :** Comparison fragility curves of original and updated Cambazkaya bridge model for soil class A. ..... 82
**Figure B.10 :** Comparison fragility curves of original and updated Cambazkaya bridge model for soil class B. ..... 83
**Figure B.11 :** Comparison fragility curves of original and updated Cambazkaya bridge model for soil class C. ..... 84
**Figure B.12 :** Comparison fragility curves of original and updated Cambazkaya bridge model for soil class A-B-C. ..... 85
**Figure C.1 :** Fragility curves of original Ceyhan bridge model for soil class A. ..... 86
**Figure C.2 :** Fragility curves of original Ceyhan bridge model for soil class B. ..... 87
**Figure C.3 :** Fragility curves of original Ceyhan bridge model for soil class C. ..... 88
**Figure C.4 :** Fragility curves of original Ceyhan bridge model for soil class C. ..... 89
**Figure C.5 :** Fragility curves of updated Ceyhan bridge model for soil class A..... 90
**Figure C.6 :** Fragility curves of updated Ceyhan bridge model for soil class B. ..... 91
**Figure C.7 :** Fragility curves of updated Ceyhan bridge model for soil class C. ..... 92
**Figure C.8 :** Fragility curves of updated Ceyhan bridge model for soil class A-B-C. ..... 93
**Figure C.9 :** Comparison fragility curves of original and updated Ceyhan bridge model for soil class A. ..... 94
**Figure C.10 :** Comparison fragility curves of original and updated Ceyhan bridge model for soil class B. ..... 95

**Figure C.11 :** Comparison fragility curves of original and updated Ceyhan bridge model for soil class C. ..... 96
**Figure C.12 :** Comparison fragility curves of original and updated Ceyhan bridge model for soil class A-B-C. ..... 97

## FRAGILITY EVALUATION OF STEEL TRUSS RAILWAY BRIDGES IN TURKEY

## SUMMARY

The objective of this thesis is to investigate the probability of failure of existing steel railway bridges in Turkey. In order to accomplish that objective, two multispan continuous bridges with total length of 154.5 m and 103.8 m; one simply supported bridge with total length of 96 m were investigated. Finite element models of those bridges were constructed through SAP2000 software based on original design drawings that were provided by TCDD, and they referred to as original bridge models. Furthermore, original models were compared with field measurements if available. In absence of field measurements, comparison was done with dynamic parameters which were obtained from previous studies. In case of more than 1% difference between relevant parameters, it was decided to develop original models. Consequently, new model, which was named as updated model, was generated with updating process.

Three different soil classes were studied and earthquake records were determined with intent to obtain general earthquake behavior within the scope of typically used earthquakes in literature and Turkey. Subsequently, original and updated finite elements models were subjected to nonlinear time history analyses with selected earthquake records. According to obtained results from these analyses, fragility analyses of original and updated bridge models were performed and vulnerability curves of these were obtained. Fragility assessments were carried out for both circumstances and results were compared to each other.

This thesis is composed of five chapters. In Chapter 1, general information about the study and the aim of the study are represented.

Chapter 2 includes history and general characteristics about steel truss bridges, specifications of fragility curve development methodologies and summaries of previous studies related to fragility evaluation procedures.

Chapter 3 describes the generation of analytically derived fragility curves within the scope of this study. The principles of selection of ground motion records, nonlinear time history analysis and modal updating procedure are included.

Chapter 4 presents fragility evaluation results of case studies on selected single span and multispan continuous bridges.

Finally, Chapter 5 is devoted to summary and conclusion of the study. Recommendations based on the results and conclusions of the study are also given in this chapter.

# TÜRKİYE'DEKİ ÇELİK KAFES DEMİRYOLU KÖPRÜLERİNİN HASAR GÖREBİLİRLİK EĞRİLERİNİN ELDE EDİLMESİ

## ÖZET

Sunulan bu tez çalışmasının amacı Türkiye'de mevcut çelik demiryolu köprülerinin hasargörebilirlik olasılıklarının incelenmesidir. Bu doğrultuda hazırlanan tez çalışması kapsamında, Türkiye'deki çelik demiryolu köprülerinin genel durumunu yansıtması amacıyla toplam uzunlukları sırasıyla 154.5 m, 103.8 m ve 96 m olan bir adet üç açıklıklı sürekli köprü, bir adet iki açıklıklı sürekli köprü ve bir adet tek açıklıklı köprü incelemesi yapılmıştır. Üç adet çelik demiryolu köprüsüne ait sonlu elemanlar modeli, TCDD tarafından sağlanan orijinal çizimlerine göre SAP2000 yazılımı aracılığı ile oluşturulmuş ve bu modeller orijinal modeller olarak adlandırılmıştır. Sonrasında, orijinal modeller, eğer mevcut ise güncel arazi ölçümlerinden, mevcut değil ise önceki çalışmalarda sunulan arazi ölçümlerinden elde edilen dinamik parametreler ile kıyaslanmıştır. İlgili parametreler arasındaki farkın 1% den büyük olması durumunda orijinal modellerin geliştirilmesine karar verilmiştir ve uygulanan geliştirme işlemleri sonucunda elde edilen yeni model, geliştirilmiş model olarak adlandırılmıştır.

Köprülerin genel deprem davranışının bulunması amacıyla, literatürde yaygın olarak kullanılan ve Türkiye'de de gözlenen deprem etkilerini kapsayacak şekilde önceki yıllarda üç farklı zemin sınıfında gözlenmiş deprem ivme kayıtları belirlenmiştir. Ardından, oluşturulan orijinal ve geliştirilmiş sonlu elemanlar modelleri, seçilen deprem kayıtları altında doğrusal olmayan zaman-tanım alanında analizlere maruz bırakılmıştır. Bu analizlerden elde edilen sonuçlara göre, orijinal ve geliştirilmiş köprü modellerinin hasargörebilirlik analizleri yapılmış ve hasargörebilirlik eğrileri elde edilmiştir. Her iki durum için hasargörebilirlik değerlendirmeleri yapılmış ve sonuçlar birbiriyle kıyaslanmıştır.

Beş bölümden oluşan tez çalışmasının ilk bölümünde çalışmanın amacından bahsedilmiş ve çalışma hakkında genel bilgiler sunulmuştur.

İkinci bölümde, çelik kafes köprülerin tarihçesi ve yapısal özellikleri ile ilgili genel bilgilere yer verilmiş, hasargörebilirlik eğrilerinin elde edilme yöntemleri anlatılmış ve hasargörebilirlik eğrilerinin elde edilmesi konusu ile alakalı önceki yıllarda yapılan çalışmalara değinilmiştir.

Üçüncü bölüm, tez çalışmasının ana konusu olan hasargörebilirlik eğrilerinin elde edilmesi kapsamında takip edilen yöntemi içermektedir. Bu kapsamda kullanılmak üzere öncelikle uygun deprem kayıtlarının seçilmesi, doğrusal olmayan zaman-tanım alanında analizin uygulanması, sonlu elemanlar modelinin arazi ölçümleri ile kıyaslanması ve köprülere ait hasargörebilirlik eğrilerinin elde edilmesi başlıklarına yer verilmiştir.

Dördüncü bölümde, bu tez çaışması kapsamında yapılmış sayısal örneklere yer verilmiştir. Bu bağlamda iki adet çok açıklıklı sürekli ve bir adet tek açıklıklı köprü uygulama örneği olarak seçilmiştir. Uygulama örneklerine ait sonuçlara bu bölümde yer verilmiştir.

Beşinci bölümde çalışmanın genel hatlarına yer verilmiş ve çalışmaya ait sonuçlar ve öneriler sunulmuştur.

# 1. INTRODUCTION

Since Turkey is located in the area which has active fault lines, research projects related to earthquake have invariably come to the forefront. Hence, everyday-life structures with having main concerns in catastrophic areas are required to conserve their stability. As bridges are considered as foremost elements in transportation, serviceability of these key elements plays an important role in the state of emergency after earthquakes.

Ground transportation consists of two major components as highway transportation and railway transportation in Turkey. Although highway transportation seems more effective, railway transportation is widely accepted as a substantial solution. Construction of railway lines in Turkey dates back about 150 years and many railway bridges were constructed in the earlier phases of that construction stages. Therefore, most of those bridges giving service on railway network might already complete their projected life. In fact, failure problems of bridges are generally related to man-made and natural troubles. However, aging-related problems should undoubtedly be kept in mind, and to gain maximum use out of bridges rather than breaking down, also the performance of existing bridges should be assessed and taken into account. Therefore, it is critical to determine seismicity of existing bridges in case of preventing structural damages and losses. This also has economic aspects for future generations.

In the sequel of growing importance of this issue, researchers have been interested in enhancing principles of fragility analysis and its application to various structure. However, little has been done for railways in this regard, even though they are important segments of lifeline system. Hence, emphasis of this thesis has been made on steel truss railway bridges and scope of this research is to investigate seismic fragility of three existing steel truss railway bridges through nonlinear dynamic analysis. These analyses were conducted with finite element analysis software SAP2000. On this purpose, one simply supported (SS) and two multispan continuous (MSC) steel bridges were selected as case study examples.

First, original finite element models which referred to as “original bridge model” of selected case study bridges were constructed based on original design drawings. Modal parameters such as mode shapes and corresponding frequencies were obtained and they were compared with experimental results that gained from previous reports or in-situ field testings. Thus, original finite element models were updated, and another finite element models which referred to as “updated bridge model” were generated based on experimental modal identification studies. Nonlinear dynamic analyses were conducted on both original and updated bridge models. Once the analyses have been concluded, fragility analysis was carried out, and fragility curves of each bridge were developed. Seismic vulnerability of those bridges was evaluated and discussed according to fragility curves of those.

This thesis is composed of five chapters. In Chapter 1, general information about the study and the aim of the study are represented.

Chapter 2 includes general characteristics about steel truss bridges, specifications of fragility curve development methodologies and summaries of previous studies related to fragility evaluation procedures.

Chapter 3 describes the generation of analytically derived fragility curves within the scope of this study. The principles of selection of ground motion records, nonlinear time history analysis, and modal updating procedure are included.

Chapter 4 presents fragility evaluation results of case studies on selected single span and multispan continuous bridges.

Finally, Chapter 5 is devoted to summary and conclusion of the study. Recommendations based on the results and conclusions of the study are also given in this chapter.

# 2. LITERATURE REVIEW

## 2.1 Scope of Literature Review

Fragility assessment of structures is a rather contemporary issue in which many researchers attend to put effort into the development of this topic. However, in the literature, fragility assessment of steel truss bridges do not take wider place. Therefore, the scope of literature review includes studies related to steel truss bridges, bridges other than steel truss bridges and buildings.

In this chapter, first, general information about steel truss bridges are introduced. Then, the methods of generating fragility curves are outlined, and previous studies related to this subject are summarized.

## 2.2 Review of Steel Truss Bridges

Balance among cost-effective structure and future traffic volume is an important aspect to be managed for a bridge, which is one of the fundamental members of the transportation system. Alongside strength is always a primary issue and presenting potential for handling all required span options, steel bridges have suggested as suitable solutions for design aspects. (Barker and Pucket, 2013).

Steel bridge enables to have a lighter and appropriate design solutions. The smallest foundations comparing to classical reinforced concrete bridges; industrialized and rapid construction process; greater control of members, substructures, and connections; easy dismantling and reuse procedures are the advantages of steel solutions (Pipinato and De Miranda, 2016).

Moreover, steel truss bridges could provide reasonable and cost-effective solutions. Following distinctive features about truss bridges were defined by O'Connor (1971) and were summarized by Barker and Puckett (2013) as:

- A bridge truss provides two main structural profits that have influence to lead the economy in material and to reduce dead weight: First, the primary member

forces are axial loads; Second, the open-web system enables the utilization of larger overall depth rather than a similar solid-web girder. In case of achieving a probability for more rigid structure, reduced deflections should be provided which can be presented by increased depth.

- The conventional truss bridge is considered as an economical solution for medium spans. Traditionally, among the plate girder and the stiffened suspension bridge, truss bridge has been chosen for spans in between. Present construction methods and materials have influenced to increase the economical span of both steel and concrete girders. The cable-stayed girder bridge has become a competitor to the steel truss for the intermediate spans. Eventually, under these circumstances with considering significant construction costs of a truss, the number of truss spans have been tended to reduce in recent years.
- In comparison with possible solutions, the truss encroachment has two options: first, large opening below with upper chord level deck; second, small opening below with lower level chord deck if the traffic runs through the bridge. For railway overpasses carrying a railway above a road or another railway, the small construction depth of a through truss bridge is a favorable solution. In several construction options, the combination of both arrangements has advantageous as providing a through truss over the main span with a small construction depth and approaching with the deck at upper chord level.

Each truss consists of a top and bottom chord, end-posts, and web members. The web members are further divided into hip verticals, intermediate posts, and diagonals as shown in Figure 2.1 (Prell, 1908).

### 2.2.1 History of truss bridges

A truss is a series of members dividing stress in the direction of their length, combined together into a triangular system, which is able to sustain a range of loads applied at the points where the members cross when placed upon supports with a calculated distance in between (Prell, 1908). In principle, the intersection point of each member at a joint is free to pivot independently of the other members creating the joint. If this condition cannot be fulfilled, secondary stresses are led to the members. Also if loads occur other than at panel points, or joints, bending stresses are produced in the members (Kulicki, Prickett, & LeRoy, 1999).

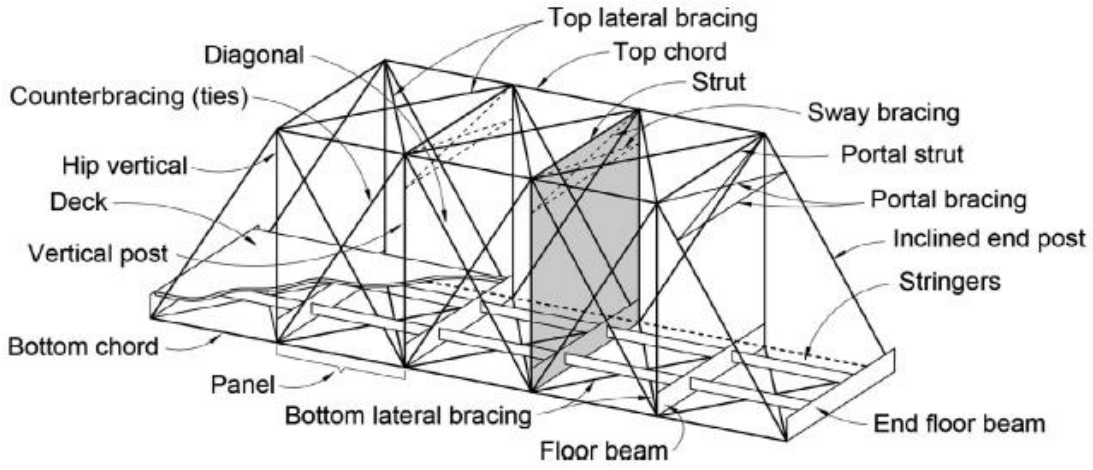


**Figure 2.1 :** Truss main components (Pipinato and De Miranda, 2016).

Even though trusses come across since the ancient Roman period, the first concept of modern truss system was developed by Andrea Palladio, an architect from 16th-century Italy (Gosh, 2006), who utilized king-post truss as shown in Figure 2.2. The following century of Palladio's development, Theodore Burr re-discovered the truss that named after him, which, in reality, a series of king-post trusses. This was considered to be unstable under moving loads, and was therefore reinforced by the implementation of an arch to the system, or was built somehow as an arch, there being considerable rise at the center of the span as shown in Figure 2.3 and Figure 2.4 (Dufour, 1909).

The first truss timber bridge in America was constructed and patented by Ithiel Town, a prominent American architect and civil engineer, in 1820 (Gosh, 2006).

The Howe truss was the first patented truss to introduce iron into the timber structure (1840), which carries the name of its developer, William Howe. The Howe truss has top and bottom chords as well as the diagonal bracings in timber and the vertical members made of hammered iron rods. In 1844, the patenting of the Pratt truss followed this development, which reversed the material combination of the Howe truss by using timber for the vertical and wrought iron for the diagonal members.

In 1847, the first all-iron truss -a bow string truss- was constructed by Squire Whipple, with cast iron top chord and verticals, and hammered iron bottom chord and diagonals. Later on, during the late 19th century, steel truss bridges with various compositions came to be built. Apart from the Pratt and Howe trusses, Baltimore, Warren, and K-type compositions became known (Gosh, 2006).

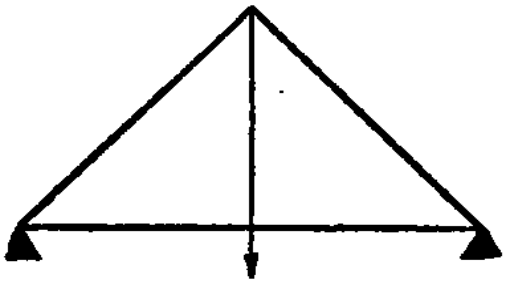

**Figure 2.2 :** King-post truss (Dufour, 1909).

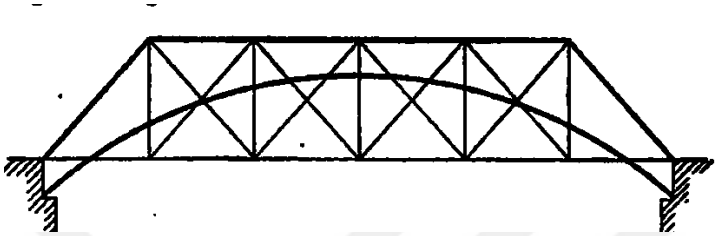

**Figure 2.3 :** King-post truss bridge stiffened by arch (Dufour, 1909).

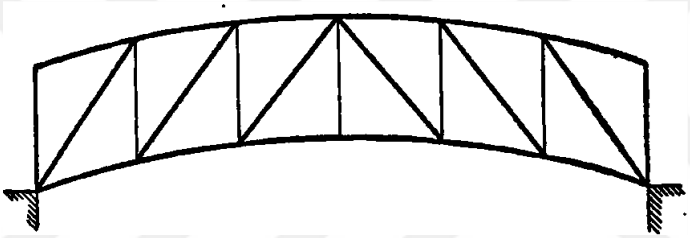

**Figure 2.4 :** Burr truss bridge, arched (Dufour, 1909).

Antecedent truss systems can be considered variations of arch systems. Those systems were designed to apply horizontal thrusts at the abutments, as well as vertical reactions (Kulicki, Prickett, & LeRoy, 1999). The first great bridge of history, whose main structure was an arch-formed steel, is the St. Louis Bridge passing over the the river Mississippi in the United States of America, a design of James B. Eads and built in 1874, with three 152+157+152m span arches (Troyano, 2003) (see Figure 2.5).

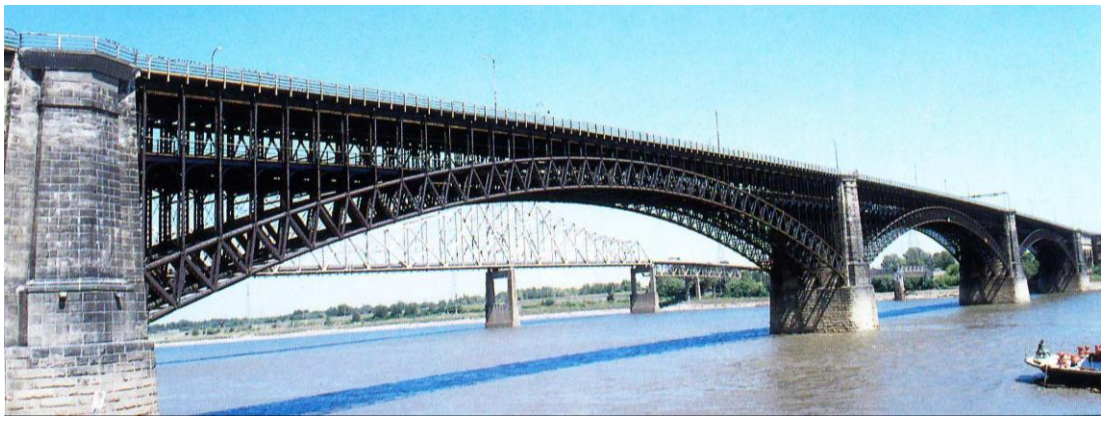

**Figure 2.5 :** St. Louis bridge over Mississippi river, United States (Troyano, 2003).

The Queensboro bridge passing over the East River in New York City was constructed in 1909. This bridge was formed by a continuous truss configuration with a 192-meters central span and two 360-meters main spans (Gosh, 2006) (see Figure 2.6).

**Figure 2.6 :** Queensboro bridge over East River, United States (www. nyc.gov).

### 2.2.2 Types of trusses

A wide number of truss types have been built up for special purposes. Those truss forms may be categorized according to their names, character of their chords, and system of webbing (Prell, 1908). Common truss types and their characteristics are listed in Table 2.1.

In addition to these, truss bridges may be made continuous over a number of piers. However, since the stresses in the members are quite sensitive to the settlement of supports, this type of bridge is suitable only in case where the differential settlements of abutments and piers are not significant. With utilizing continuous truss bridge system, larger spans between the span ranges of 150 m and 400 m are conceivable in comparison to simply supported trusses. Moreover, a continuous truss is accepted as comparatively more rigid and is a statically indeterminate structure (Gosh, 2006).

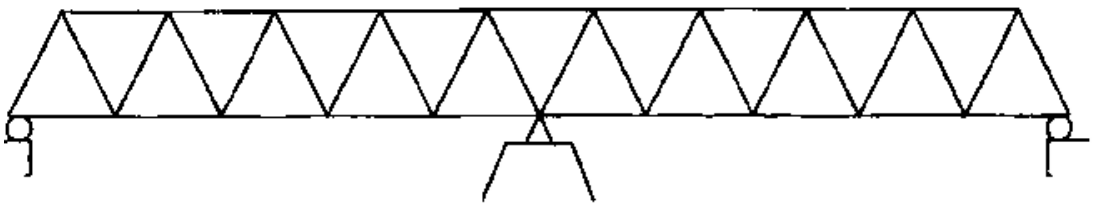

**Figure 2.7 :** An example of continuous truss bridge (Gosh, 2006).

**Table 2.1 :** Truss typologies (Pipinato and De Miranda, 2016).

| Designation | Geometric Scheme | When First Used | Typical Length | Comments |
|---|---|---|---|---|
| Pratt |  | 1844 | 9m-75 m | Diagonals in tension, verticals in compression, except for hip verticals adjacent to inclined end post. |
| Baltimore | 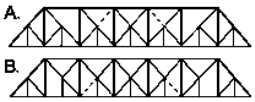  | 1871 | 75m-180 m | A: with substruts, B:with subties |
| Warren | 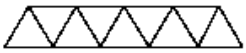 | 1848 | 15m-120 m | Triangular in outline, the diagonals carry both compressive and tensile forces. An original Warren truss has equilateral triangles. |
| Pratt half-hip |  | Late 19th century | 9m-45 m | A Pratt with inclined end posts that do not horizontally extend the length of a full panel. |
| Pennsylvania (petit) | 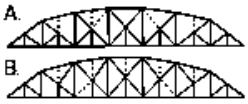  | 1875 | 75m-180m | A: Parker with substruts, B: Parker with subties |
| Warren |  | Mid-19th century | 15m-120 m | Diagonals carry both compressive and tensile forces; verticals serve as bracing for triangular web system. |
| Truss leg bedstead | 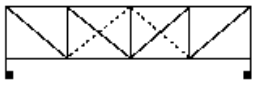 | Late 19th century | 9m-30 m | A Pratt with vertical end posts embedded in their foundations. |
| Lenticular-parabolic |  | 1878 | 5m-110 m | A Pratt with top and bottom chords parabolic curved over the entire length. |

**Table 2.1 (continued) :** Truss typologies (Pipinato and De Miranda, 2016).

| Designation | Geometric Scheme | When First Used | Typical Length | Comments |
|---|---|---|---|---|
| Double intersection Warren | 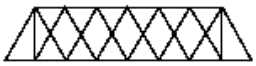 | Mid 19th century | 23m-120 m | Structure is indeterminate; members act in both compression and tension; two triangular web systems are superimposed upon each other with or without verticals. |
| Parker |  | Mid-to-late 19th century | 12m-75 m | A Pratt with a polygonal top chord. |
| Pegram |  | 1887 | 45m-195 m | A hybrid between the Warren and Parker trusses; upper chords are all of equal length. |
| Howe |  | 1840 | 9m-45 m | Diagonals in compression, verticals in tension (wood, verticals of metal). |
| Camelback |  | Late 19th century | 30m-90 m | A Parker with a polygonal top chord of exactly five slopes. |
| Double intersection Pratt |  | 1847 | 21m-90 m | An inclined end-post Pratt with diagonals that extend across two panels. |
| Post |  | 1865 | 30m-90 m | A hybrid between the Warren and the Double intersection Pratt. |
| Bowstring arch-truss |  | 1840 | 15m-40 m | A tied arch with diagonals serving as bracing and verticals supporting the deck. |

**Table 2.1 (continued) :** Truss typologies (Pipinato and De Miranda, 2016).

| Designation | Geometric Scheme | When First Used | Typical Length | Comments |
|---|---|---|---|---|
| Camelback | 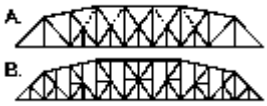  | Late 19th century | 30m-150 m | A: Pennsylvania truss with a polygonal top chord of exactly five slopes, B: Same as A, with horizontal struts |
| Schwelder |  | Late 19th century | 30m-90 m | A double-intersection Pratt positioned in the center of a Parker. |
| Bollman |  | 1852 | 13m-30 m | Verticals in compression, diagonals in tension; diagonals run from end posts to every panel point. |
| Waddell A-truss |  | Late 19th century | 8m-23 m | Expanded version of the king post truss, usually made of metal. |
| Kellogg |  | Late 19th century | 23m-30 m | A variation on the Pratt with additional diagonals running from upper chord panel points to the center of the lower chords. |
| K-truss |  | Early 20th century | 60m-240 m | Takes the name from the particular shape remembering K members. |
| Fink |  | 1851 | 23m-45 m | Verticals in compression; diagonals in tension; longest diagonals run from end posts to center panel points. |
| Wichert | 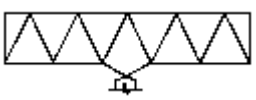 | 1932 | 122m-305 m | Identified by a pin connected support system over the piers; truss is continuous over piers. |

## 2.3 Review of Fragility Curve Development Methods

Fragility curves basically indicate the likelihood of seismic demand imposed on the structure is greater than or equal to the capacity of the structure. These curves can be constructed for a particular segment, or for a class of structures. Fragility information gives a broad idea regarding the possibility of a structural system to be damaged by an earthquake.

Due to the inherent uncertainty included in the development of fragility curves, there is not an absolute method or strategy. However, in literature, there are several approaches to derive fragility curves as expert-base, empirical, analytical and hybrid fragility curve considering the response data, which might be obtained from the opinions of experienced researchers, the field examinations after earthquake events or the results of analytical studies. Each data source has related profits and drawbacks. The succeeding section gives an overview of existing procedures to conduct the assessment of vulnerability of bridges.

### 2.3.1 Expert-base fragility curves

When available information about bridge response data is incomplete, inadequate or nonexistent, the probability function of bridge can be derived from observations of expert engineers in the area of earthquake engineering about expected damage from ground motions.

The most efficient methodology for development of expert-base fragility curves is presented by Applied Technology Council in the report of ATC-13 (ATC, 1985). In that method, expert engineers were asked to make estimates of the probable damage distributions when bridge was subjected to various earthquake levels (Rossetto and Elnashi, 2003). That method includes Delphi procedure that includes systematic questionnaires, gathering insights from experts for the questionnaires, continuously iterating questionnaires until project manager can control information feedback rounds, and lastly cumulating the feedbacks by statistical operation methods. In accordance with each intensity level of ground motion, probability distributions of damage factor were criticized depending those questionnaires. After probability distribution discretization, damage probability matrices were gathered. Besides the damage probability matrices, various types of statistics were gathered (ATC-13).

In spite of these conveniences, however, that method contains a few drawbacks. It is possible to incorporate an individual who does not qualify as an expert or the individual may introduce himself as an expert despite the fact that he was not. Furthermore, outcomes of the Delphi method also depend upon subjective judgment of the experts. Nevertheless, the likelihood of all these occasions happening at the same time is very low. Furthermore, inbreeding and motivational biases can be avoided by assuring diversity in backgrounds of the experts.

### 2.3.2 Empirical fragility curves

Another method of deriving fragility curve is primarily based on actual damage data collected from field investigations after earthquakes or experiments in different sites. Empirical method of generating fragility curves is considered as the most realistic approach since the existing damage state of a bridge is examined and evaluated in detail for all components (Rosetto and Elnashi, 2003). Advantage of the observational method is being profitable for characterizing the structural performance of a set of similar structures. However, damage state definition which depends on visual investigation at every location of the work is a challenge with this method. Additionally, advanced statistical methods should be applied in case of obtaining the parameters of the curve.

Pursuing after severe earthquakes around the world, empirical bridge fragility curves turned out to be more prevalent in consequence of more ground motion and more bridge damage data available. Several researchers utilized observational methods considering distinctive earthquakes or combination of several earthquakes and their related bridge damage data. Yamazaki et al. (2000), Karim and Yamazaki (2001) and Shinozuka et al. (2000a) considered only the Kobe earthquake. Basöz et al. (1999) considered only Northridge earthquake. Additionally, Basoz and Kiremidjian (1997) used the Loma Prieta and Northridge earthquakes. Furthermore, Shinozuka et al. (2003) and Elnashai et al. (2004) used both Northridge and Kobe earthquakes.

Yamazaki et al. (2000) developed empirical fragility curves of 216 bridge structures along the Chugoku Expressway. PGA, PGV and JMA (Japan Meteorological Agency) intensity were used as a measure of earthquake. Moreover, Kriging technique which is a method of stochastic interpolation was employed to estimate spatial distribution of ground motion indices for the 1995 Hyogo-ken Nanbu (Kobe) earthquake records.

However, empirical fragility curves, which were acquired following this approach, do not introduce structural parameters and variation of input ground motion as a result of deficiency of data. Hence, these curves may not be applicable to the class of structures (Karim Yamazaki 2001).

Shinozuka et al. (2000a) presented the development of both empirical and analytical fragility curves for the Hanshin Expressway Public Corporation's (HEPC's) bridges (columns) on the basis of damage data that was recorded during the 1995 Hyogo-ken Nanbu (Kobe) earthquake and seismic response of bridges under dynamic analysis. Statistical analysis was conducted through two-parameter lognormal distribution functions, PGA was used to represent ground motion intensity. Also Additionally, testing goodness of fit of fragility curves was included in this study. Results of that testing procedure showed that both empirical and analytical assumptions demonstrated above 90% confidence.

In order to analyze seismic condition of highway bridges in Greater Los Angeles area, Basöz et al. (1999) generated empirical fragility curves and damage probability matrices which introduced relationships between ground motion and bridge damage data that recorded during the 1994 Northridge earthquake using logistic regression analysis. Classification of bridge inventory and damage state descriptions were done by the method developed in Basöz and Kiremidjian (1996). Contrary to the work done by Yamazaki et al. (2000), observed damage data were segregated by structural characteristics. Thus, these empirical fragility curves were compared to those provided in the ATC-13 (ATC, 1985). According to the comparison, results do not correlate thoroughly to the observed damage. Similar procedure was conducted in Basöz et al. (1997). Report presented the results of comprehensive study which evaluated seismic vulnerability of bridge inventory that experienced 1989 Loma Prieta and 1994 Northridge earthquakes. PGA values were used to characterize the ground motion levels, and a complete set of the empirical curves was developed from the logistic regression analysis. A comparison was done with the fragility curves which were provided in HAZUS. Results showed that those fragility curves overestimate the exceedance probabilities in all ground motion levels for any given damage state.

Shinozuka et al. (2003) constructed empirical fragility curves utilizing bridge damage data obtained from damage report for Caltrans' bridges and HEPC's report that established after the 1994 Northridge and the 1995 Hyogo-ken Nanbu (Kobe)

earthquakes, respectively. Two parameter lognormal distribution functions were employed to represent fragility curves. Researchers proposed two methods that conducted parameter estimation, hypothesis testing and confidence interval estimation in distinctive ways. Briefly, first method, which was more traditional, was utilized when the fragility curves were independently constructed for different states of damage, while second method was used when they were developed dependent from each other.

Elnashi et al. (2004) proposed a simple procedure to derive fragility curves that utilized the overstrength ratio of bridges which were the part of same bridge class but have different properties. Hence, that feature enables the proposed method to use in extensive projects which include many bridges to have similar configurations. This method considered four limit states and two data sets for bridge damage that gathered during the 1994 Northridge and the 1995 Hyogo-ken Nanbu (Kobe) earthquakes. Results indicated that both normal and lognormal distributions were acceptable models for the sample under consideration.

### 2.3.3 Analytical fragility curves

#### 2.3.3.1 Elastic spectral analysis

Elastic spectral analysis method is known as the simplest approach to constructing analytical fragility curves (Hwang et al., 2000). Hwang et al. (2000) and Jernigan and Hwang (2002) utilized this approach for the development of the fragility curves for Memphis bridges. This method assessed seismic damage potential of various components of bridge with determination of capacity/demand ratios and correlation with particular damage states for various levels of intensity measures. Thus, a bridge damage frequency matrix was generated which is used for developing fragility curves (Billah and Alam, 2015).

Hwang et al. (2000) proposed a procedure for seismic evaluation of bridges and highway networks which consist of developing a classification system for bridge inventory, derivation of fragility curves, estimation of site condition parameters and determination of seismic damage. The capacity and seismic demand of the components were calculated according to FHWA (1995) and an elastic spectral analysis method specified in AASHTO (1996), respectively. The capacity/demand ratios and

corresponding damage states were determined, and damage data were statistically analyzed in order to develop fragility curves for various bridge types.

Subsequently, Jernigan and Hwang (2002) presented similar analytical method which employed elastic spectral analysis in the determination of the seismic demand of bridge components. This method was used to develop the fragility curves for a bridge type which was commonly found in Memphis Highway systems.

Despite the fact that this method is the easiest, it has a few restrictions. Elastic spectral analysis method gives satisfactory results for bridges that rely upon only in linear elastic range. This method fails to predict the demand accurately whereas the bridge is subjected to serious nonlinearity. So that, it makes the accuracy of constructed fragility function debatable.

#### 2.3.3.2 Nonlinear static analysis

Nonlinear static analysis method or capacity spectrum method is another approach to developing derived fragility curves analytically. Various researchers (Dutta and Mander, 1998; Mander and Basoz, 1999; Mander, 1999; Shinozuka et al., 2000b; Monti and Nistico, 2002; Banerjee and Shinozuka, 2007) put effort to enhance this method for generating fragility curves for bridges. Nonlinear static analysis reveals the advantage of considering nonlinearity in finite element model. Thus, the limitations of elastic spectral analysis can be overcome. This method is implemented by calculation of the capacity using nonlinear static pushover analysis and estimation of demand through reduction of the elastic response spectrum. Then, as shown in Figure 2.8, these spectra are plotted in same graph, the intersection of two curves result in the expected performance level of the bridge in a deterministic analysis. Using the intersection of capacity and demand distribution, the probability of failure can be determined for a particular level of selected intensity measure. Fragility curves for the bridges can be generated using these spectra.

Mander (1999) investigated to set up reliable fragility curves in the light of limited available data. Probability distributions were plotted over both capacity and demand curves, then they were expressed in the form of fragility curve given by a log-normal cumulative probability density function. The parameters of median and a normalized standard deviation of fragility curve were assessed with capacity spectrum method which assumes displacement-based nonlinear static analysis procedure as it defined in

AASHTO. Additionally, analytical fragility curves for various different bridge types were compared with empirically derived fragility curves based on bridge damage data obtained from 1994 Northridge and 1989 Loma Prieta earthquakes. Moreover, methodology described in this study was illustrated with a three-span simply supported prestressed concrete highway bridge.

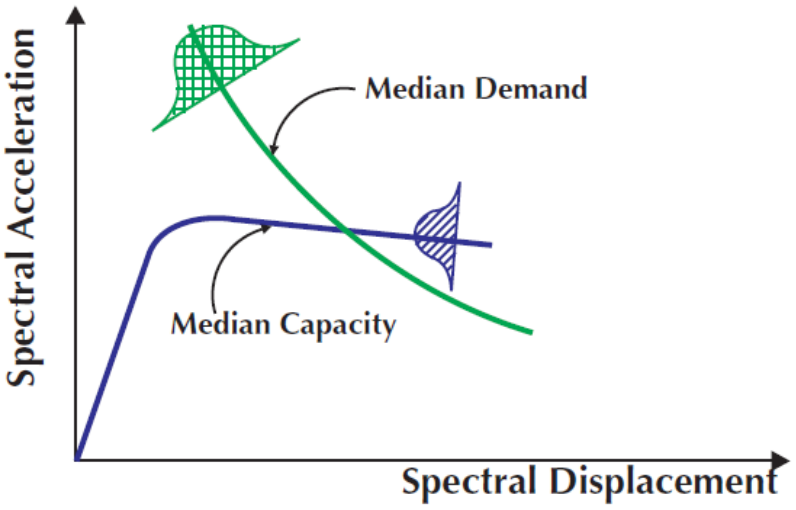


**Figure 2.8 :** Intersection of capacity-demand acceleration-displacement spectra (Mander, 1999).

Shinozuka et al. (2000b) investigated the probability of damage of structures based on nonlinear static procedure. In this study, capacity spectrum method (CSM) was employed as stated in ATC 1996. Moreover, fragility curves developed with that procedure were compared with those obtained by dynamic analysis. Although comparison results were convenient for at least minor damage state, it was concluded that as the damage states increased, the agreement in fragility curves decreased.

Monti and Nistico (2002) presented a simplified method for evaluating the damage state of bridge in terms of fragility curves. The method was based on the probabilistic approach of three predefined performance levels through a simple damage function. The likelihood of exceeding each performance level as a function of the PGA corresponded to fragility curve. Also, the method was evaluated with representative four highway bridge typologies with different piers.

Apart from advantages of this method, it was practically developed based on the recommendations from ATC 40 (ATC, 1996) which was related to buildings. Furthermore, this method needs defining the bridge structure types and the estimation

of effective hysteretic damping, which plays an essential role in seismic performance evaluation (Billah and Alam, 2015).

### 2.3.3.3 Nonlinear dynamic analysis

According to Shinozuka et al. (2000b), nonlinear dynamic analysis is the most reliable method for estimating the inelastic seismic demands of the structures to derive analytical fragility curves. This method considers both geometric and material nonlinearity to obtain seismic response under earthquake loads.

Many researchers (Hwang et al., 2001; Cornell et al., 2002; Choi et al., 2004; Elnashai et al., 2004; Nielson and DesRoches, 2006; Nielson and DesRoches, 2007; Pan et al, 2010) have utilized this procedure. In case of employing nonlinear dynamic analysis, first, finite element model of the bridge with considering nonlinearity is constructed with a suitable set of earthquake ground motion records that represents the seismicity of the bridge region. Then, nonlinear time history analysis is conducted for each bridge model to record maximum critical responses of bridge components. After the utilization of those demand records, analytical fragility curves are constructed by regression analysis or maximum likelihood method. Typical procedure is summarized in Figure 2.9.

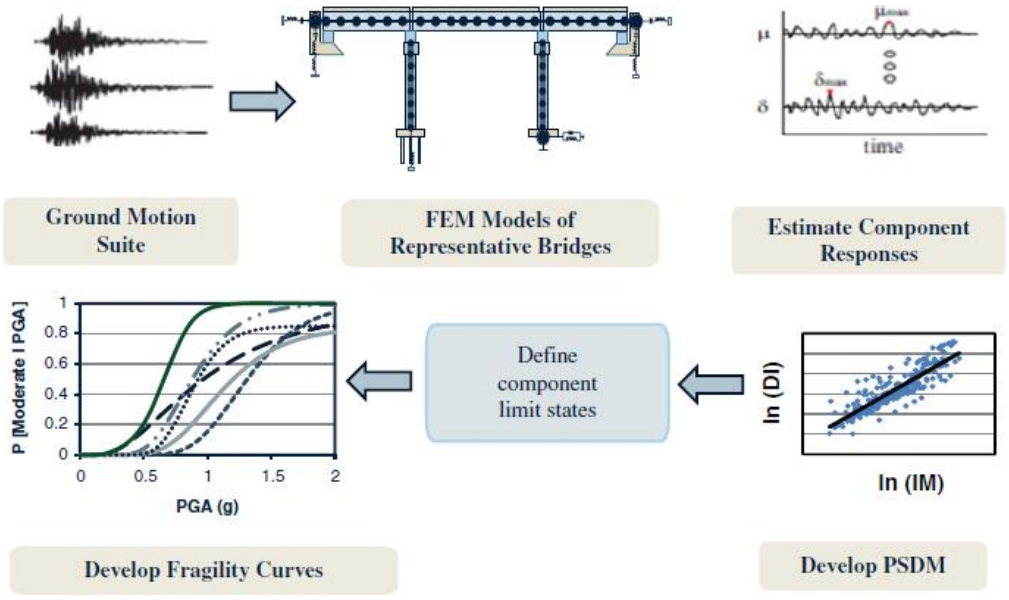


**Figure 2.9 :** Schematic representation of the NDA procedure to develop fragility curves (Billah, 2015).

Hwang et al. (2001) presented an analytical approach for generating fragility curves of highway bridges by performing nonlinear time history analyses for each ground motion, site condition and bridge samples. That approach provided easy verification and refinement of uncertainties in modeling parameters.

Cornell et al. (2002) introduced a formal probabilistic basis for the 2000 SAC FEMA (FEMA, 2000) to assess performance of structures under seismic loads. Presented method rested on nonlinear dynamic displacement-based approach. Performance levels were identified with the quantification of structural demand and structural capacity. In addition, spectral acceleration Sa was involved as ground motion intensity measure into the assessment procedure.

Choi et al. (2004) generated a set of fragility curves for the identified four typical bridges found in the United States. Individually developed fragility curves of each component for each bridge class then were synthesized into main fragility curves to represent the whole bridge system based on first order reliability. According to those fragility curves, it was concluded that exceeding 50% probability of slight damage, PGA differs in the range of 0.19 to 0.24g. That study reveals that the most and the least vulnerable bridge types were multispan simply supported steel-girder bridges and multispan continuous prestressed concrete-girder bridges, respectively.

Nielson and DesRoches (2006) presented an expanded methodology to derive analytical fragility curves for highway bridges that struggles to reveal the effects of main components of the bridge to its overall system fragility. Nonlinear time history analyses were used to assess seismic demand, and demand and capacity of the structural components were assumed to follow a lognormal distribution. The methodology was illustrated with a case study for a multispan class of bridges which were simply supported by concrete slab. It was concluded that the most fragile bridge components are abutments. Additionally, in another study of the researchers, (Nielson and DesRoches, 2007), seismic fragility curves for nine classes of bridges were developed, and then a comparison was made with fragility curves of those were constructed based on the proposed methodology which was found in HAZUS-MH. Results revealed that vulnerability level is lesser than presented in HAZUS-MH, relying on the presented fragility curves.

Pan et al. (2010) presented the results of the fragility analysis of a typical multispan simply supported steel bridge in New York State. Distinctive 10 ground motions, in case of covering a wide range of PGA's, were selected and employed to every bridge sample. Then, 100 simulated earthquake ground motions were utilized to nonlinear time history analyses of a set of 10 bridge samples. A quadratic regression between fragility parameters was assumed and yielded more reliable fragility results than a linear regression. It was concluded that the vulnerability of fixed steel bearings in bridge was higher than other components.

#### 2.3.3.4 Incremental dynamic analysis

Incremental dynamic analysis is a special type of a nonlinear time history analysis where ground motions are incrementally scaled to cover the entire range of structural responses from elasticity, to yielding, and finally, global dynamic instability and a series of analyses is performed at rapidly increasing intensity levels. This method was first mentioned by Bertero (1977), developed by Luco and Cornell (1998) and described in detail by Vamvatsikos and Cornell (2002). Consistently, this method is useful to derive collapse fragility curves of structures.

Strong side of this method is that prior assumptions are not compulsory in terms of probabilistic distribution of seismic demand (Zhang & Huo, 2009). However, incremental scaling of a large set of ground motions can cause higher computational demand. Likewise, the procedure contains selection and scaling of ground motions, which may bring on over or under estimation of the fragility of the structures (Baker, 2013).

Kirçil and Polat (2006) developed the fragility curves of mid-rise R/C buildings in terms of spectral acceleration, peak ground acceleration (PGA) and spectral displacements under the effect of twelve artificial ground motions. Incremental dynamic analyses were employed in order to obtain capacity of the structures for the considered damage levels. Fragility curves were generated with the method based on two parameter log-normal distribution functions of the occurrence of damage.

### 2.3.4 Hybrid fragility curves

In case of reducing computational effort and providing an objective evaluation, hybrid approach which fundamentally considers several of previously explained methods can

be employed. The first attempt of this objective was taken by Penelis et al. (1989) that combines inelastic dynamic analysis and earthquake database of Thessaloniki,1978. Likewise, Kappos et al. (1995) extensively presented the origin of hybrid approach and essential concepts as previously presented in Kappos et al. (1991). Moreover, Kappos et al. (1998), Kappos et al. (2006) and Kappos and Panagopoulos (2010) utilized the hybrid fragility curves in order to evaluate the reinforced concrete and masonry buildings in Greece. Concerning structural typology and available damage data resemblance of the area were embodied under those studies. It was also combined with analytical damage statistics which were derived from the utilization of nonlinear analysis of typical structures (Kappos et al., 2006).

Kappos et al. (1995) presented a hybrid methodology of fragility analysis that considers empirical and analytical assumptions. The methodology consists of correlating damage estimates from available data and concerns the effect of soil conditions on site. However, that hybrid methodology experiences a few limitations. Foremost, substantial damage statistics of preceding earthquakes are considered reliable for that method, however, under inadequate statistical sample condition, this is not valid. Besides, there is a controversial relationship between structural damage and earthquake intensity (Kappos 2016).

Summary of the four methods which are utilized for developments of fragility curves can be found in Table 2.2 with limitations and a few essential aspects.

**Table 2.2 :** Categorization of vulnerability curve (Kwon and Elnashi, 2006).

| Category | | Characteristics |
|---|---|---|
| Empirical vulnerability curve | Features | Based on post-earthquake survey<br>Most realistic |
| | Limitations | Highly specific to a particular seismo-tectonic, geotechnical and built environment<br>The observational data used tend to be scarce and highly clustered in the low-damage, low-ground motion severity range<br>Include errors in building damage classification<br>Damage due to multiple earthquakes may be aggregated |
| Judgemental vulnerability curve | Features | Based on expert opinion<br>The curves can be easily made to include all factors |
| | Limitations | The reliability of the curves depends on the individual experience of the experts consulted<br>A consideration of local structural types, typical configurations, detailing and materials inherent in the expert vulnerability prediction |
| Analytical vulnerability curve | Features | Based on damage distributions simulated from the analyses<br>Reduced bias and increased reliability of the vulnerability estimate for different structures |
| | Limitations | Substantial computational effort involved and limitations in modeling capabilities<br>The choices of the analysis method, idealization, seismic hazard, and damage models influence the derived curves and have been seen to cause significant discrepancies in seismic risk assessments |
| Hybrid vulnerability curve | Features | Compensate for the scarcity of observational data, subjectivity of judgmental data, and modeling deficiencies of analytical procedures<br>Modification of analytical or judgment based relationships with observational data and experimental results |
| | Limitations | The consideration of multiple data sources is necessary for the correct determination of vulnerability curve reliability |

# 3. DEVELOPMENT OF ANALYTICAL FRAGILITY CURVES

The flow chart shown in Figure 3.1 summarizes methodology which adopted within the scope of this thesis. After generation of original analytical bridge models, nonlinear dynamic analyses were applied to that original model. Then, experimental identification of bridges was done through in-situ testing or based on previous reports. Furthermore, those experimental results were compared to the results of original models, and If error percentage between results was greater that 1%, modal updating procedure was employed. Once again, nonlinear dynamic analyses were conducted on updated bridge models. Once the analyses have been concluded, fragility analysis was carried out, and fragility curves of each bridge were developed for both original and updated models.

## 3.1 Selection of Ground Motion Records

Within the scope of development of analytical fragility curves, first step is to determine appropriate ground motion data set for nonlinear time history analysis. In this study, a variety of ground motion records is examined. After that, an adequate number of these records which represents seismic hazard conditions of regions of interest is chosen to provide a set of ground motion. However, owing to the fact that recorded ground motions which were acquired from the previous earthquakes in Turkey are not adequate to be used as a part of the development of bridge fragility curves, earthquake records from different locations of the world are investigated. Likewise, as it is mentioned in Turkish Seismic Code (TSC)-2007, peak ground acceleration (PGA) value for the first degree of earthquake zone is equal to 0.4g (see Figure 3.2). As a consequence, different 60 earthquake ground motions are selected in a broader range.

Earthquake ground motion data are selected from actual records, and all records are downloaded from PEER (Pacific Earthquake Engineering Research Center) database (PEER, 2016). Soil class definitions according to FEMA 450 (2003) are given in Table 3.1, and details related to ground motion records are listed in Table 3.2, Table 3.3, Table 3.4. The response spectra of selected 20 ground motions for each soil class are

given in Figure 3.3, Figure 3.4, and Figure 3.5; also, the response spectra of all ground motions are presented in Figure 3.6.

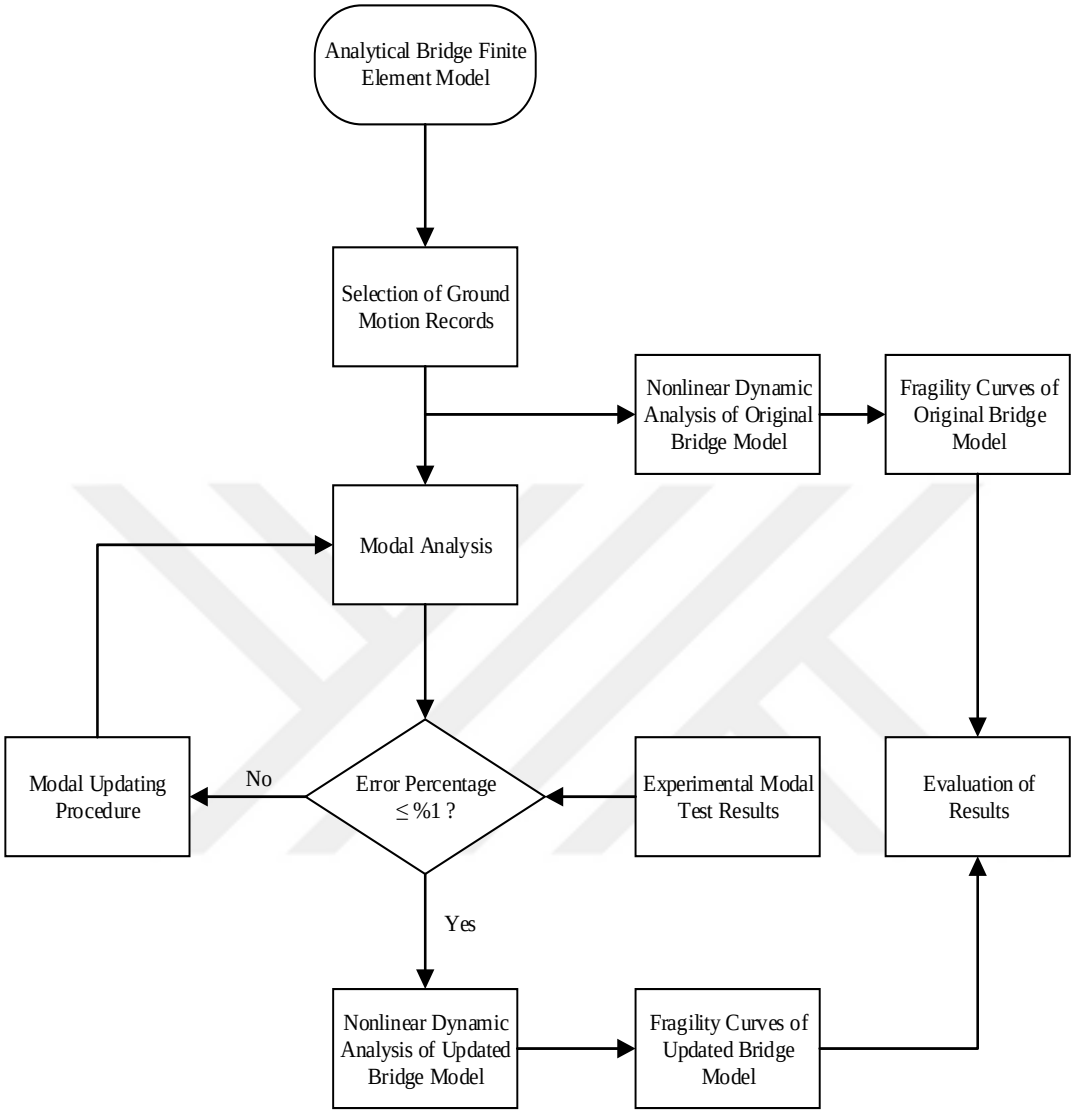


**Figure 3.1 :** Flow chart for presented approach.

**Table 3.1 :** Site class definitions **(FEMA 450, 2003)**.

| Site Class | Site profile wave | Soil shear wave velocity, $\upsilon_s$ (m/s) |
|---|---|---|
| A | Hard rock | $\upsilon_s > 1500$ |
| B | Rock | $760 < \upsilon_s < 1500$ |
| C | Very dense soil and soft rock | $360 < \upsilon_s < 760$ |
| D | Stiff soil | $180 < \upsilon_s < 360$ |
| E | Soft clay soil | $\upsilon_s < 180$ |

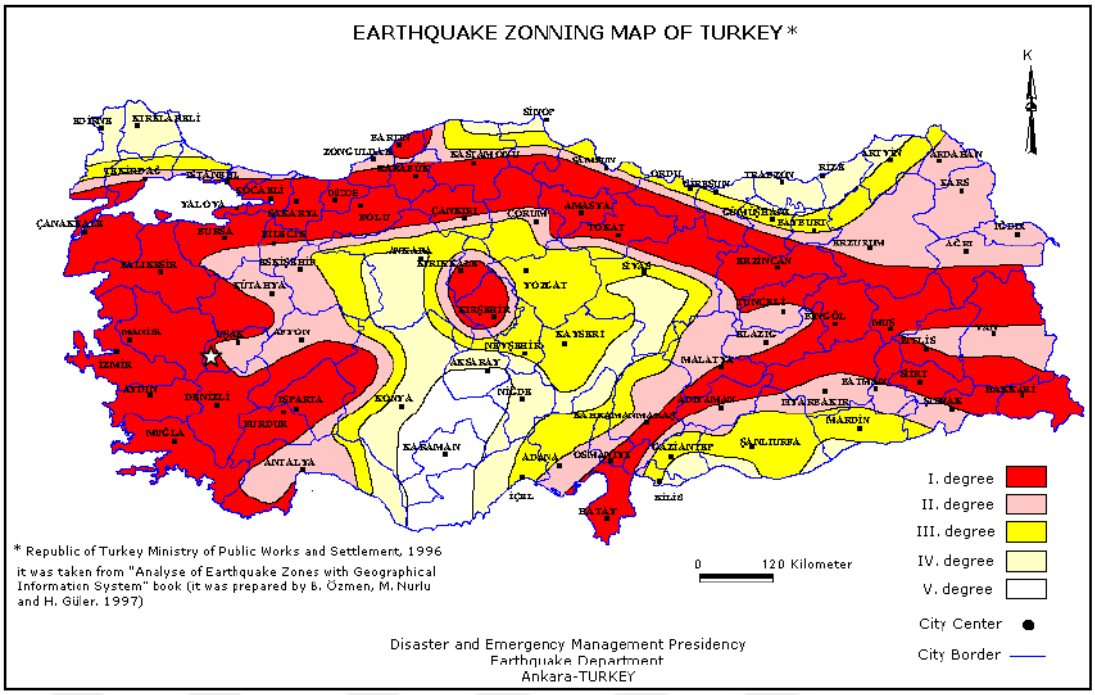


**Figure 3.2 :** Earthquake zoning map of Turkey (www.deprem.gov.tr, 2016).

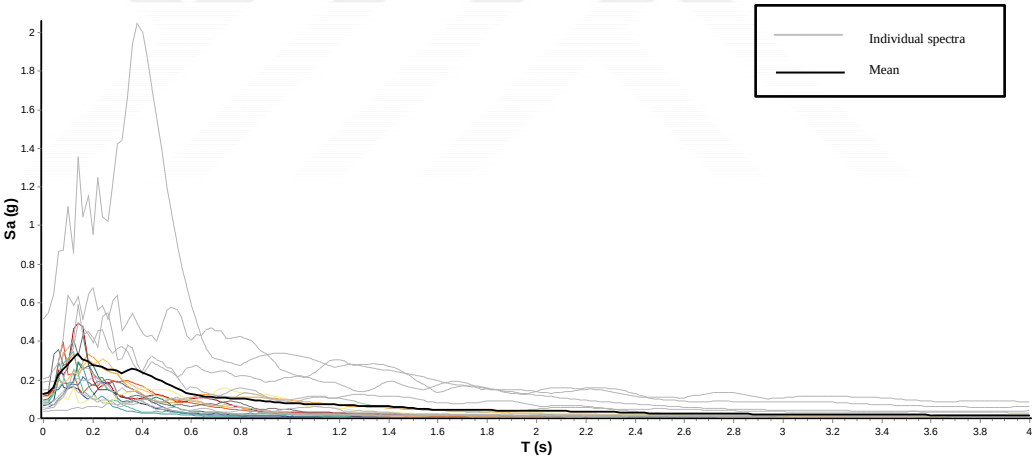


**Figure 3.3 :** Response spectra of selected 20 ground motions of soil class A.

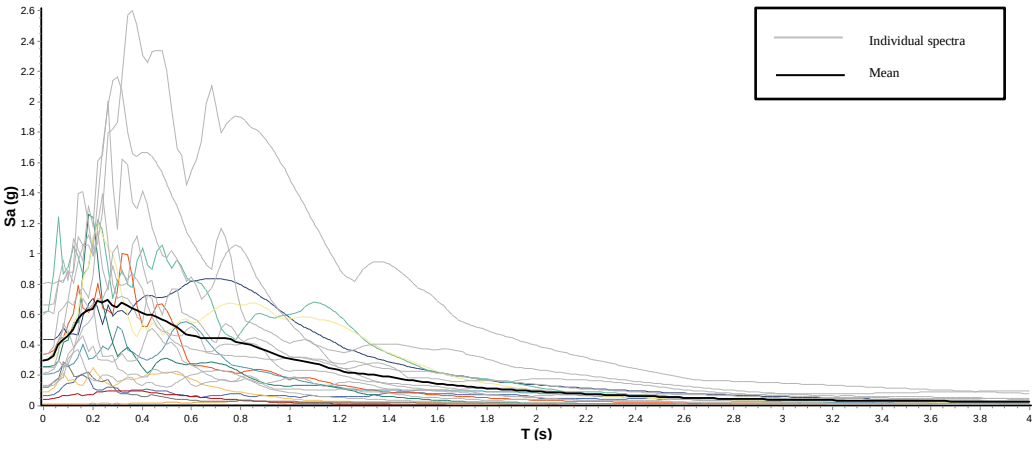


**Figure 3.4 :** Response spectra of selected 20 ground motions of soil class B.

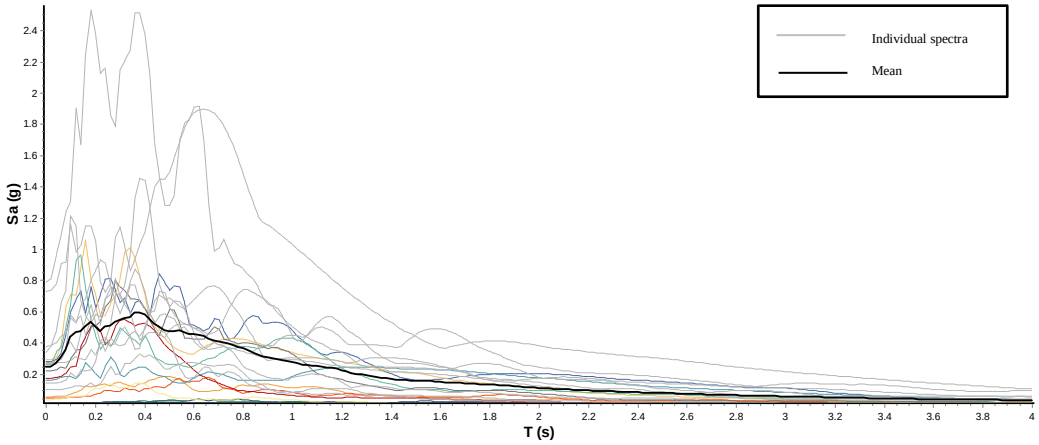


**Figure 3.5 :** Response spectra of selected 20 ground motions of soil class C.

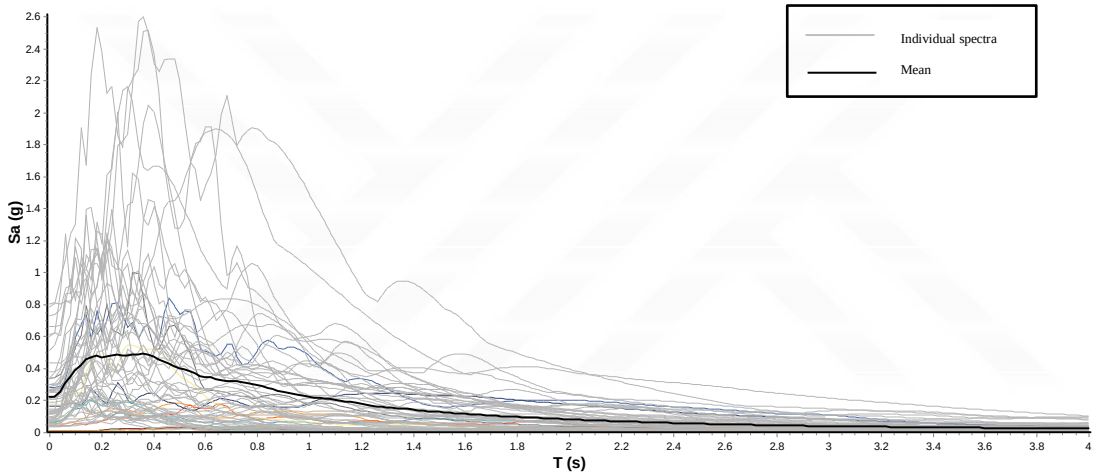


**Figure 3.6 :** Response spectra of selected 60 ground motions of soil class A-B-C.

## 3.2 Nonlinear Time History Analysis

Since nonlinear dynamic analyses are capable of producing highly accurate outcomes and comparatively small uncertainty as a result of utilization of ground motion acceleration combination, it is considered as a powerful tool and reliable analysis of seismic assessment (FEMA 440, 2005). That analysis provides direct application of earthquake loads to structures so that it is assumed as nonlinear time history analysis ideally simulates structural behavior (Li, 1996). Integration of equations of the motion of the structure by gradually taking into account as nonlinear behavior is the main objective of that method. Displacement, plastic deformation and internal forces occurred in the system, and maximum values of them which were experienced during earthquake is determined incrementaly (Çavdar and Bayraktar, 2014).

When nonlinear dynamic procedure is accurately carried out, it introduces very precise dynamic response results. The structural response is determined and relevant demand parameters of response history data are obtained resulting in response history data. On the point of nonlinear dynamic analysis, it includes fewer assumptions and depends on fewer limitations. Nonetheless, the consistency of the outcomes relies on how the analysis model is constructed and reflects structural behavior. Under the circumstances of controlled degradation and reliable nonlinear dynamic analysis models, acceptance criteria generally specify maximum value of structural component deformations upon values.

To conduct nonlinear time history analysis, direct integration with Newmark method is preferred to be used. Rayleigh damping with coefficients which are defined by natural frequencies of structure is applied. Also, geometric nonlinearity is considered as nonlinear P-Δ effect which is caused by gravity loads acting on the deformed configuration of the structure. Finally, the analysis starts after the structure dead load is fully loaded. For each ground motion record, maximum seismic response of each bridge is recorded as shown in Figure 3.7.

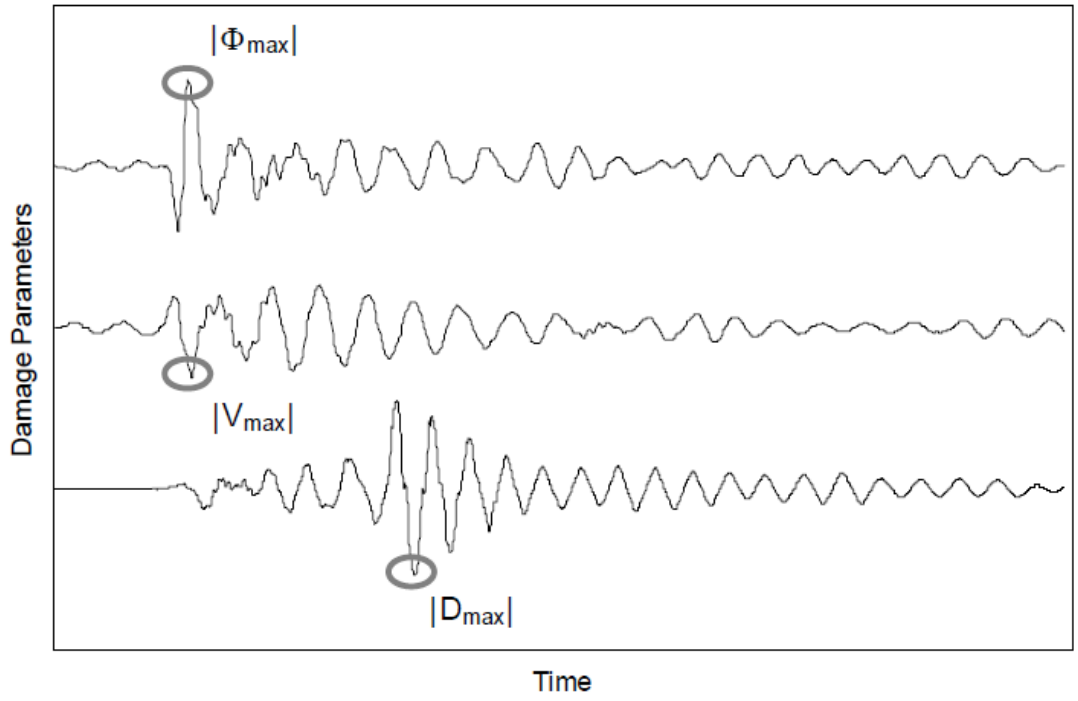


**Figure 3.7 :** Maximum seismic response of different damage parameters (Avşar, 2009).

**Table 3.2 :** Selected ground motion records for soil class A.

| ID | Earthquake | Date | Magnitude ($M_w$) | Record | PGA (g) | Distance (km) | Type |
|---|---|---|---|---|---|---|---|
| 1 | Anza (Horse Cany)-1 | 25/02/1980 | 4.9 | AZF315 | 0.066 | 12.1 | Lateral Strike |
| 2 | Morgan Hill | 24/04/1984 | 6.2 | G01320 | 0.098 | 16.2 | Lateral Strike |
| 3 | Coyote Lake | 06/08/1979 | 5.7 | G01320 | 0.132 | 9.3 | Lateral Strike |
| 4 | Landers-1 | 28/06/1992 | 7.3 | GRN180 | 0.041 | 141.6 | Lateral Strike |
| 5 | Landers-2 | 28/06/1992 | 7.3 | ABY090 | 0.146 | 69.2 | Lateral Strike |
| 6 | Landers-3 | 28/06/1992 | 7.3 | SIL000 | 0.05 | 51.7 | Lateral Strike |
| 7 | Landers-4 | 28/06/1992 | 7.3 | 29P000 | 0.08 | 42.2 | Lateral Strike |
| 8 | Loma Prieta-1 | 18/10/1989 | 6.9 | G01090 | 0.473 | 11.2 | Reverse/ Oblique |
| 9 | Loma Prieta-2 | 18/10/1989 | 6.9 | SGI360 | 0.06 | 30.6 | Reverse/ Oblique |
| 10 | Loma Prieta-3 | 18/10/1989 | 6.9 | MCH000 | 0.073 | 44.8 | Reverse/ Oblique |
| 11 | Loma Prieta-4 | 18/10/1989 | 6.9 | PTB297 | 0.072 | 78.3 | Reverse/ Oblique |
| 12 | Lytle Creek | 12/09/1970 | 5.9 | CSM095 | 0.071 | 88.6 | Reverse/ Oblique |
| 13 | N. Palm Springs-1 | 08/07/1986 | 6.0 | AZF225 | 0.099 | 20.6 | Reverse/ Oblique |
| 14 | N. Palm Springs-2 | 08/07/1986 | 6.0 | ARM360 | 0.129 | 46.7 | Reverse/ Oblique |
| 15 | N. Palm Springs-3 | 08/07/1986 | 6.0 | H02090 | 0.093 | 45.6 | Reverse/ Oblique |
| 16 | N. Palm Springs-4 | 08/07/1986 | 6.0 | CFRUP |  | 27 | Reverse/ Oblique |
| 17 | Whittier Narrows | 01/10/1987 | 5.3 | MTW000 | 0.123 | 20.4 | Reverse/ Oblique |
| 18 | Anza (Horse Cany)-2 | 25/02/1980 | 4.9 | PTF135 | 0.131 | 13 | Lateral Strike |
| 19 | Anza (Horse Cany)-3 | 25/02/1980 | 4.9 | TVY135 | 0.081 | 5.8 | Lateral Strike |
| 20 | Anza (Horse Cany)-4 | 25/02/1980 | 4.9 | BAR225 |  |  | Lateral Strike |

**Table 3.3:** Selected ground motion records for soil class B.

| ID | Earthquake | Date | Magnitude ($M_w$) | Record | PGA (g) | Distance (km) | Type |
|---|---|---|---|---|---|---|---|
| 1 | Parkfield | 28/06/1966 | 5.6 | C12320 | 0.0633 | 14.7 | Lateral Strike |
| 2 | Morgan Hill-1 | 24/04/1984 | 6.2 | GIL067 | 0.1144 | 16.2 | Lateral Strike |
| 3 | Kocaeli-1 | 17/08/1999 | 7.4 | ARC000 | 0.2188 | 17 | Lateral Strike |
| 4 | Morgan Hill-2 | 24/04/1984 | 6.2 | G06090 | 0.2920 | 11.8 | Lateral Strike |
| 5 | Coyote Lake | 06/08/1979 | 5.8 | G06230 | 0.4339 | 3.1 | Lateral Strike |
| 6 | Northridge-1 | 17/01/1994 | 6.7 | ORR090 | 0.5683 | 22.6 | Reverse/ Oblique |
| 7 | Loma Prieta | 18/10/1989 | 7.1 | CLS000 | 0.6437 | 5.1 | Reverse/ Oblique |
| 8 | Kobe | 16/01/1995 | 6.9 | KJM000 | 0.8213 | 6.9 | Lateral Strike |
| 9 | Santa Barbara | 13/08/1978 | 7.2 | SBA222 | 0.203 | 14.0 | Reverse/ Oblique |
| 10 | Livemor | 27/01/1980 | 7.4 | LMO355 | 0.252 | 8.0 | Lateral Strike |
| 11 | N. Palm Springs-1 | 08/07/1986 | 6.0 | CAB180 | | | Reverse/ Oblique |
| 12 | N. Palm Springs-2 | 08/07/1986 | 6.0 | FVR045 | 0.129 | 13.0 | Reverse/ Oblique |
| 13 | Northridge | 17/01/1994 | 6.7 | TPF000 | 0.364 | 37.9 | Reverse/ Oblique |
| 14 | San Fernando | 02/09/1971 | 6.6 | ORR021 | 0.324 | 24.9 | Reverse/ Oblique |
| 15 | Whitter Narrows | 10/01/1987 | 6.0 | ALH180 | 0.333 | 13.2 | Reverse/ Oblique |
| 16 | Kocaeli-2 | 17/08/1999 | 7.4 | SKR090 | 0.376 | 3.1 | Lateral Strike |
| 17 | Victoria, Mexica | 09/06/1980 | 6.1 | CPE045 | 0.62 | 34.8 | Lateral Strike |
| 18 | Anza (Horse Cany)-1 | 25/02/1980 | 4.9 | BAR225 | 0.047 | 40.6 | Lateral Strike |
| 19 | Anza (Horse Cany)-2 | 25/02/1980 | 4.9 | RDA045 | 0.097 | 19.6 | Lateral Strike |
| 20 | Borrego Mtn | 09/04/1968 | 6.8 | PAS270 | 0.090 | 203.0 | Lateral Strike |

**Table 3.4 :** Selected ground motion records for soil class C.

| ID | Earthquake | Date | Magnitude ($M_w$) | Record | PGA (g) | Distance (km) | Type |
|---|---|---|---|---|---|---|---|
| 1 | Borrego Mtn-1 | 09/04/1968 | 6.8 | A-ELC180 | 0.13 | 46.0 | Lateral Strike |
| 2 | Borrego Mtn-2 | 09/04/1968 | 6.8 | A-PEL090 | 0.012 | 217.4 | Lateral Strike |
| 3 | Borrego Mtn-3 | 09/04/1968 | 6.8 | A-TLI249 | 0.01 | 195.0 | Lateral Strike |
| 4 | Coyote Lake-1 | 06/08/1979 | 5.7 | G02140 | 0.339 | 7.5 | Lateral Strike |
| 5 | Coyote Lake-2 | 06/08/1979 | 5.7 | G03050 | 0.272 | 6.0 | Lateral Strike |
| 6 | Coyote Lake-3 | 06/08/1979 | 5.7 | G04270 | 0.248 | 4.5 | Lateral Strike |
| 7 | Coyote Lake-4 | 06/08/1979 | 5.7 | HVR150 | 0.039 | 31.2 | Lateral Strike |
| 8 | Imperial Valley-1 | 15/10/1979 | 7.0 | I-ELC180 | 0.313 | 8.3 | Lateral Strike |
| 9 | Imperial Valley-2 | 15/10/1979 | 7.0 | H-AEP045 | 0.327 | 8.5 | Lateral Strike |
| 10 | Imperial Valley-3 | 15/10/1979 | 7.0 | H-BCR230 | 0.775 | 2.5 | Lateral Strike |
| 11 | Imperial Valley-4 | 15/10/1979 | 6.5 | H-BRA315 | 0.220 | 8.5 | Lateral Strike |
| 12 | Imperial Valley-5 | 15/10/1979 | 6.5 | H-CX0225 | 0.275 | 10.6 | Lateral Strike |
| 13 | Hollister | 28/11/1974 | 5.2 | A-HCH271 | 0.177 | 10.0 | Lateral Strike |
| 14 | Cape Mendocino | 25/04/1992 | 7.1 | PET090 | 0.662 | 9.5 | Reverse/ Oblique |
| 15 | Coalinga-1 | 02/05/1983 | 6.4 | H-C05270 | 0.147 | 47.3 | Reverse/ Oblique |
| 16 | Coalinga-2 | 02/05/1983 | 6.4 | H-C08000 | 0.098 | 50.7 | Reverse/ Oblique |
| 17 | Kern County-1 | 21/07/1952 | 7.4 | HOL180 | 0.057 | 120.5 | Reverse/ Oblique |
| 18 | Kern County-2 | 21/07/1952 | 7.4 | PEL180 | 0.058 | 120.5 | Reverse/ Oblique |
| 19 | Loma Prieta-1 | 18/10/1989 | 6.9 | HCH090 | 0.247 | 28.2 | Reverse/ Oblique |
| 20 | Loma Prieta-2 | 18/10/1989 | 6.9 | G02000 | 0.367 | 12.7 | Reverse/ Oblique |

### 3.3 Modal Updating

To obtain consistent results during seismic performance evaluation, appropriateness of finite element model should be checked Since initial model of structure does not take into account of variability of material properties and time-dependent stiffness changes, differences might be observed between analytical model and real structure. To reduce those alterations, finite element model of the bridge must be calibrated (Banerjee and Shinozuka, 2008).

In model updating procedure, it is aimed to obtain matching frequencies and mode shapes with both analytical and experimental results. It can be characterized as a modification of current analytical model considering measured field vibration test. Frequency analysis of calibrated finite element model should be conducted and close agreement should be obtained from dynamic site investigation results. After calibration process, the updated final model is expected to represent the dynamic behavior of the structure more accurately, Thus, it can be used with confidence for further investigation process.Therefore, modal updating procedures are established which intend to enhance the original finite element model by utilizing modal field test results (Jung, 1992).

To perform model calibration, a parametric study was first executed and the sensitive parameters which effect structural dynamic characteristics were determined. According to the results, bearing spring stiffness in longitudinal, lateral and vertical directions are found as the most sensitive parameters to have effect on modal characteristics (Caglayan et al., 2012). In this matter, they were selected as primary calibration parameters in this study. The finite element model calibration was carried out by adjusting those selected parameters until reasonable matches in the natural frequencies and modal shapes were observed. Only the most structurally significant modes and frequencies are used in the model calibration process until obtaining high level of confidence (Caglayan et al., 2012).

### 3.4 Fragility Curve Development Methodology

In general perspective, fragility of a structure is defined as the probability of exceeding certain damage levels which were specified for structures under various ground motions. Therefore, vulnerability of a structure could be evaluated by fragility curves. These curves demonstrate the probability of structural damage as a function of

intensity measures such as ground motion indices (IM) or various design parameters. Intensity measure of the probabilistic expressions can be selected as a single measure of the intensity of a seismic event. Mathematically, fragility curves are expressed as:

$$P[D > C|IM]$$

In this study, while fragility curves are developing, the methodology which is presented by Kirçil and Polat (2006) is adopted. According to that study, fragility curves are constructed in terms of obtained direct displacements from nonlinear time history analysis. Assumption is made while generating the fragility curves in the form of two-parameter lognormal distribution functions. Based on this assumption, the cumulative probability of the occurrence of damage equal to or greater than damage level D is expressed as:

$$P[D > C|IM] = \Phi\left(\frac{ln\,X-\lambda}{\zeta}\right) \quad (1)$$

where $\Phi$ is the standard normal distribution, $X$ is the lognormal distributed response displacement; $\lambda$ and $\zeta$ are the mean and standard deviation of $ln\ X$, respectively. Determination the mean and standard deviation are performed according to plot of $ln\ X$ versus the interrelated standard normal variable on a lognormal scale and to execute a linear regression analysis (Gündüz,1996). The relationship between the standard normal variable and the mean and standard deviation of $ln\ X$ can be expressed as follows:

$$s = \frac{\ln X-\lambda}{\zeta} \quad (2)$$

where $s$ is the standard normal variable.

# 4. CASE STUDIES

Three case studies are conducted in the content of this thesis to conduct fragility assessment of steel truss railway bridges in Turkey. These case studies are selected to represent truss bridge inventory of railways in Turkey as two multispan continuous truss bridges which are Karaçam and Cambazkaya Railway Bridges and one single span truss bridge which is Ceyhan Railway Bridge. Finite element models of selected case study bridges are generated through finite element software SAP2000 (CSI, 2015). During modeling phase, directions of X, Y and Z are fixed to corresponding longitudinal, transversal and vertical directions, respectively.

## 4.1 Case Study 1: Karaçam Bridge

### 4.1.1 General

In the present study, Karaçam Railway Bridge, a multispan continuous steel truss bridge having three equal spans with each length of 51.50 m, is selected as first case study. This bridge is located in Istanbul – Ankara main railway connection, 142 km east of Istanbul. The bridge was designed and built by US-Steel in 1946 to cross Sakarya River, and total length of bridge is 154.50 m. Height and width of truss are 7.35 m and 4.90 m, respectively. Additionally, angle of skewness of bridge with respect to railway axis is 33.47$^{o}$ (Uzgider, 1996a). General view of Karaçam Railway Bridge is given in Figure 4.1.

As it was mentioned in Uzgider et al. (1996a), the bottom chord members, diagonals, and truss hangers were designed and constructed of wide flange American hot rolled I-sections. Stringers and floor beams were 762 mm and 927 mm deep American hot-rolled I-sections, respectively. The skew floor beams located only over abutments and piers were 630 mm deep built-up I sections. The bottom lateral bracings were American hot rolled T-type sections. The diagonal members of the top lateral bracing system consisted of sections with angles and double angles.

**Figure 4.1 :** General view of Karaçam Railway Bridge.

### 4.1.2 Experimental results

Experimental modal parameters such as modal frequencies and related mode shapes are taken from Uzgider et al. (1996a). In that study, test train, provided by Turkish State Railways Administration (TCDD), was used as the excitation mechanism for the bridge, and it was passed six times over the bridge to record the acceleration response. Measurements were conducted with bi-axial accelerometers and a 16-channel data acquisition system. Hence, as given in Figure 4.2, first three modes of bridge were identified as 2.4400 Hz, 5.0781 Hz, and 6.3477 Hz in torsional and flexural directions, respectively.

### 4.1.3 Analytical results

#### 4.1.3.1 Original bridge model

Original bridge model of Cambazkaya Railway Bridge is generated based on original design drawings that provided by TCDD, and modal analysis is carried out to obtain mode shapes and corresponding frequencies as seen in Figure 4.3. According to original analytical model, frequencies of first three modes of bridge are calculated as 2.0582 Hz, 4.9413 Hz, and 7.0673 Hz in torsional and flexural directions, respectively.

#### 4.1.3.2 Fragility curves of original bridge model

Fragility curves of original Karaçam Railway Bridge model are generated based on methodology described in Chapter 3, and they are presented in Figure A.1 to Figure A.4. According to those fragility curves of original bridge model, following results are concluded:

- The failure rate for 5 mm displacement in X direction of span 1 is 60% for soil class A; 30% for soil classes B and C; 40% for fragility curve that involves three soil classes A-B-C. Span 2 introduces 85% for soil class A; 50% for soil class B; 40% for soil class C; 55% for fragility curve that involves three soil classes A-B-C. Additionally, Span 3 introduces 85% for soil class A; 60% for soil class B; 55% for soil class C; 65% for fragility curve that involves three soil classes A-B-C.

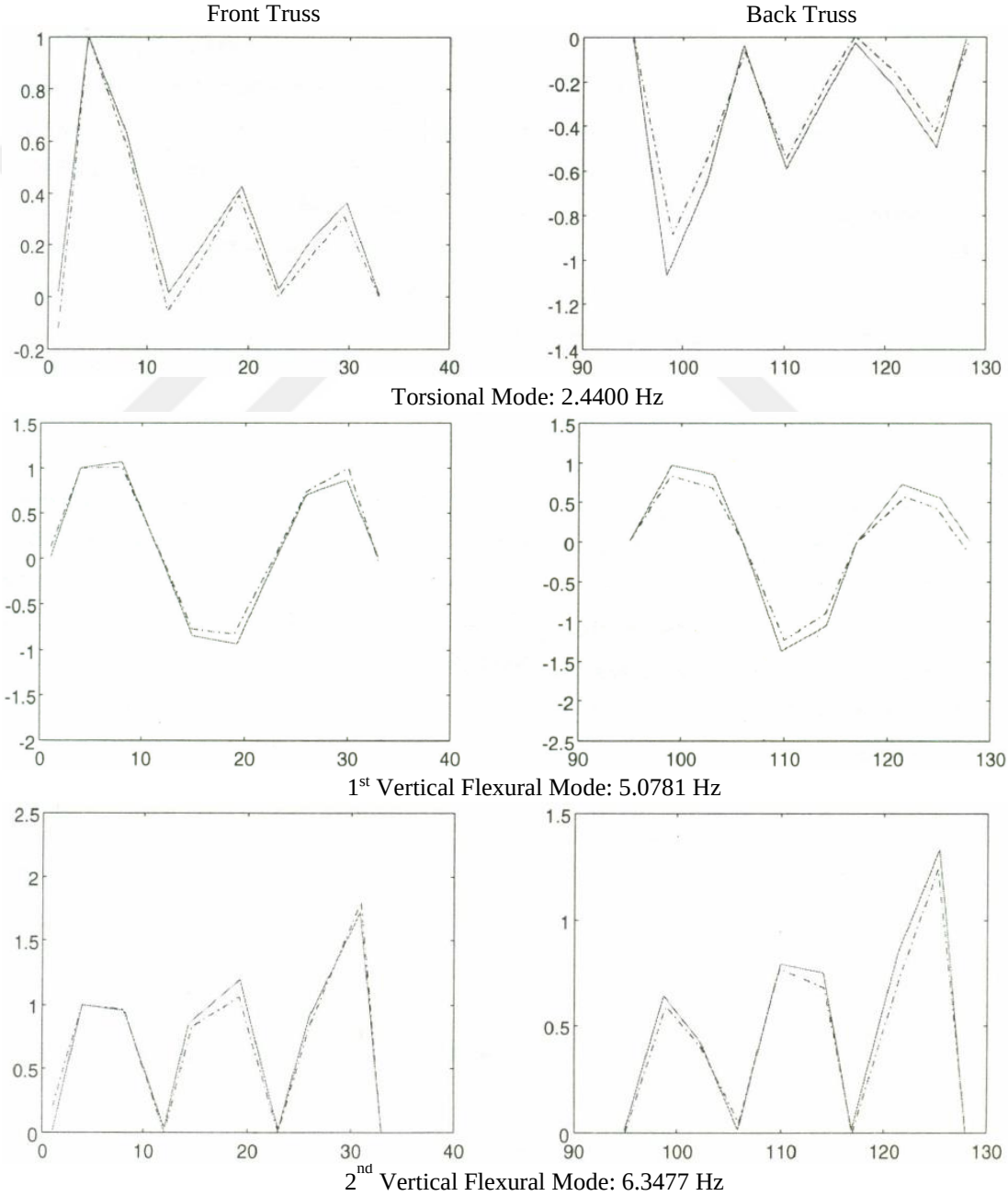


**Figure 4.2 :** Experimental mode shapes and corresponding frequencies of Karaçam Railway Bridge (Uzgider et al., 1996a).

- The failure rate for 10 cm displacement in Y direction is 80% for soil class A; 35% for soil classes B and C; 45% for fragility curve that involves three soil classes A-B-C. However, span 2 introduces 5% higher results than span 1 and span 2.
- The failure rate for 2 cm displacement in Z direction of span 1 is 90% for soil class A; 55% for soil classes B; 65% for soil class C; 70% for fragility curve that involves three soil classes A-B-C. Span 2 introduces 85% for soil class A; 45% for soil classes B and C; 55% fragility curve that involves three soil classes A-B-C. Additionally, span 3 introduces 5% lower results than span 2.

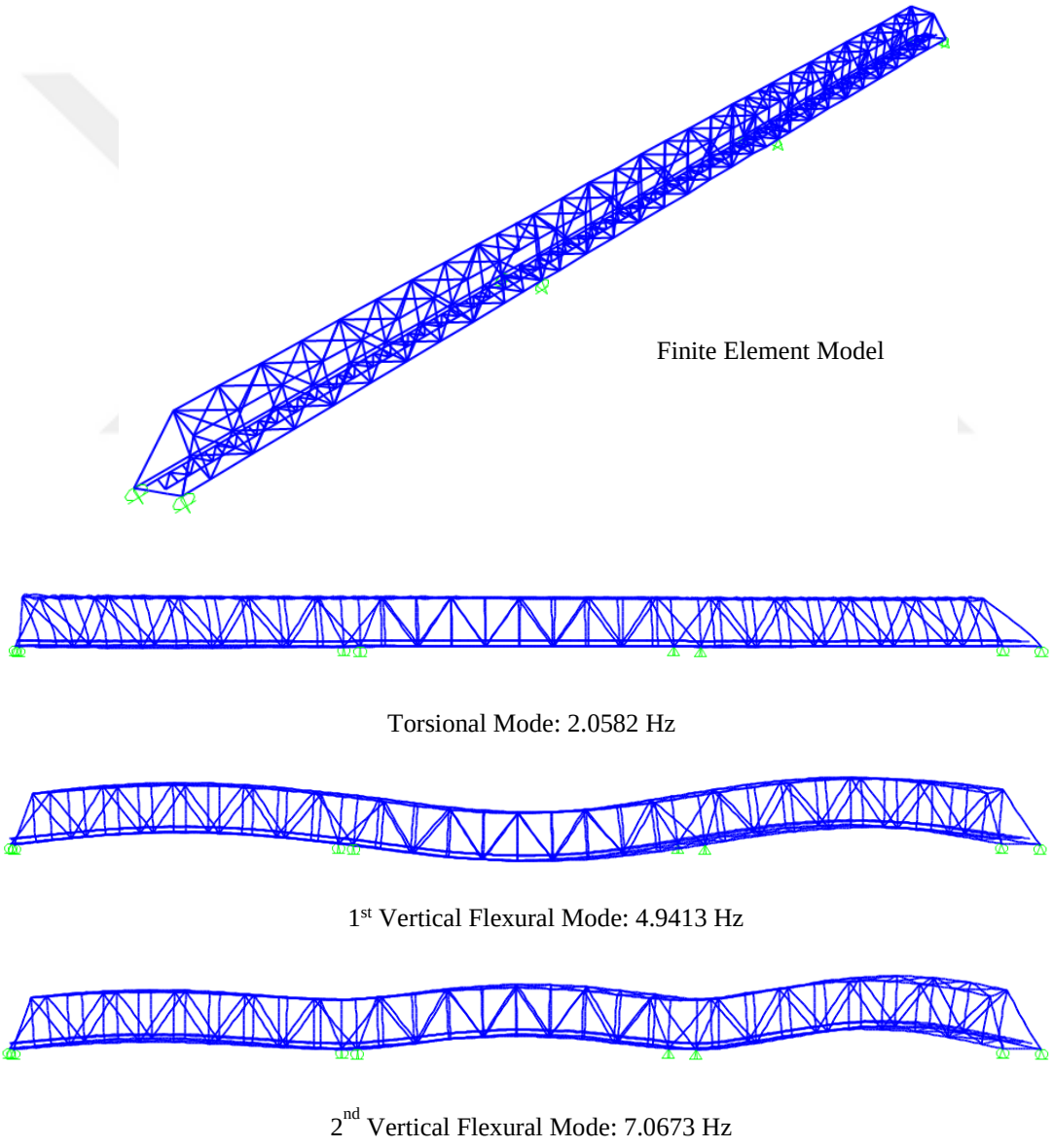


**Figure 4.3 :** Analytical frequencies of original Karaçam bridge model.

#### 4.1.3.3 Modal updating of bridge model

To quantify the performance of the bridge, the finite element model of the bridge must be calibrated. Hence, the analytical results become consistent with the experimental results (Banerjee and Shinozuka, 2008). Moreover, in the model updating procedure, it is aimed to obtain the matching frequencies and mode shapes with both analytical and experimental results.

In this study, when comparison was done between finite element model and identified site investigation results, approximately 15% difference is observed. That kind of difference might occur due to variability of material properties and time-dependent stiffness changes. Thus, finite element model should be updated based on site investigation results, and modal parameters of that model after calibration, which is further referred as updated model of Karaçam Railway Bridge should be calculated.

The updated modal parameters of bridge are given in Figure 4.4. Frequencies of first three modes of bridge are calculated as 2.4509 Hz, 5.0255 Hz, and 6.4008 Hz in torsional and flexural directions, respectively after calibration.

Frequency analysis of the calibrated finite element model revealed a close agreement with dynamic site investigation results. The comparative results before and after model updating process and differences between them are given in Table 4.1. With modal updating procedure, the maximum difference is observed to reduced to under 1%.

**Table 4.1 :** Analytical and experimental frequencies before and after model calibration of Karacam Railway Bridge.

| Mode | Analytical frequencies (Hz) | | Experimental frequencies (Hz) | Error percentage (%) | |
|---|---|---|---|---|---|
| | Before calibration | After calibration | | Before calibration | After calibration |
| Torsional mode | 2.0582 | 2.4509 | 2.4400 | 15.7 | 0.4 |
| 1st vertical mode | 4.9413 | 5.0255 | 5.0781 | 2.7 | 1.0 |
| 2nd vertical mode | 7.0673 | 6.4008 | 6.3477 | 11.3 | 0.8 |

#### 4.1.3.4 Fragility curves of updated bridge model

Fragility curves of updated Karaçam Railway Bridge model are presented in Figure A.5 to Figure A.8. According to those fragility curves of updated bridge model, following results are concluded:

- The failure rate for 5 mm displacement in X direction is 100% for soil class A and 80% for soil classes B and C; 90% for fragility curve that involves three soil classes A-B-C for span 1 and span 3. Additionally, span 2 introduces 5% lower results only for soil classes B and C.

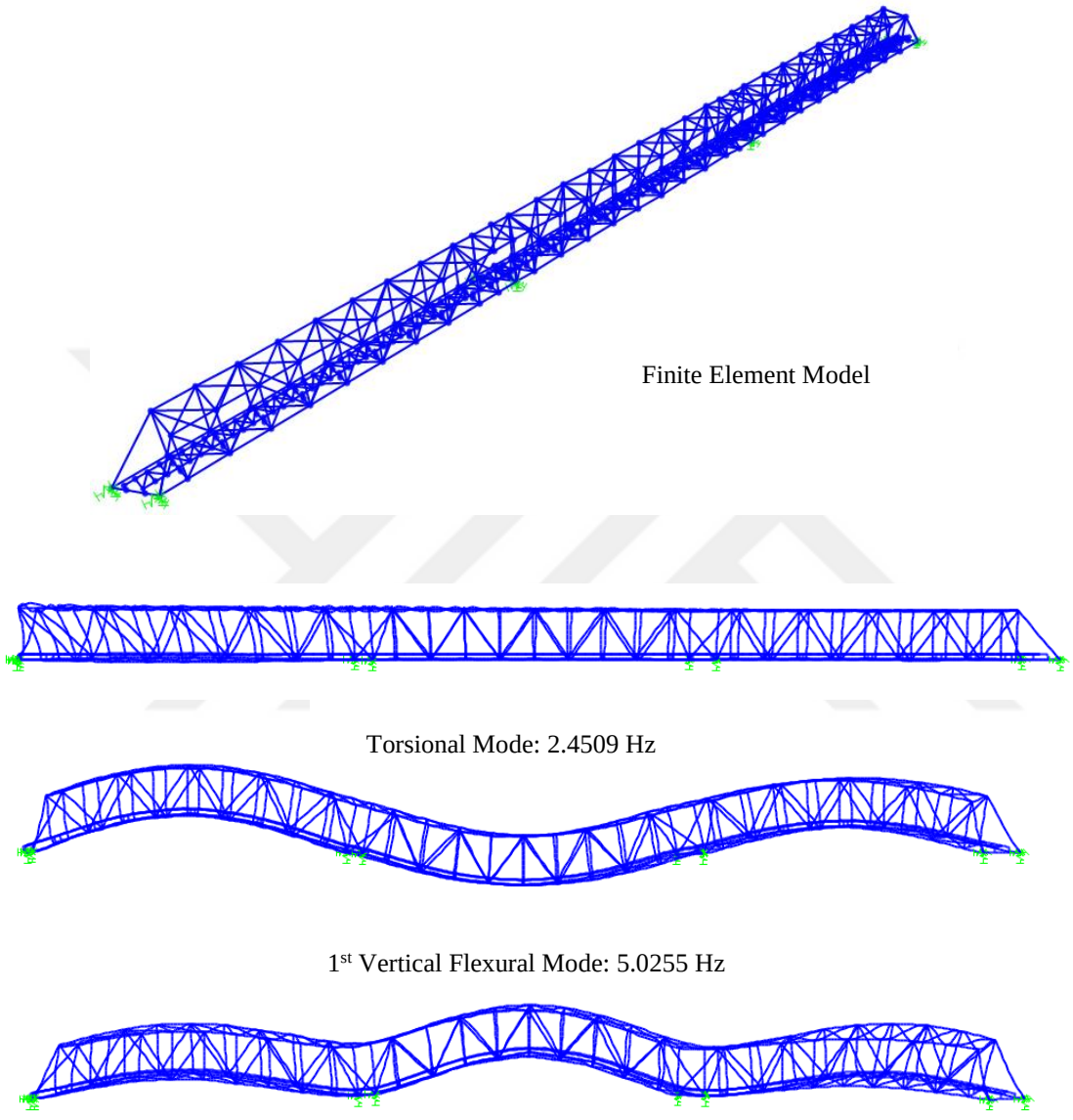


**Figure 4.4 :** Analytical frequencies of updated Karaçam bridge model.

- The failure rate for 10 cm displacement in Y direction of span 1 is 100% for soil class A; 80% for soil class B; 70% for soil class C; 85% for fragility curve that involves three soil classes A-B-C. However, span 2 and span 3 introduce 90% for soil class A; 15% for soil class B and C; 25% for fragility curve that involves three soil classes A-B-C.

- The failure rate for 2 cm displacement in Z direction of span 1 and span 3 is 100% for soil class A; 70% for soil class B; 80% for soil class C; 90% for fragility curve that involves three soil classes A-B-C. However, span 2 introduces 15% lower results.

#### 4.1.3.5 Comparison of fragility curves

Comparison fragility curves of Karaçam Railway Bridge model are presented in Figure A.9 to Figure A.12. According to those comparison curves that involve three soil classes A-B-C, probability of failures of original and updated models are changing as follows:

- For displacement of 5 mm in X direction of all spans, the probability of failure of updated model is observed 2 times higher in average for all soil classes except A.
- For displacement of 10 cm in Y direction of span 1, the probability of failure of updated model is observed 2 times higher in average for all soil classes except A. However, the decrease in half is observed for span 2 and span 3 for all soil classes except A.
- For displacement of 2 cm in Z direction of all spans, approximately 20% increase in probability of failure of updated model is observed for all soil classes.

Hence, it is revealed that the most critical part is span 1 in Karaçam Railway Bridge. Any failure in this span leads to failure of whole bridge. Additionally, in general, span 2 and span 3 revealed lower results than span 1.

## 4.2 Case Study 2: Cambazkaya Bridge

### 4.2.1 General

As a second case study, Cambazkaya Railway Bridge, a multispan continuous steel railway bridge having two equal spans with each length of 51.90 m, is selected and analyzed. This bridge is located in Istanbul – Ankara main railway connection, 188 km east of Istanbul. The bridge was designed and constructed by Fried and Krupp A. G. & Friedrich-Alfred-Hütte Rheinhausen in 1933 to cross Sakarya River, and total length of bridge is 103.80 m. Height and width of truss are 6.80 m and 4.90 m,

respectively. Additionally, angle of skewness of bridge with respect to railway axis is 25.53º (Uzgider, 1996b). General view of Cambazkaya Railway Bridge is given in Figure 4.5.

**Figure 4.5 :** General view of Cambazkaya Railway Bridge.

As it was mentioned in Uzgider et al. (1996b), the bottom and top chord members were constructed of built-up channels. End posts and truss diagonals consisted of hot-rolled and built up I-section and channels. The decking system consisted of floor beams which were 700 mm deep hot-rolled I-sections with exception of skew floor beam having built-up I-section; stringers which were constructed of 450 mm deep built-up I sections; bottom lateral bracings which were composed of double angles. Also, the diagonals of the top lateral cross bracing system consisted of double angles.

### 4.2.2 Experimental results

According to field studies that conducted by Uzgider et. Al. (1996b), frequencies of first three modes of bridge were identified as 8.8379 Hz, 4.8828 Hz, and 5.6641 Hz in torsional and flexural directions, respectively, as given in Figure 4.6.

### 4.2.3 Analytical results

#### 4.2.3.1 Original bridge model

Original bridge model of Cambazkaya Railway Bridge is generated based on original design drawings, and modal analysis is carried out to obtain mode shapes and corresponding frequencies as seen in Figure 4.7. According to original analytical model, frequencies of first three modes of bridge are calculated as 7.3973 Hz, 4.6064 Hz, and 6.1676 Hz in torsional and flexural directions, respectively.

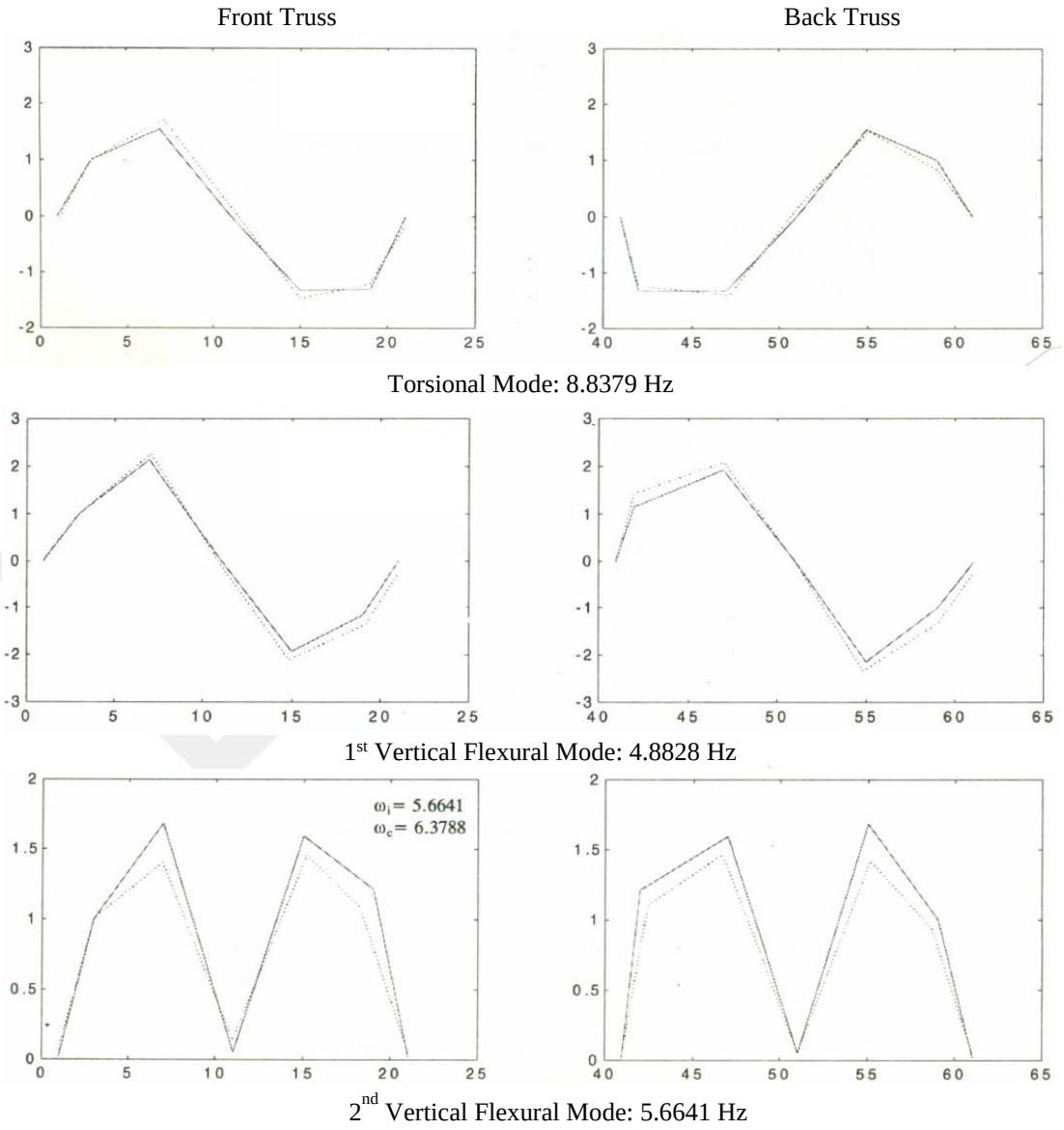


**Figure 4.6 :** Experimental mode shapes and corresponding frequencies of Cambazkaya Railway Bridge (Uzgider et al., 1996b).

### 4.2.3.2 Fragility curves of original bridge model

Fragility curves of original Cambazkaya Railway Bridge model are presented in Figure B.1 to Figure B.4. According to those curves of original bridge model, following results are concluded:

- The failure rate for 1 mm displacement in X direction of span 1 is 100% for soil class A, and 90% for other soil classes. For span 2, approximately 1% to 5% lesser results are observed in comparison to span 1.

- The failure rate for 4 cm displacement in Y direction, 90% and 80% for span 1 and span 2 respectively for soil class A; 25% for other soil classes for both spans.
- The failure rate for 1 cm displacement in Z direction of span 1, 100% for soil class A; 40% for soil class B and C; 50% for fragility curve that involves three soil classes A-B-C for span 1. However, in these curves, span 2 reveals 10% lower results than span 1.

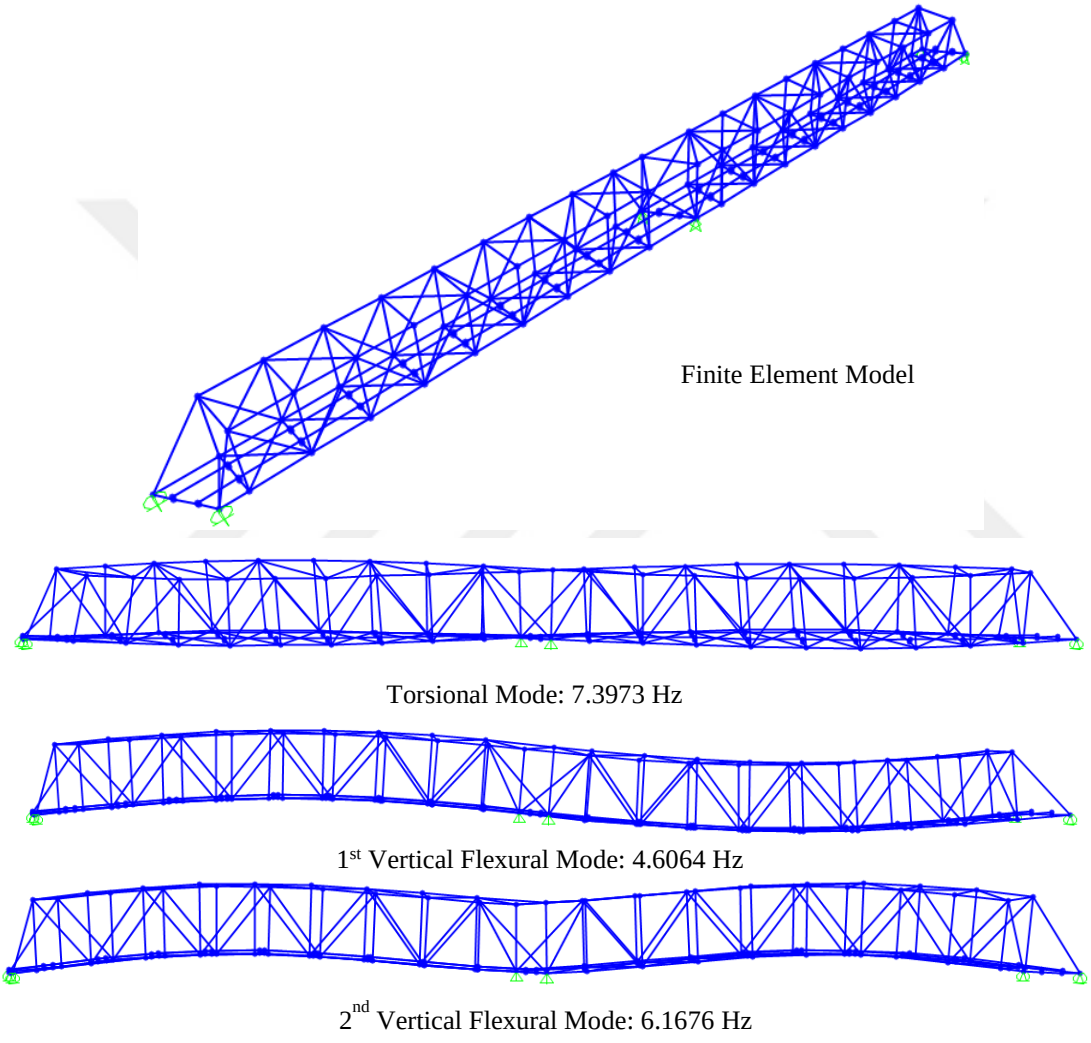


**Figure 4.7 :** Analytical frequencies of original Cambazkaya bridge model.

### 4.2.3.3 Modal updating of bridge model

For Cambazkaya Railway Bridge, approximately 15% difference between experimental and analytical model is observed alike previous case study. Therefore, modal updating procedure is applied. Thus, modal parameters after calibration of finite

element model of Cambazkaya Railway Bridge are calculated one more time, and related modal parameters are given in Figure 4.8.

Frequencies of first three modes of bridge after calibration are calculated as 8.7894 Hz, 4.8660 Hz, and 5.6375 Hz in torsional and flexural directions, respectively. With that updating procedure, the maximum difference is observed to reduced to under 1% which can be accepted as a close agreement with dynamic site investigation results. All frequencies and differences between analytical and experimental modes are given in Table 4.2 in comparison with before and after model updating process.

**Table 4.2 :** Analytical and experimental frequencies before and after model calibration of Cambazkaya Railway Bridge.

| Mode | Analytical frequencies (Hz) | | Experimental frequencies (Hz) | Error percentage (%) | |
|---|---|---|---|---|---|
| | Before calibration | After calibration | | Before calibration | After calibration |
| Torsional mode | 7.3973 | 8.7894 | 8.8379 | 16.3 | 0.5 |
| 1st vertical mode | 4.6064 | 4.8660 | 4.8828 | 5.7 | 0.3 |
| 2nd vertical mode | 6.1676 | 5.6375 | 5.6641 | 8.9 | 0.5 |

#### 4.2.3.4 Fragility curves of updated bridge model

Fragility curves of updated Cambazkaya Railway Bridge bridge model are presented in Figure B.5 to Figure B.8. According to those curves of updated bridge model, following results are concluded:

- The failure rate for 1 mm displacement in X direction is 100% for soil class A; 90% for soil classes B and C; 100% for fragility curve that involves three soil classes A-B-C.
- The failure rate for 4 cm displacement in Y direction, 100% for soil class A; 80% for soil class B; 85% for soil class C; 95% for fragility curve that involves three soil classes A-B-C for both spans.
- The failure rate for 1 cm displacement in Z direction, 100% for soil class A; 90% for soil class B; 100% for soil class C and fragility curve that involves three soil classes A-B-C for span 1. However, only for soil classes B and C, span 2 reveals 10% lower results than span 1.

#### 4.2.3.5 Comparison of fragility curves

Comparison fragility curves of Cambazkaya Railway Bridge model are presented in Figure B.9 to Figure B.12. According to those comparison fragility curves that involve three soil classes A-B-C, probability of failures of original and updated models are changing as follows:

- For displacement of 1 mm in X direction, the ratio is increasing from 90% to 100%.
- For displacement of 4 cm in Y direction, the increase in probability of failure of updated model is observed around 3.5 times higher for all soil classes except A.
- For displacement of 1 cm in Z direction, the probability of failure of span 1 and span 2 in original model are 50% and 40% respectively. However, It is observed 100% probability in updated model. Updated model gives 2 times higher results for all soil classes except A.

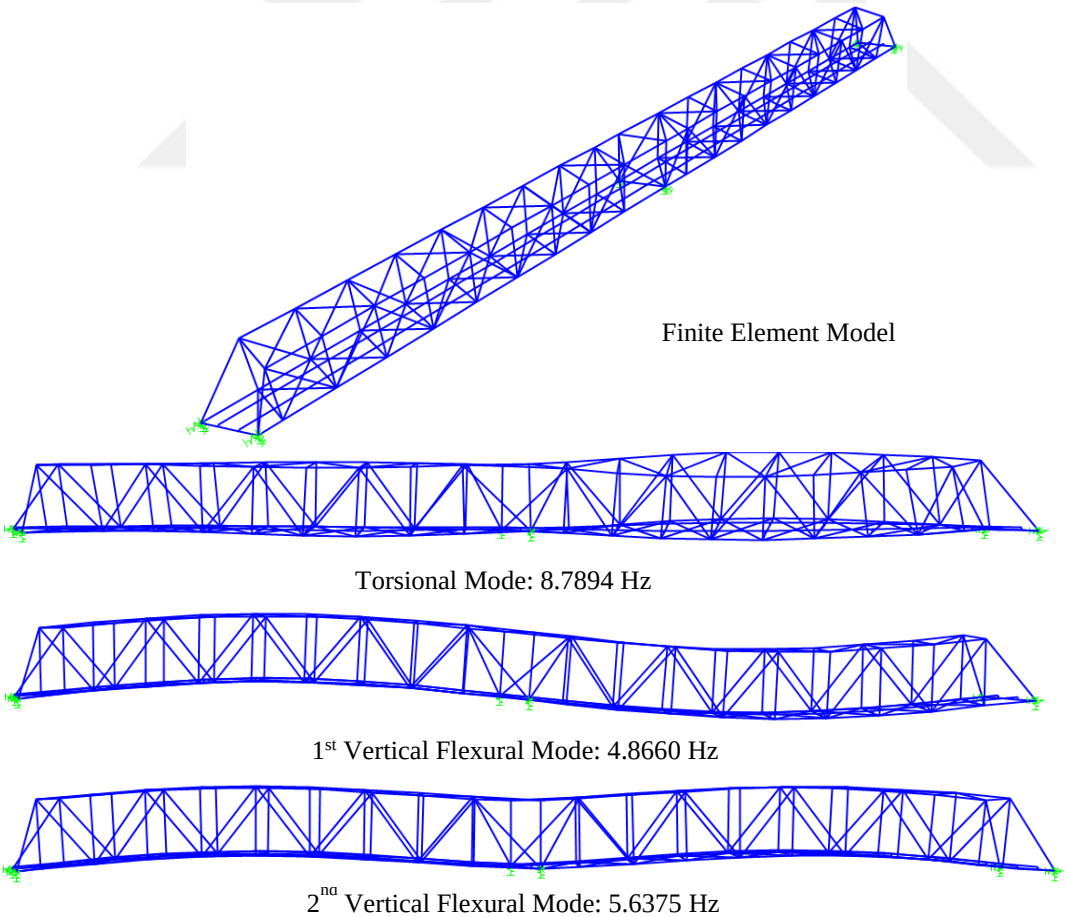


**Figure 4.8 :** Analytical frequencies of updated Cambazkaya bridge model.

Hence, maximum differences between original and updated models are revealed as 10%, 70% and 50% for X, Y, and Z directions respectively. Approximate difference between both spans is determined around 10%.

## 4.3 Case Study 3: Ceyhan Bridge

### 4.3.1 General

Third and final case study in the scope this thesis is conducted through Ceyhan Railway Bridge which is a single span simply supported steel truss railway bridge having span length of 96.00 m. This bridge is located in Konya-Fevzipaşa-Hudut main railway line at Km 371+194. The bridge was designed and constructed in 1912 to cross Ceyhan River. Height and width of truss are 13.50 m and 5.00 m, respectively. General view of Ceyhan Railway Bridge is given in Figure 4.9.

The bottom and top chord, truss diagonal members of bridge consisted of hot rolled and built-up sections. The decking system was constructed of floor beams which were made of 900 mm-deep built-up I-sections, stringers which were made of 550 mm-deep hot-rolled I sections and bottom lateral bracings which were made of angles. The diagonals of the top lateral cross bracing system also consisted of angles.

### 4.3.2 Experimental results

In order to conduct experimental study, test train provided by TCDD was operated to generate excitation on the case study bridge. That train was passed six times over the bridge with speed of 50 km/h. With each pass, the acceleration response of bridge was recorded through single and bi-axial accelerometers. An example bi-axial accelerometer unit and data acquisition system are shown in Figure 4.10 and Figure 4.11, respectively.

Sixteen accelerometers were mounted on bridge in longitudinal, transversal and vertical directions based on previous reports (Uzgider et al., 1996a;1996b) to obtain modal parameters. Test was conducted through two setups since measurements were conducted with a 16-channel data acquisition system. Setup 1 and Setup 2 with locations of accelerometers on bridge sketch are shown in Figure 4.12.

**Figure 4.9 :** General view of Ceyhan Railway Bridge.

**Figure 4.10 :** An example bi-axial accelerometer unit.

**Figure 4.11 :** 16-channel data acquisition system.

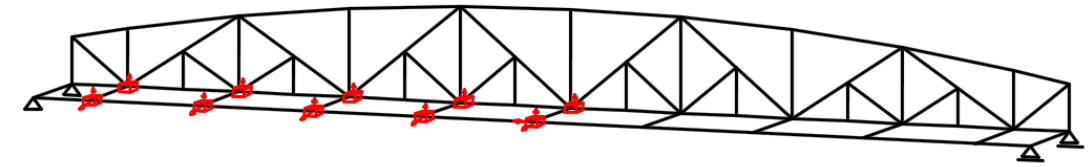

Setup-1

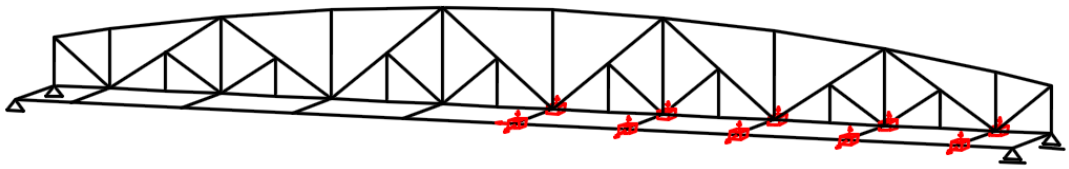

Setup-2

**Figure 4.12 :** Locations of accelerometers on Ceyhan Railway Bridge.

According to field studies, frequencies of first three modes of bridge are identified as 1.343 Hz, 3.113 Hz, and 5.737 Hz in torsional and flexural directions, respectively, as given in Figure 4.13.

### 4.3.3 Analytical results

#### 4.3.3.1 Original bridge model

Original bridge model of Ceyhan Railway Bridge is generated based on original design drawings, and modal analysis is carried out to obtain mode shapes and corresponding frequencies as seen in Figure 4.14. According to original analytical model, frequencies of first three modes of bridge are calculated as 1.4066 Hz, 3.0997 Hz, and 5.3784 Hz in torsional and flexural directions, respectively.

#### 4.3.3.2 Fragility curves of original bridge model

Fragility curves of original Ceyhan Railway Bridge model are presented in Figure C.1 to Figure C.4. Regarding those curves that investigate probability of failure of original bridge model, following results are concluded:

- The failure rate for 1 mm displacement in X direction is 100% for soil class A; 70% for soil classes B and C; 80% for fragility curve that involves three soil classes A-B-C.
- The failure rate for 25 cm displacement in Y direction is 90%, 15%, 10%, 20%, for soil classes A, B, C and A-B-C, respectively.
- The failure rate for 1.5 cm displacement in Z direction is 95% for soil class A and 30% for other soil classes.

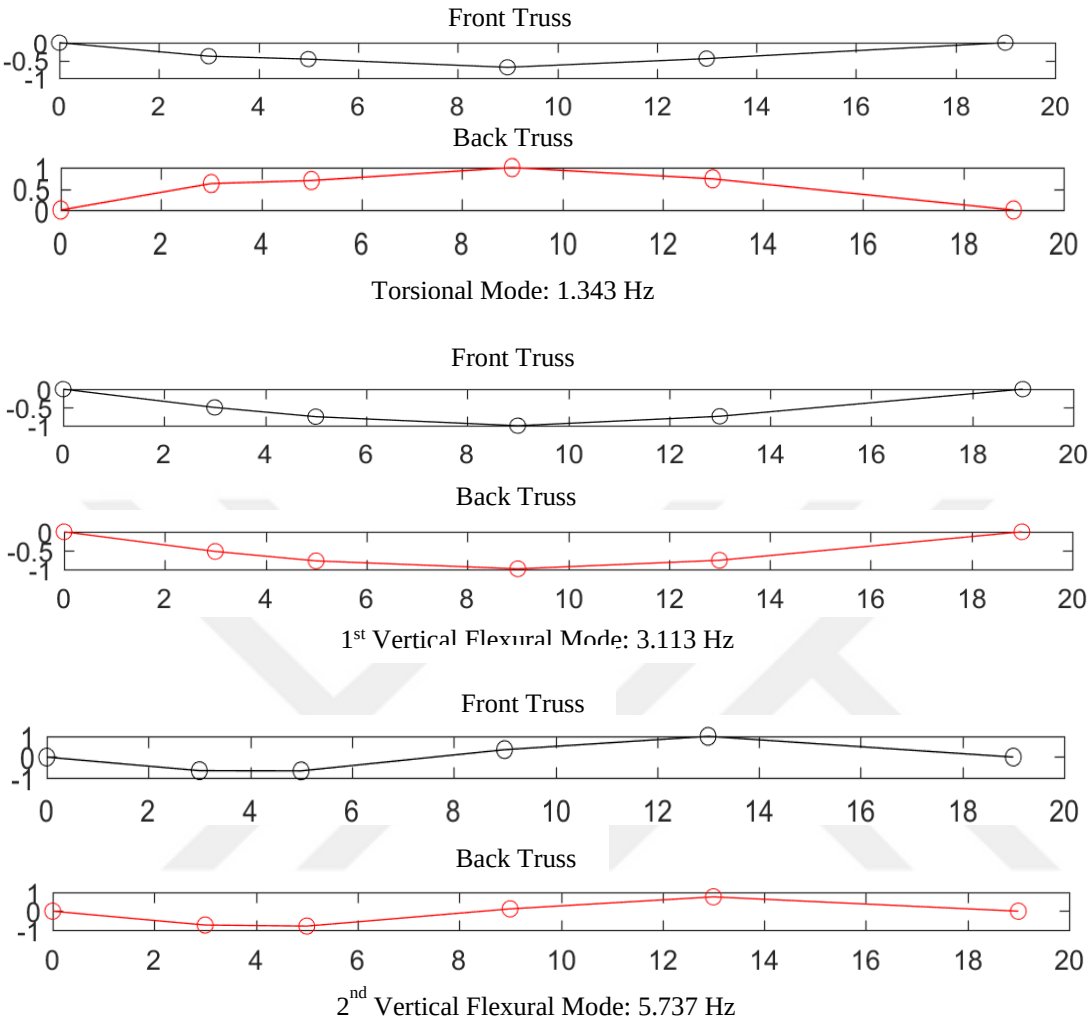


**Figure 4.13 :** Experimental mode shapes and corresponding frequencies of Ceyhan Railway Bridge.

### 4.3.3.3 Modal updating of bridge model

For Ceyhan Railway Bridge, approximately 7% difference between experimental and analytical model is observed. Therefore, modal updating procedure is applied in order to provide matching mode shapes with field investigations. Thus, modal parameters after calibration of finite element model of Ceyhan Railway Bridge are calculated as given in Figure 4.15. Frequencies of first three modes of bridge after calibration are determined as 1.3422 Hz, 3.1102 Hz, and 5.7765 Hz in torsional and flexural directions, respectively. With that updating procedure, the maximum difference is observed to reduced to under 1% which can be accepted as a close agreement with

dynamic site investigation results. All frequencies and differences are given in Table 4.3 in comparison with before and after modal updating process.

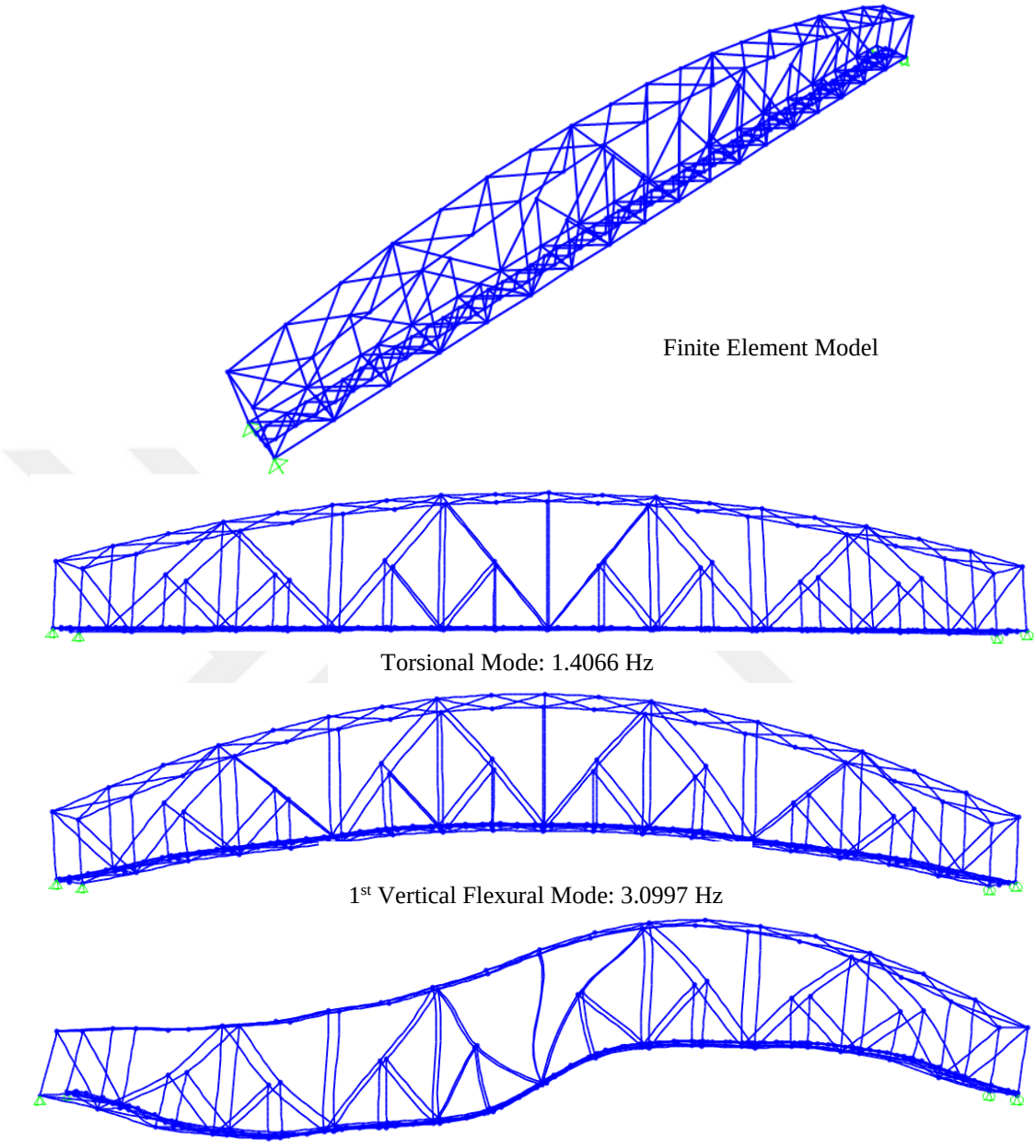


**Figure 4.14 :** Analytical frequencies of the original Ceyhan bridge model.

#### 4.3.3.4 Fragility curves of updated bridge model

Fragility curves of updated Ceyhan Railway Bridge bridge model are presented in Figure C.5 to Figure C.8. Regarding those curves that investigate probability of failure of original bridge model, following results are concluded:

- The failure rate for 1 mm displacement in X direction is 100% for soil class A and 50% for other soil classes.

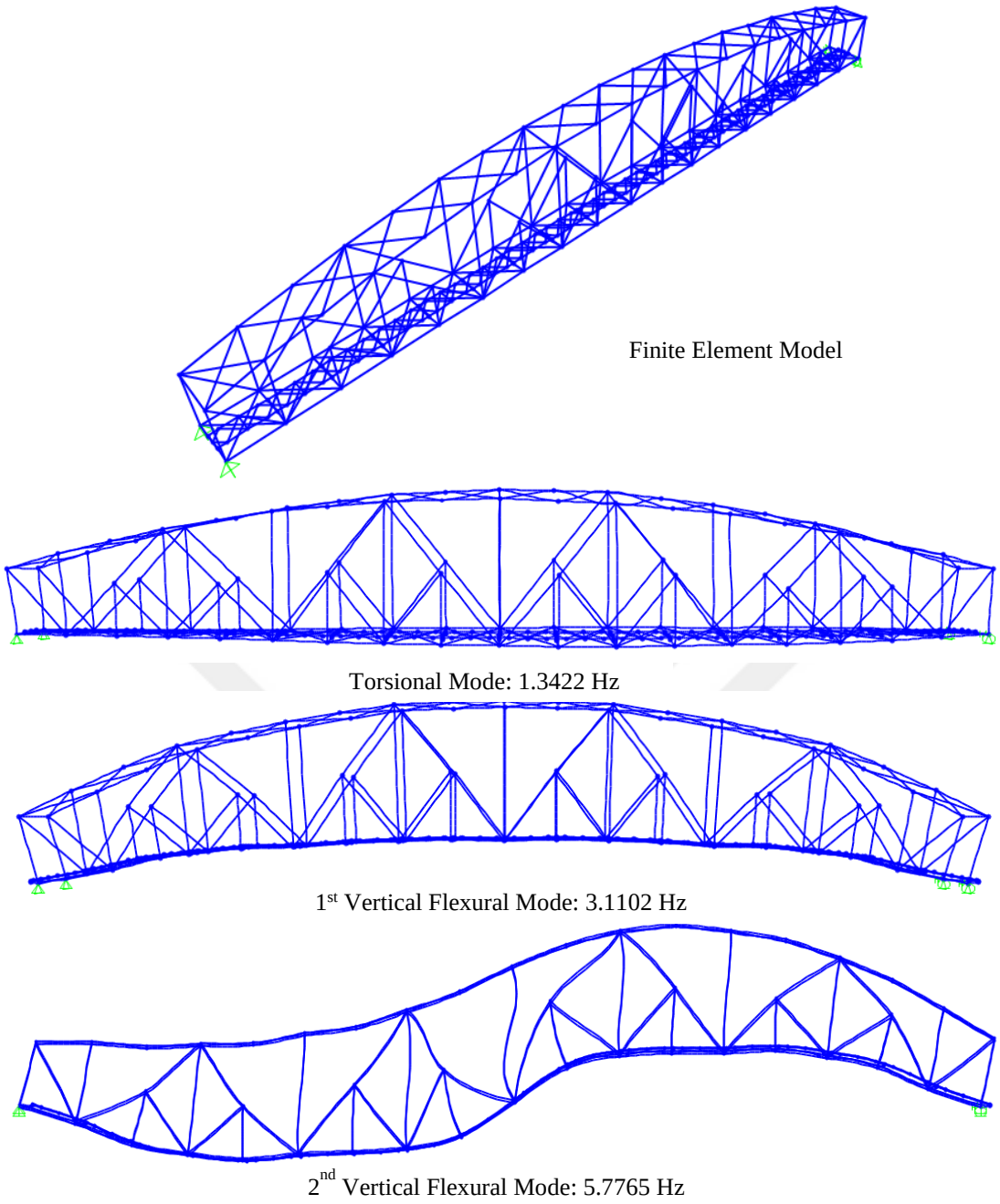


**Figure 4.15 :** Analytical frequencies of updated Ceyhan bridge model.

**Table 4.3 :** Analytical and experimental frequencies before and after model calibration of Ceyhan Railway Bridge.

| Mode | Analytical frequencies (Hz) | | Experimental frequencies (Hz) | Error percentage (%) | |
|---|---|---|---|---|---|
| | Before calibration | After calibration | | Before calibration | After calibration |
| Torsional mode | 1.4066 | 1.3422 | 1.343 | 4.7 | 0.1 |
| 1st vertical mode | 3.0997 | 3.1102 | 3.113 | 0.4 | 0.1 |
| 2nd vertical mode | 5.3784 | 5.7765 | 5.7337 | 6.2 | 0.7 |

- The failure rate for 25 cm displacement in Y direction is 70% for soil class A; 15% for soil classes B and C; 20% for fragility curve that involves three soil classes A-B-C.
- The failure rate for 1.5 cm displacement in Z direction is 80% for soil classes A and 20% for other soil classes.

#### 4.3.3.5 Comparison of fragility curves

Comparison fragility curves of Ceyhan Railway Bridge bridge models are presented in Figure C.9 to Figure C.12. According to those comparison curves that involve three soil classes A-B-C, probability of failures of original and updated models are changing as follows:

- For displacement of 1 mm in X direction, the failure rate is decreasing from 90% to 60%.
- For displacement of 25 cm in Y direction, the ratio is equalized to 20%. However, above that displacement value, the increase in probability of failure is observed around 10%.
- For displacement of 1.5 cm in Z direction, the ratio is decreasing from 30% to 20%. However, above the displacement of 2.5 cm, the tendency of increase in probability of failure is observed around 10% in a similar manner as Y direction.

In conclusion, It is revealed that for single span bridge type, probability of failure of bridge is changing around 10% when original bridge model is updated through field investigations.

# 5. CONCLUSIONS AND RECOMMENDATIONS

In this thesis, 3 different railway bridges, which were constructed at the beginning of 20$^{th}$ century in Turkey, were investigated as case studies under 60 different ground motion records from 3 soil classes. In this regard, original finite element models of selected bridges were generated based on original design drawings. Dynamic analyses were conducted, and modal parameters were determined for each bridge. Concurrently, experimental modal parameters were obtained from field investigation, and they were compared with analytical results. Depending on those experimental results, analytical models were updated by changing boundary conditions of supports. Several different combinations with different spring stiffness were utilized in order to conform field results. Then, nonlinear dynamic analyses were applied on both original and updated bridge models. According to nonlinear dynamic analysis results, fragility curves of each bridge were generated.

The following remarks are gained in the scope of this thesis:

- Differences between modal frequencies of original model and field result were approximately 15% for MSC bridges; approximately 7% for SS bridge.
- With adjusting spring stiffnesses in vertical, transversal and longitudinal directions, error rate was decreased under 1% for all bridges.
- According to fragility curves of Karaçam Railway Bridge which has three continuous spans, it is revealed that span 1 has the most critical results. Therefore, it is concluded that overall evaluation of the bridge might be made by investigating that span.
- According to fragility curves of Cambazkaya Railway Bridge which has two continuous spans, it is observed that both spans revealed similar results. As a consequence, it is concluded that for continuous bridges having two spans, it is enough to conduct evaluation procedure for one single span.
- According to fragility curves of Ceyhan Railway Bridge which has one simply supported span, original and updated models are concluded with similar

probability of failure results. Therefore, it might be concluded that under 5% error rate, updating procedure does not consider as obligatory.

- In all cases for all bridges, it is observed that fragility curve that involves three soil classes A-B-C revealed approximately 10% higher results than individual soil classes. Therefore, instead of using 3 individual soil classes that case might be utilized for overall assessment.

This study aimed a relatively fast and simplistic approach in order to assess current seismic condition of existing railway bridges in Turkey. Further investigations might be made on different railway bridge types such as simply supported and multispan continuous steel girder railway bridges. The effect of bridge types on fragility curves might be analyzed. Another improvement might be made on selected earthquake records. The number of earthquake records might be increased or artificially generated earthquake records might be used.

## REFERENCES


**American Association of State Highway and Transportation Officials** (AASHTO). (1996). Standard specification for highway bridges. 16th Ed., Washington, D.C.

**Applied Technology Council (ATC).** (1985). *Earthquake damage evaluation data for California* (Report No: ATC-13). Redwood City, California.

**Avşar, Ö.** (2009). Fragility based seismic vulnerability assessment of ordinary highway bridges in Turkey. PhD Thesis, Middle East Technical University, Turkey.

**Baker, J.W.** (2013). Trade-offs in ground motion selection techniques for collapse assessment of structures. *Vienna Congress on Recent Advances in Earthquake Engineering and Structural Dynamics 2013 (VEESD, 2013),* Vienna, Austria.

**Banerjee, S., and Shinozuka, M.** (2007). Nonlinear static procedure for seismic vulnerability assessment of bridges. *Comput-Aided Civ Infrastruct Eng,* 22, 293–305.

**Barker, R. M., and Puckett, J. A.** (2013). Bridge Types and Selection. R. M. Barker, & J. A. Puckett içinde, Design of Highway Bridges An LRFD Approach (p. 61-73). New Jersey: John Wiley & Sons, Inc.

**Barker, R. M., and Puckett, J. A.** (2013). Introduction to Bridge Engineering. R. M. Barker, & J. A. Puckett içinde, Design of Highway Bridges An LRFD Approach (p. 1-15). New Jersey: John Wiley & Sons, Inc.

**Basöz, N. I., and Kremidjian, A. S.** (1996). *Risk assessment for highway transportation systems.* (Report No: 118) John A. Blume Earthquake Engineering Center, Civil Engineering Department, Stanford University, Stanford, CA.

**Basöz, N., and Kiremidjian, A.S.** (1997). *Evaluation of bridge damage data from the Loma Prieta and Northridge, CA earthquakes.* (Report No: 127), John A. Blume Earthquake Engineering Center, Stanford, CA.

**Basöz, N. I., Kremidjian, A. S., and King, S. A.** (1999). Statistical analysis of bridge damage data from the 1994 Northridge, CA, Earthquake. *Earthq Spectra, **15**, 1*, 25-54.

**Bertero VV.** (1977). Strength and deformation capacities of buildings under extreme environments. *In Structural Engineering and Structural Mechanics, Pister KS (ed.).* Prentice-Hall: Englewood Cli4s, NJ, 211–215.

**Billah, A. H. M. M., and Alam, M. S.** (2015). Seismic fragility assessment of highway bridges: a state-of-the-art review. *Struct Infrastruct E, **11**, 6*,804-832.

**Caglayan, B. O., Ozakgul, K. and Tezer, O.** (2012). Assessment of a concrete arch bridge using static and dynamic load testing, Structural Engineering and Mechanics, Vol. 41, No. 1, pp. 83-94.

**California Department of Transportation (Caltrans),** (1994a). *The Northridge earthquake.* Caltrans PEQIT Report, Division of Structures, Sacramento, CA.

**California Department of Transportation (Caltrans),** (1994b). *Supplementary bridge damage reports.* Division of Structures, Sacramento, CA.

**Choi, E., Desroches, R., and Nielson, B. G.** (2004). Seismic fragility of typical bridges in moderate seismic zones. *Eng Struct, 26,* 187-199.

**Computers and Structures (CSI)** (2015). CSI Analysis reference manual for SAP2000, ETABS, SAFE and CSiBridge, Berkeley, California, USA.

**Cornell, A. C., Jalayer, F., Hamburger, R. O., Foutch, D. A.** (2002). Probabilistic basis for 2000 SAC Federal Emergency Management Agency steel moment frame guidelines, J. *Struct. Eng., **128***, 526–532.

**Çavdar, Ö., and Bayraktar, A.** (2014). Pushover and nonlinear time history analysis evaluation of a RC building collapsed during the Van (Turkey) earthquake on October 23, 2011. *Nat Hazard, **70**, 1*, 657-673.

**Dufour, F. O.** (1909). Bridge Engineering: Roof Trusses; a Manual of Practical Instruction in the Calculation and Design of Steel Truss and Girder Bridges for Railroads and Highways. Chicago: American School of Correspondence.

**Dutta, A., and Mander, J.B.** (1998). Seismic fragility analysis of highway bridges. *INCEDEMCEER Center-to-Center Workshop on Earthquake Engineering Frontiers in Transportation Systems*, 311-325, Tokyo, Japan.

**Elnashai, A.S., Borzi, B., and Vlachos, S.** (2004). Deformation–based vulnerability functions for RC bridges. *Struct Eng Mech, **17**, 2*, 215-244.

**Federal Highway Administration (FHWA)**. (1995). *Seismic retrofitting manual for highway bridges.* (Report No. FHWA-RD-94-052). McLean, VA.

**Federal Emergency Management Agency (FEMA).** (2000). Recommended seismic design criteria for new steel moment-frame buildings. Rep. No. FEMA-350, SAC Joint Venture, Washington, D.C.

**FEMA 450.** (2003). NEHRP Recommended Provision for Seismic Regulation for New Buildings or Other Structures: Provision. Washington: The Building Seismic Safety Council National Institue of Building Science.

**Federal Emergency Management Agency (FEMA)**. (2003). *HAZUS-MH MR1: Technical Manual*, Washington, D.C.

**Federal Emergency Management Agency (FEMA)**. (2005). Improvement of Nonlinear Static Seismic Analysis Procedures, FEMA 440, Washington, D.C.

**Gosh, U. K.** (2006). Design and Construction of Steel Bridges. London: Taylor & Francis Group.

**Gunduz A.** (1996). Probability, statistics, risk and reliability in engineering. Istanbul: Kure publications [in Turkish].

**HAZUS.** (1997). *Standardized earthquake loss estimation methodology.* National Institute of Building Sciences, Prepared by Risk Management Solutions, Inc., Menlo Park, California.

**Hwang, H., Jernigan, J.B., and Lin, Y.W.** (2000). Evaluation of seismic damage to Memphis bridges and highway systems. *J Bridge Eng-ASCE, 5*, 322–330.

**Hwang, H., Liu, J. B., and Chiu, Y. H.** (2001). Seismic fragility analysis of highway bridges. *Technical Report* Center for Earthquake Research and Information The University of Memphis.

**Jernigan, J.B., and Hwang, H.** (2002). Development of bridge fragility curves. *In Proceedings of 7th US National Conference on Earthquake Engineering.* Boston: EERI.

**Jung, H.** (1992). Structural dynamic model updating using eigensensitivity analysis. PhD thesis Imperial College, London, UK.

**Kappos, A. J., Stylianidis, K. A., and Penelis, G. G.** (1991). Analytical prediction of the response of structures to future earthquakes. *Eur Earthq Eng, 5*, 10–21.

**Kappos, A. J., Stylianidis, K. C., and Pitilakis, K.** (1998). Development of seismic risk scenarios based on a hybrid method of vulnerability assessment. *Nat Hazards, 17*, 177–192.

**Kappos, A. J., Panagopoulos, G., Panagiotopoulos, C., and Penelis, G.** (2006). A hybrid method for the vulnerability assessment of R/C and URM buildings. *Bull Earthq Eng, 4*, 391–413.

**Kappos, A. J.** (2016). An overview of the development of the hybrid method for seismic vulnerability assessment of buildings. *Struct Infrastruct E, **12**,12*,1573-1584.

**Karim, K., and Yamazaki, F.** (2001). Effect of earthquake ground motions on fragility curves of highway bridge piers based on numerical simulation. *Earthquake Engng Struct Dyn, **30**,* 1839–1856.

**Kirçil, M. S., Polat, Z.** (2006). Fragility analysis of mid-rise R-C frame buildings *Eng Struct., 28*: 1335-1345.

**Kulicki, J. M., Prickett, J. E., and LeRoy, D. H.** (1999). Truss Bridges. R. L. Brockenbrough, & F. S. Merritt içinde, Structural Steel Designer's Handbook. McGraw Hill, Inc.

**Kwon, O. S., Elnashai, A.** (2006). The effect of material and ground motion uncertainty on the seismic vulnerability curves of RC structure. *Eng Struct, **28**,* 289-303.

**Li, Y. R.** (1996). Non-linear time history and Pushover analyses for seismic design and evaluation. PhD Thesis, University of Texas, Austin, USA.

**Luco, N., and Cornell, C.A.** (1998). Effects of random connection fractures on the demands and reliability for a three-story pre-Northridge (SMRP)

structure. *In Proceedings of the 6th U.S. National Conference on Earthquake Engineering*. Oakland, California.

**Mander J.B.** (1999). Fragility curve development for assessing the seismic vulnerability of highway bridges. Technical Report, MCEER Highway Project/FHWA.

**Mander J.B., and Basoz N.** (1999). Seismic Fragility Curve Theory for Highway Bridges. *5th US Conference on Lifeline Earthquake Engineering,* 31-40, Seattle, WA, USA.

**Monti G., and Nistico N.** (2002) Simple probability-based assessment of bridges under scenario earthquakes. *J Bridge Eng*, **7**, *2*, 104-114.

**Nielson, B. G., and Desroches, R.** (2006). Seismic fragility methodology for highway bridges. *Structures 2006.*

**Nielson, B. G., and Desroches, R.** (2007). Analytical seismic fragility curves for typical bridges in the central and southeastern United States. *Earthq Spect, 23,* 3, 615-633.

**O'Connor, C.** (1971). Design of Bridge Super Structures. New York: Wiley Interscience.

**Pan, Y., Agrawal, A. K., Ghosn, M., and Alampalli, S.** (2010). Seismic fragility of multispan simply supported steel highway bridges in new york state. ii: fragility analysis, fragility curves, and fragility surfaces. *J Bridge Eng, **15**, 5,* 462-472.

**PEER.** (2016). Pacific Earthquake Engineering Center. PEER Pacific Earthquake Engineering Center: http://peer.berkeley.edu.

**Penelis, G.G., Sarigiannis, D., Stavrakakis, E., and Stylianidis, K. C.** (1989). A statistical evaluation of damage to buildings in the Thessaloniki. Greece, earthquake of June, 20, 1978, Proceedings of 9th World Conference on Earthquake Engineering, August 1989, Tokyo- Kyoto, Maruzen, Japan, VII, 187–192.

**Pipinato, A., and De Miranda, M.** (2016). Steel and Composite Bridges. A. Pipinato içinde, Innovative Bridge Design Handbook: Construction, Rehabilitation and Maintenance (s. 247-271).

**Prell, J. S.** (1908). Cyclopedia of Civil Engineering. London: American Technical Society.

**Rossetto T., and Elnashai A.S.** (2003). Derivation of vulnerability functions for European type RC structures based on observational data. *Eng Struct, **25**, 10,* 1241-1263.

**Shinozuka, M., Feng, M.Q., Lee, J., and Naganuma, T.** (2000a). Statistical analysis of fragility curves. *J Eng Mech-ASCE, **126**, 12,* 1224-1231.

**Shinozuka, M., Feng, M. Q., Kim, H., Kim, S.** (2000b). Nonlinear static procedure for fragility curve development. *J Eng Mech., **126***(12): 1287-1295.

**Shinozuka, M., Feng, M.Q., Kim, H., Uzawa, T., and Ueda T.** (2003). *Statistical analysis of fragility curves.* (Report No. MCEER-03-0002).

**Troyano, L. F.** (2003). Bridge Engineering A Global Perspective. London: Thomas Telford.

**Uzgider, E., Sanlı, A., Piroglu, F., Ozgen A., Caglayan, B. O., and Tektunalı, A. C.** (1996a). Testing & evaluation of Karacam railway bridge. Nato Science for Stability Programme TU-850- Bridges Research Project 5.

**Uzgider, E., Gunduz, N., Aydogan, M., Piroglu, F., Caglayan, B. O., Rahmatian, P., and Ilicali, B.** (1996b). Testing & evaluation of Cambazkaya railway bridge. Nato Science for Stability Programme TU-850- Bridges Research Project 6.

**Vamvatsikos, D., and Cornell, A.C.** (2002). Incremental dynamic analysis. *Earthq Eng Struct Dyn*, *31*, 491–514.

**Yamazaki, F., Motomura, H., and Hamada, T.** (2000). Damage assessment of expressway networks in japan based on seismic monitoring. *12th World Conference on Earthquake Engineering*, Paper No. 0551

**Zhang, J., and Huo, Y.** (2009). Evaluating effectiveness and optimum design of isolation devices for highway bridges using the fragility function method. Eng Struct, *31*, 1648–1660.

**www.deprem.gov.tr.** (2016, 10 19). Republic of Prime Ministry Disaster and Emergency Management Authority: Earthquake Zoning Map of Turkey: www.deprem.gov.tr

**www. nyc.gov** (2017, 04 20). The Official Website of the City of New York: Ed Koch Queensboro Bridge

**APPENDICES**

**APPENDIX A:** Fragility curves of Karaçam bridge model.
**APPENDIX B:** Fragility curves of Cambazkaya bridge model.
**APPENDIX C:** Fragility curves of Ceyhan bridge model.

## APPENDIX A

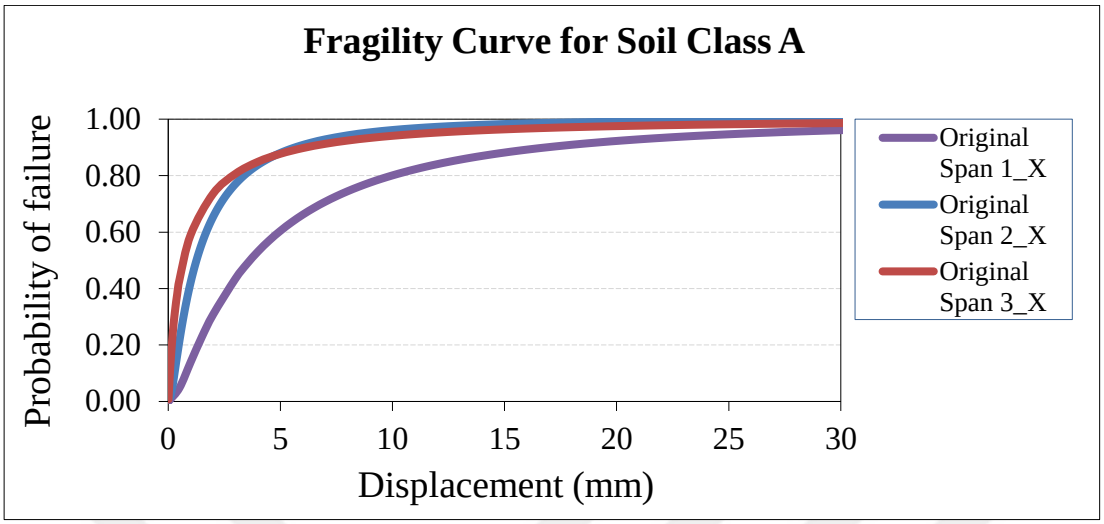


**(a)** X direction

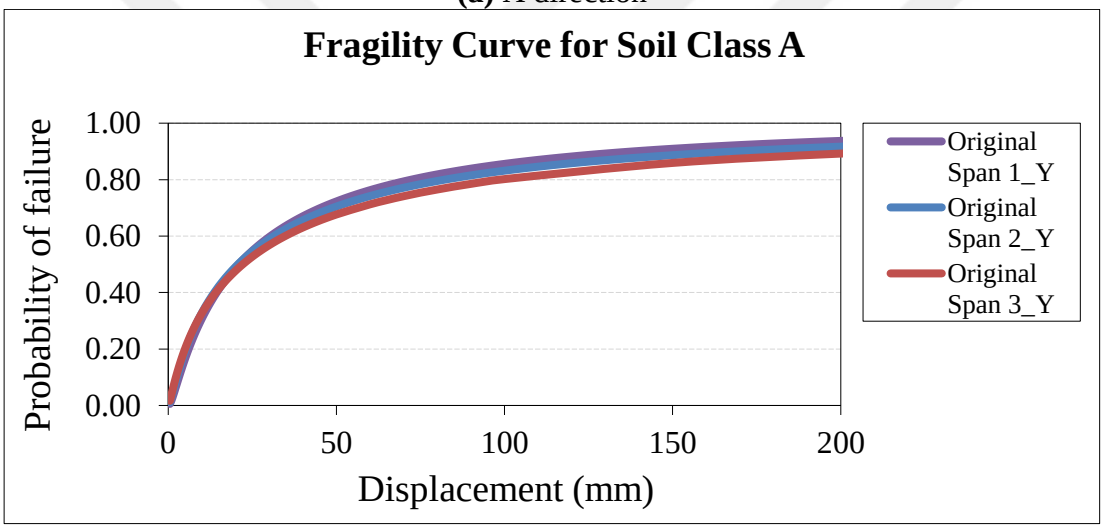


**(b)** Y direction

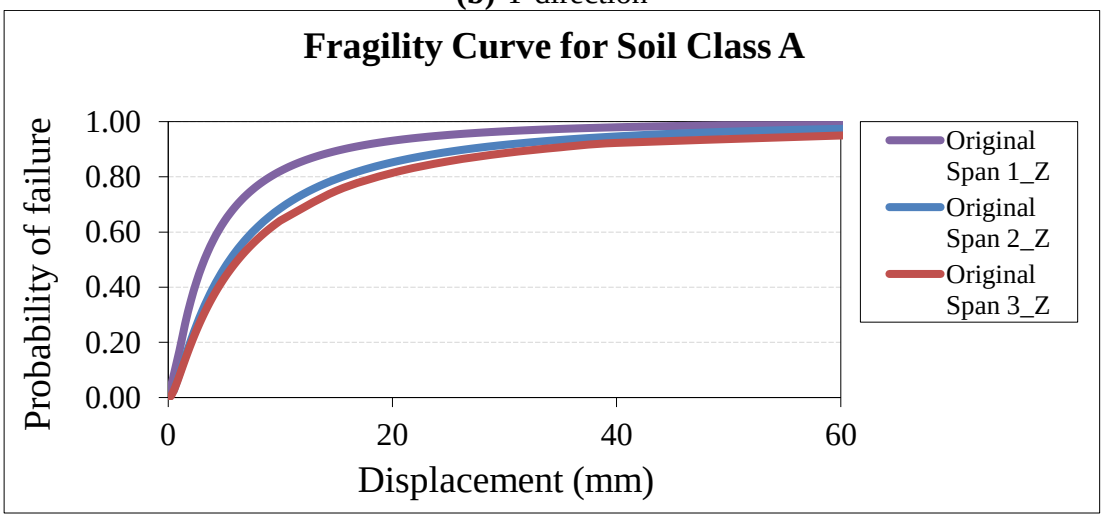


**(c)** Z direction

**Figure A.1 :** Fragility curves of original Karaçam bridge model for soil class A.

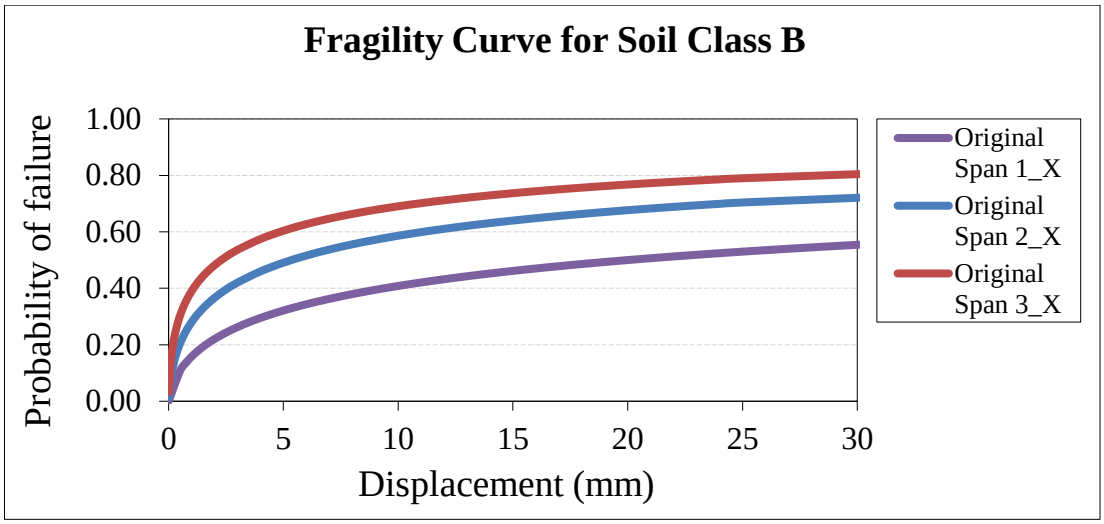


**(a)** X direction

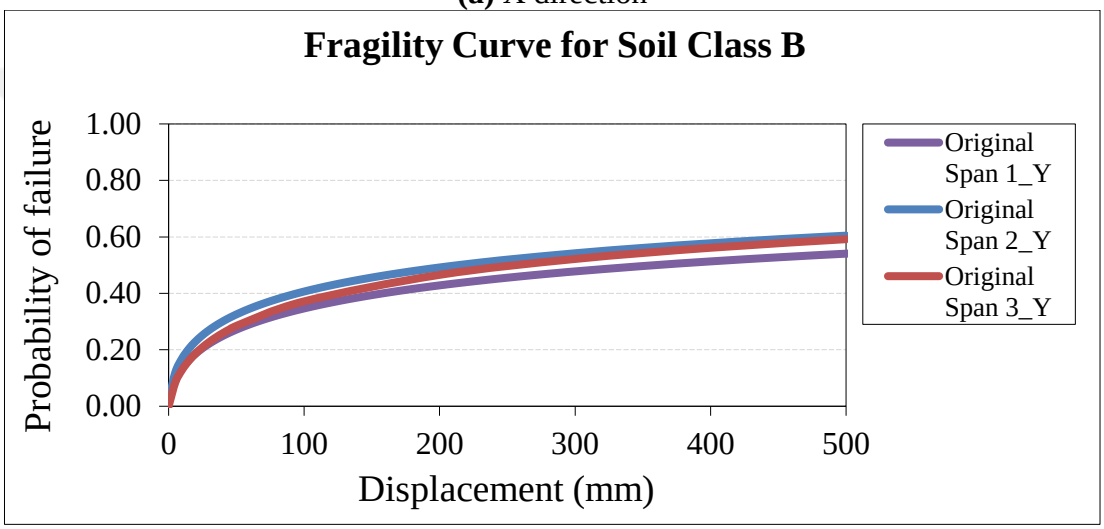


**(b)** Y direction

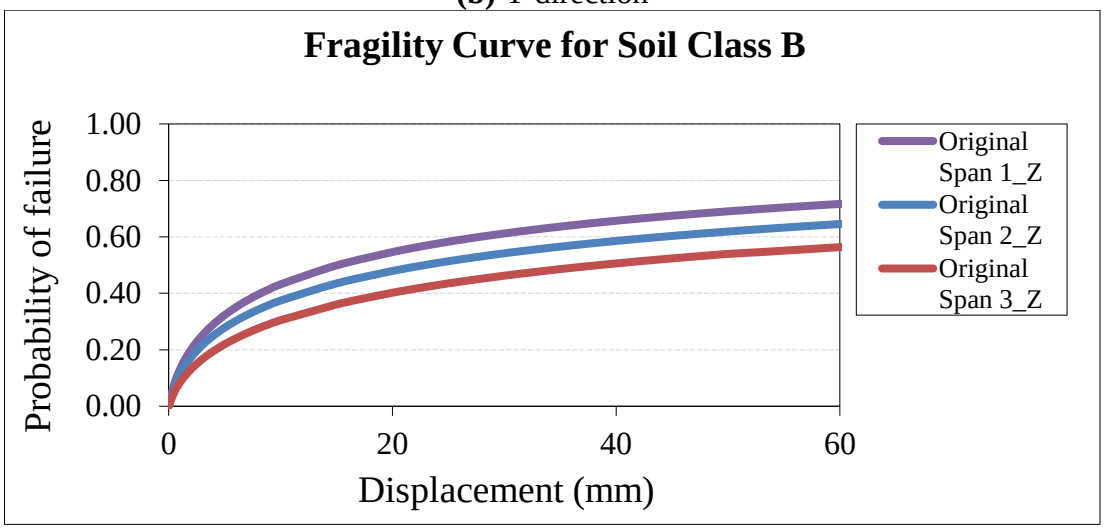


**(c)** Z direction

**Figure A.2 :** Fragility curves of original Karaçam bridge model for soil class B.

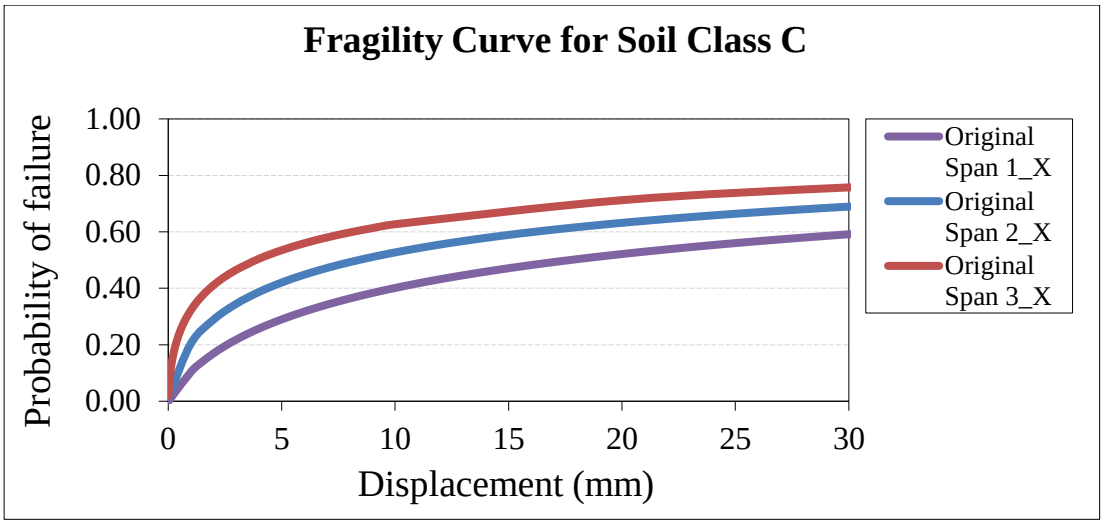


**(a)** X direction

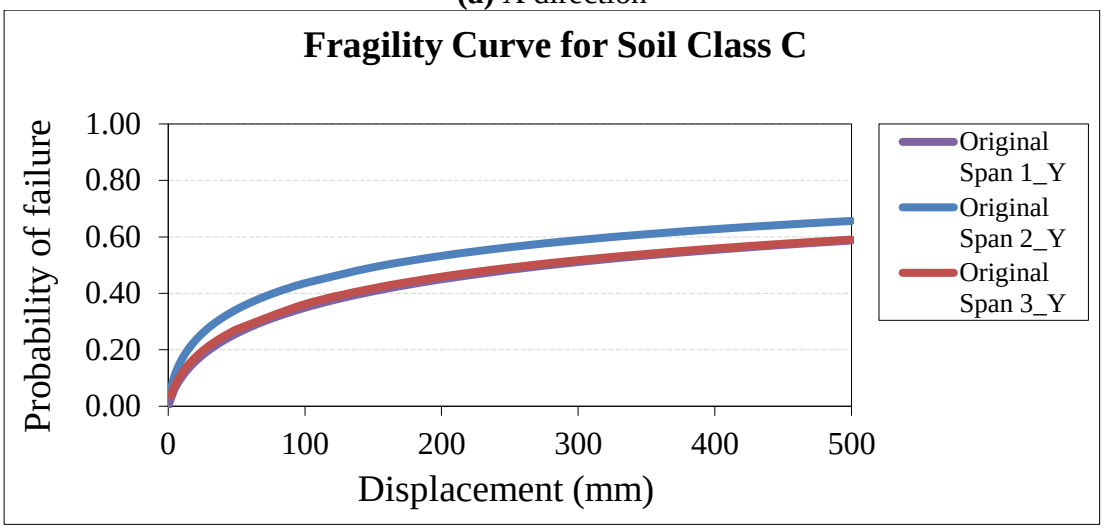


**(b)** Y direction

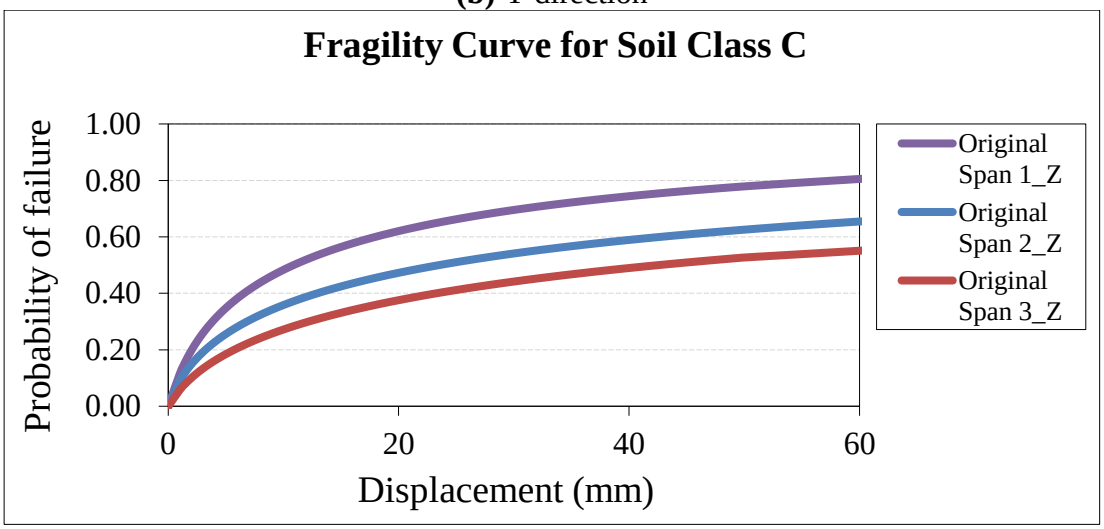


**(c)** Z direction

**Figure A.3 :** Fragility curves of original Karaçam bridge model for soil class C.

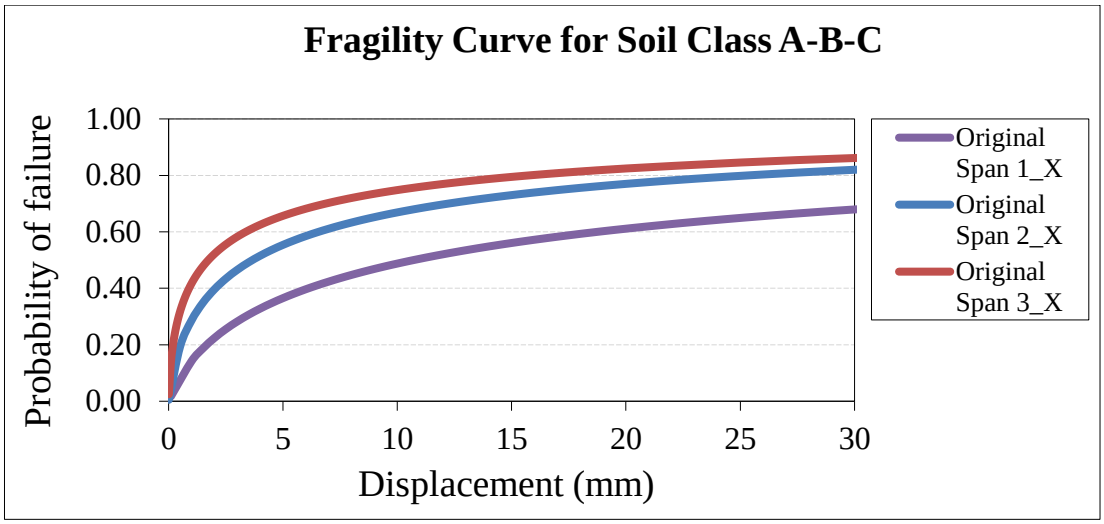


**(a)** X direction

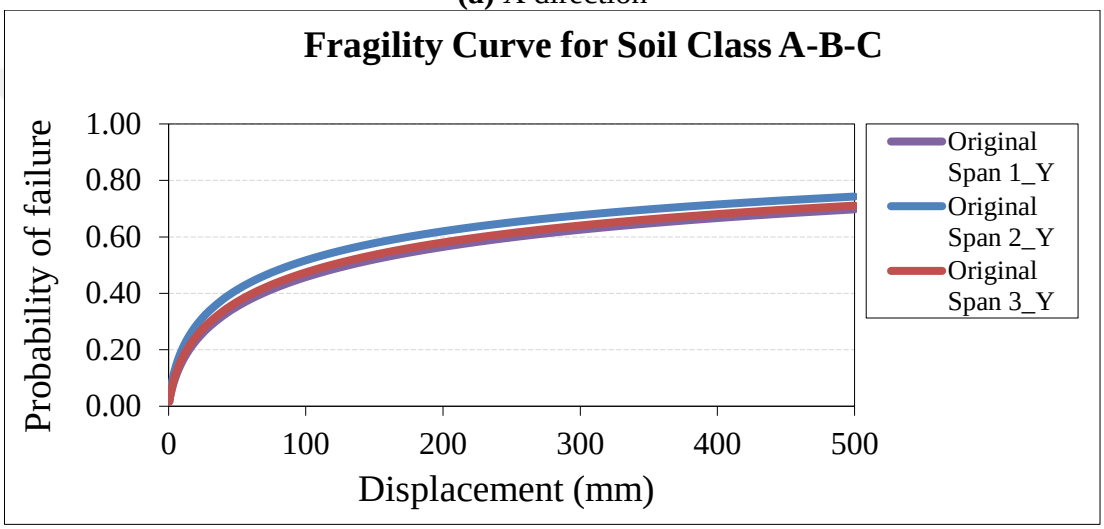


**(b)** Y direction

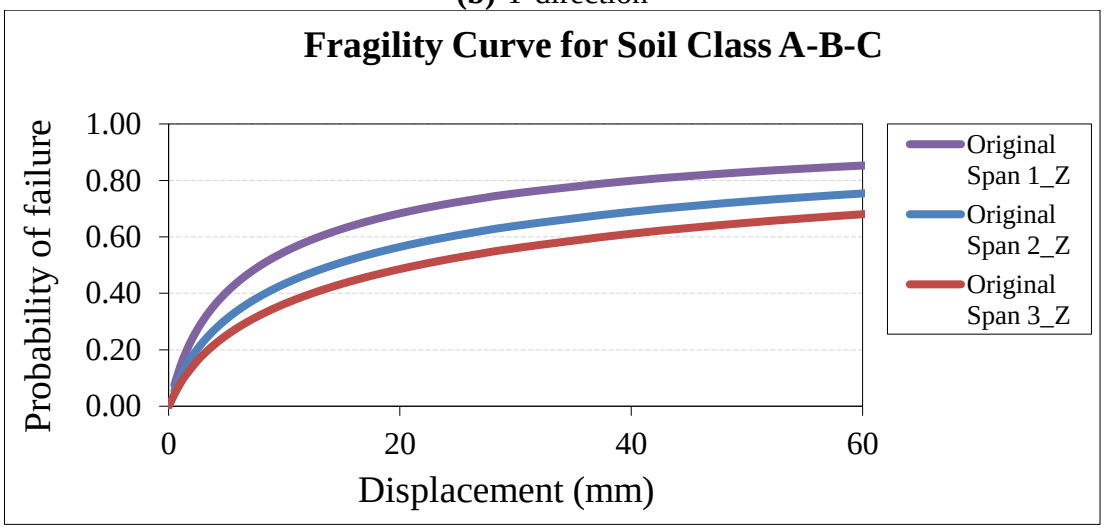


**(c)** Z direction

**Figure A.4 :** Fragility curves of original Karaçam bridge model for soil class A-B-C.

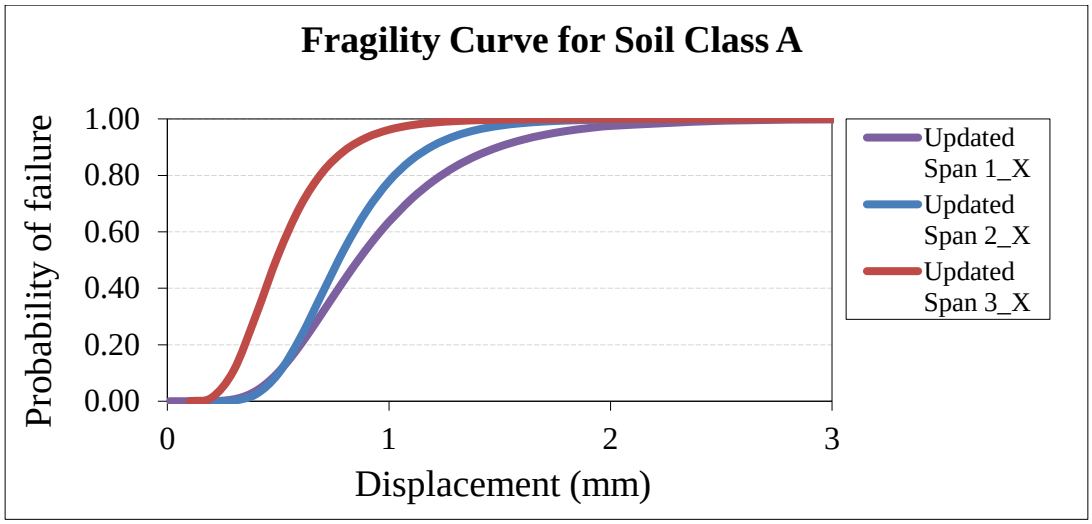


**(a)** X direction

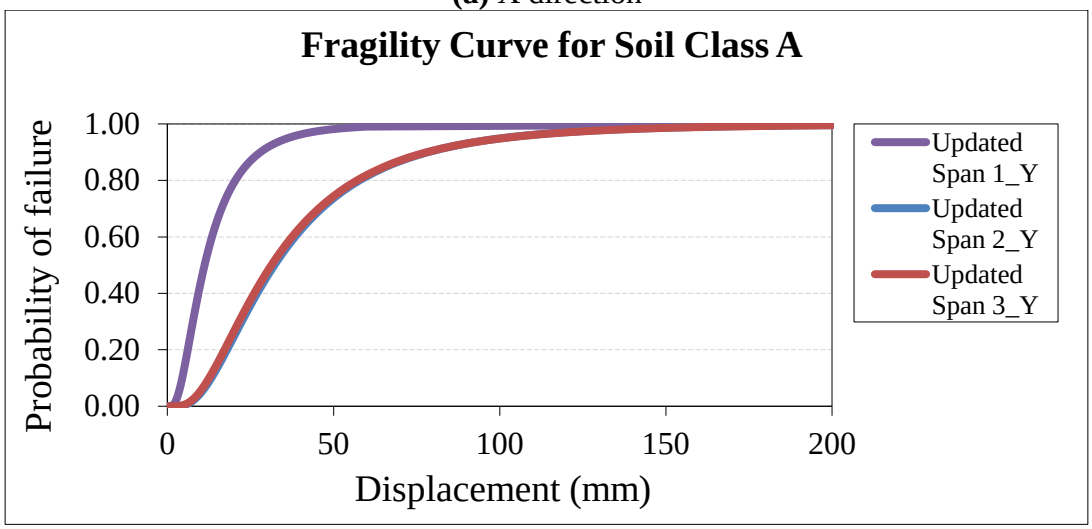


**(b)** Y direction

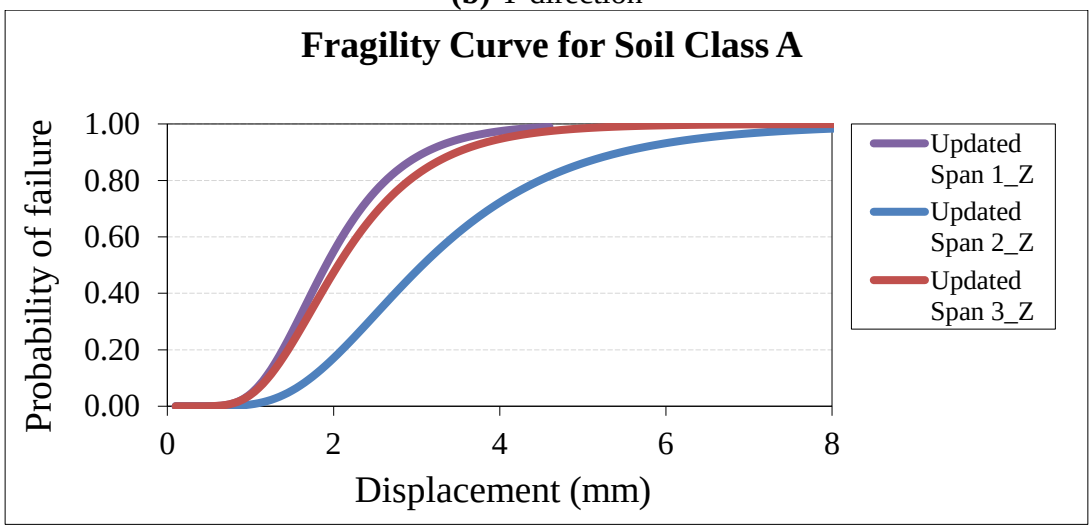


**(c)** Z direction

**Figure A.5 :** Fragility curves of updated Karaçam bridge model for soil class A.

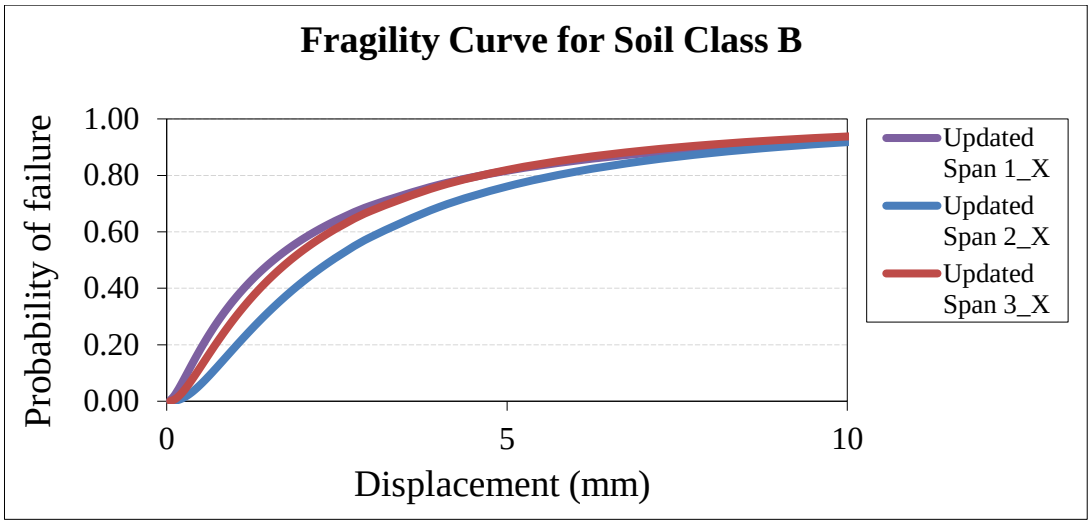


**(a)** X direction

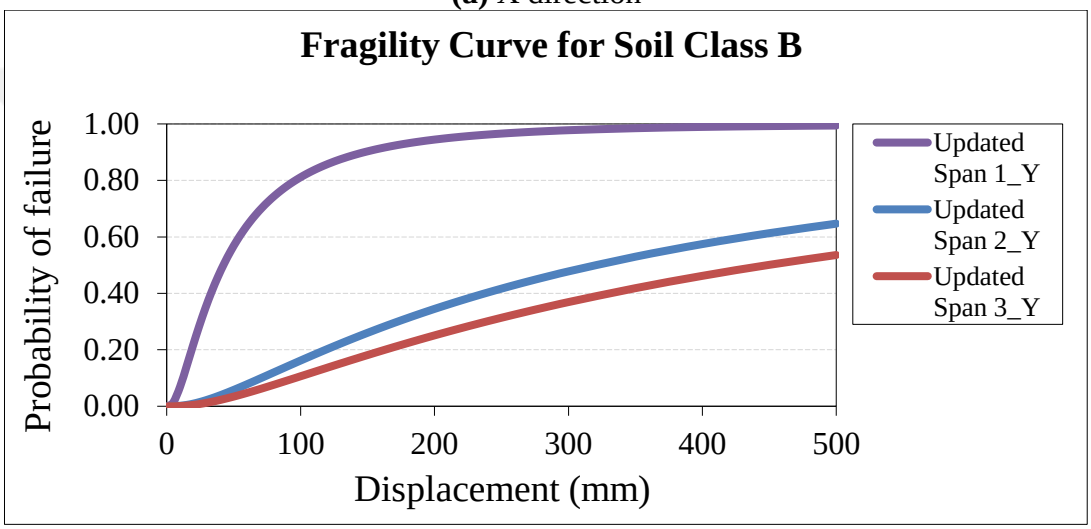


**(b)** Y direction

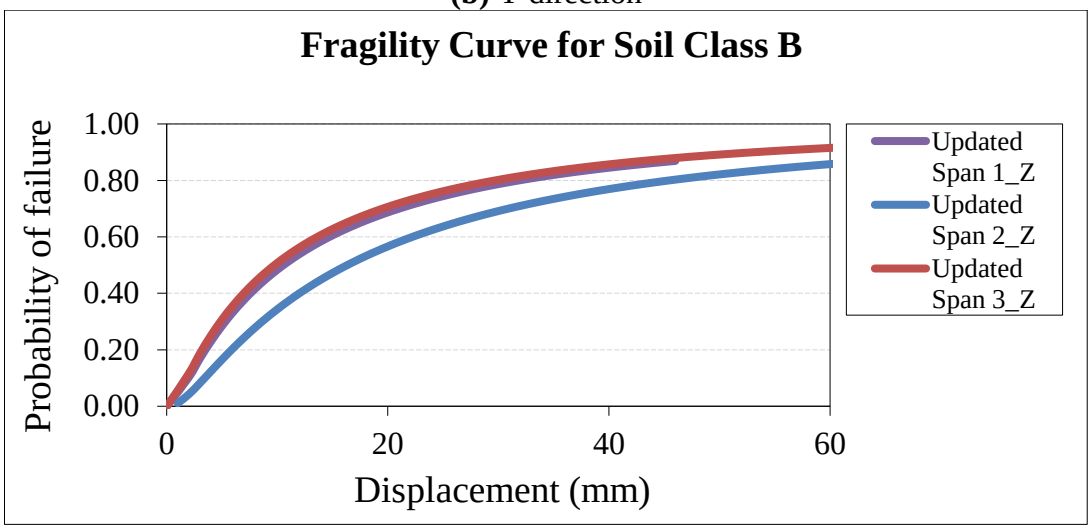


**(c)** Z direction

**Figure A.6 :** Fragility curves of updated Karaçam bridge model for soil class B.

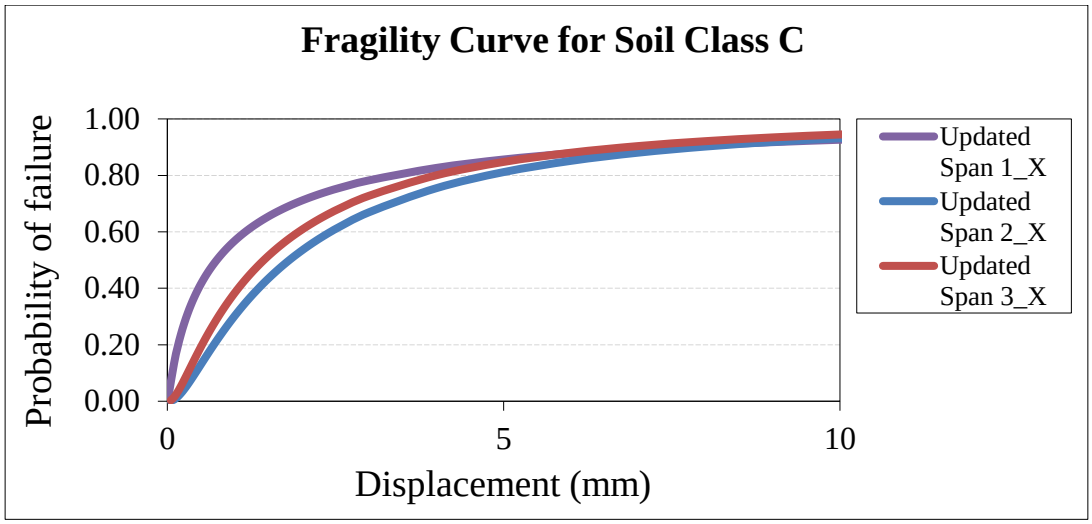


**(a)** X direction

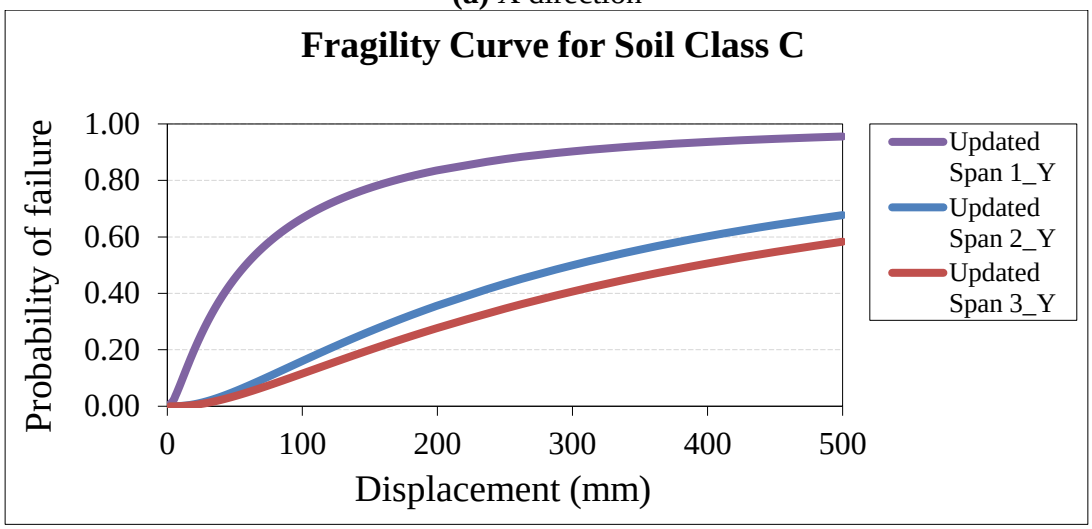


**(b)** Y direction

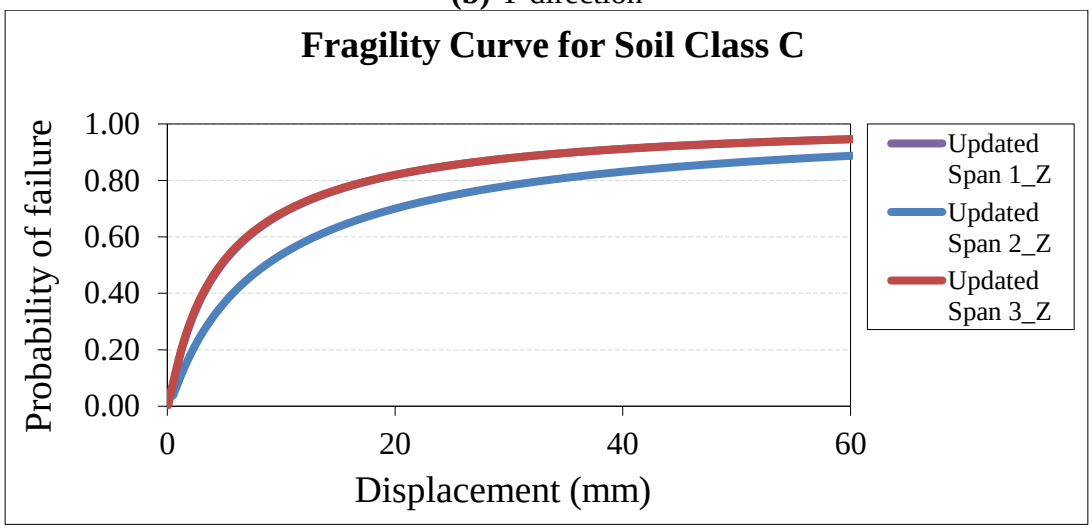


**(c)** Z direction

**Figure A.7 :** Fragility curves of updated Karaçam bridge model for soil class C.

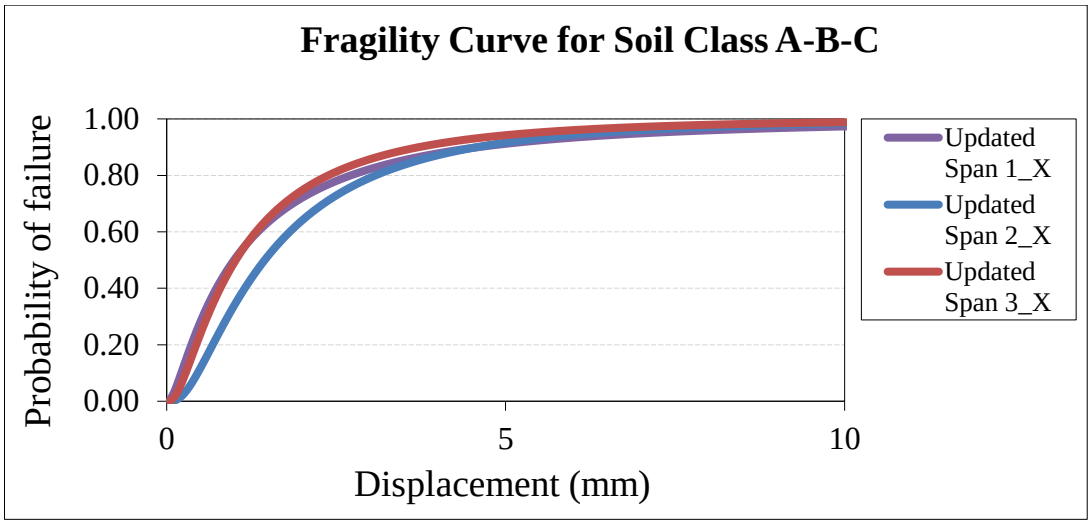


**(a)** X direction

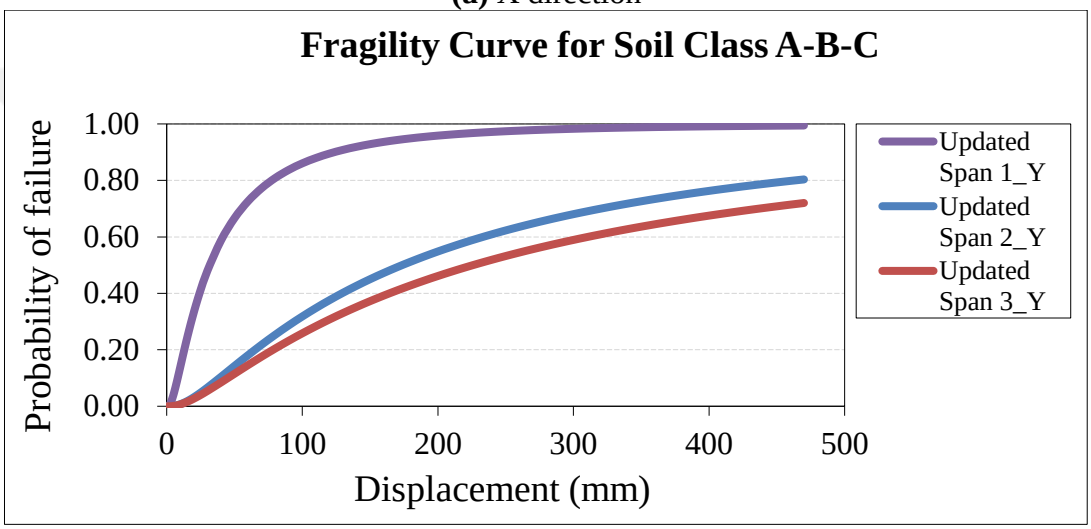


**(b)** Y direction

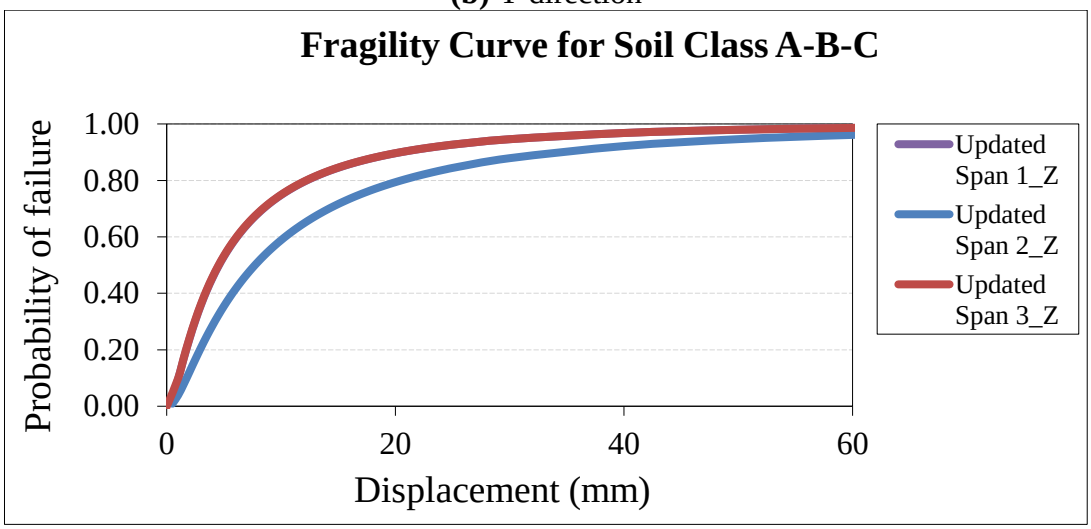


**(c)** Z direction

**Figure A.8 :** Fragility curves of updated Karaçam bridge model for soil class A-B-C.

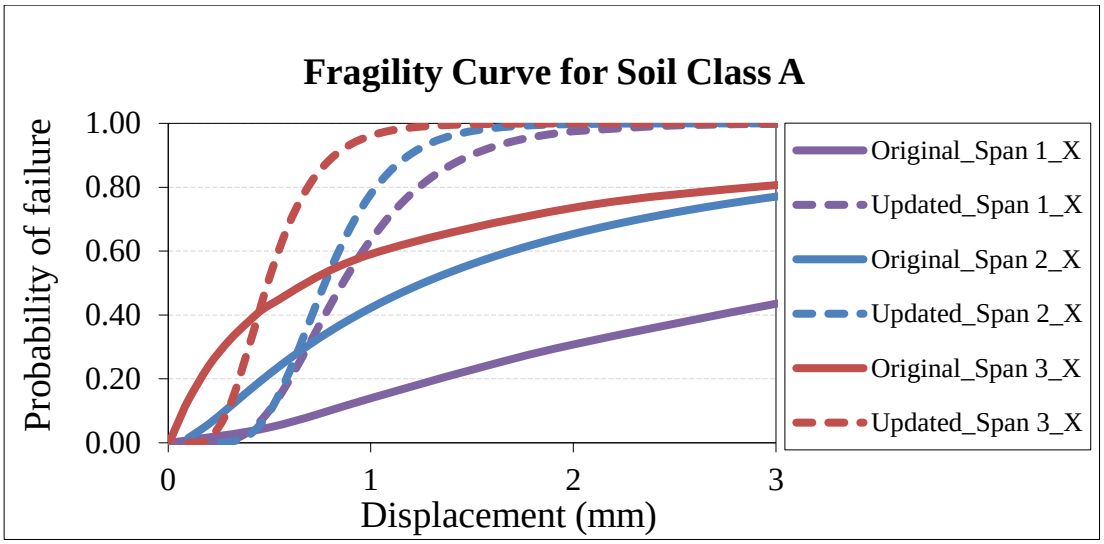


**(a)** X direction

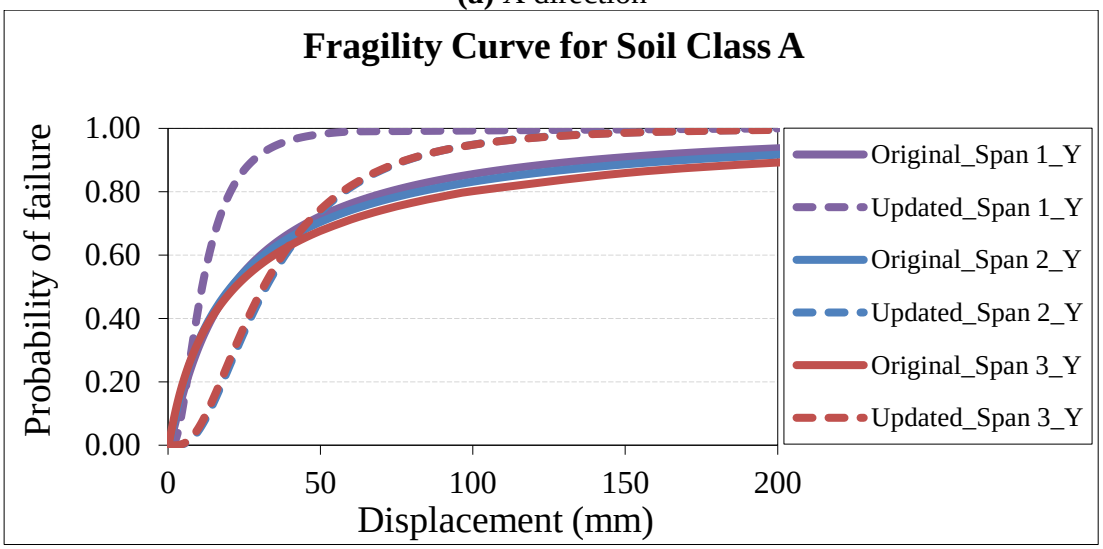


**(b)** Y direction

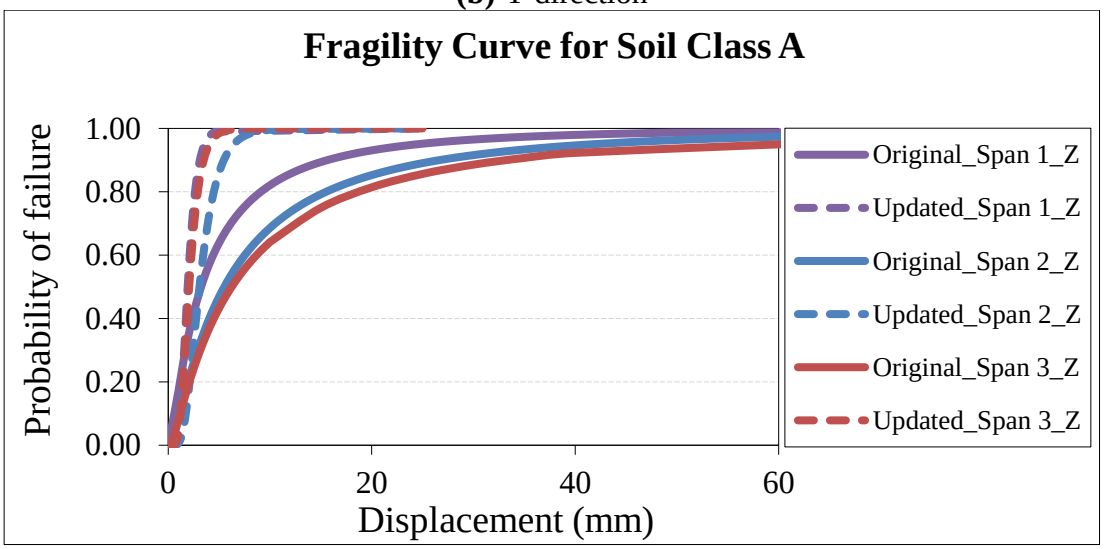


**(c)** Z direction

**Figure A.9 :** Comparison fragility curves of original and updated Karaçam bridge model for soil class A.

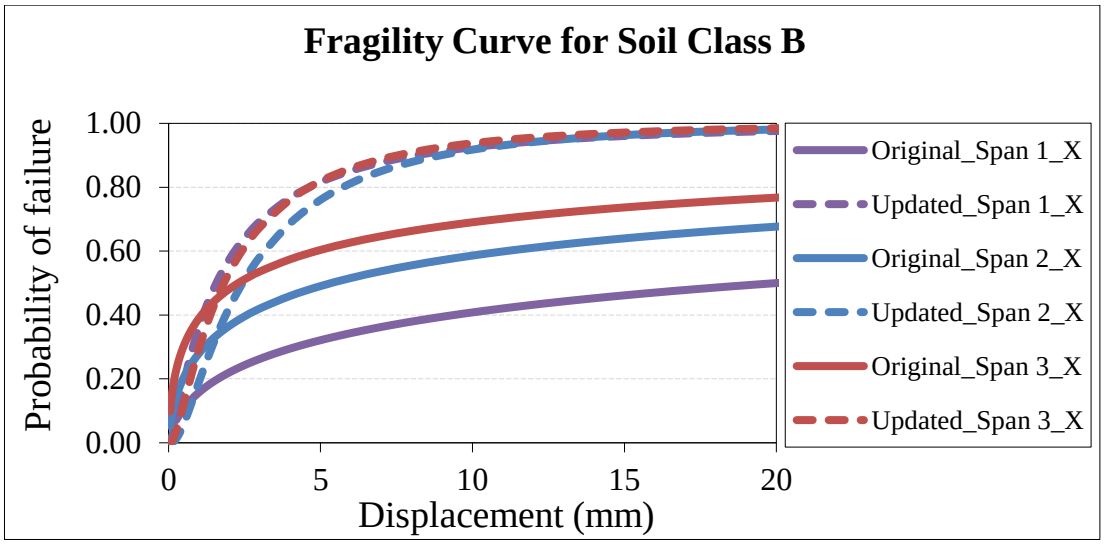


**(a)** X direction

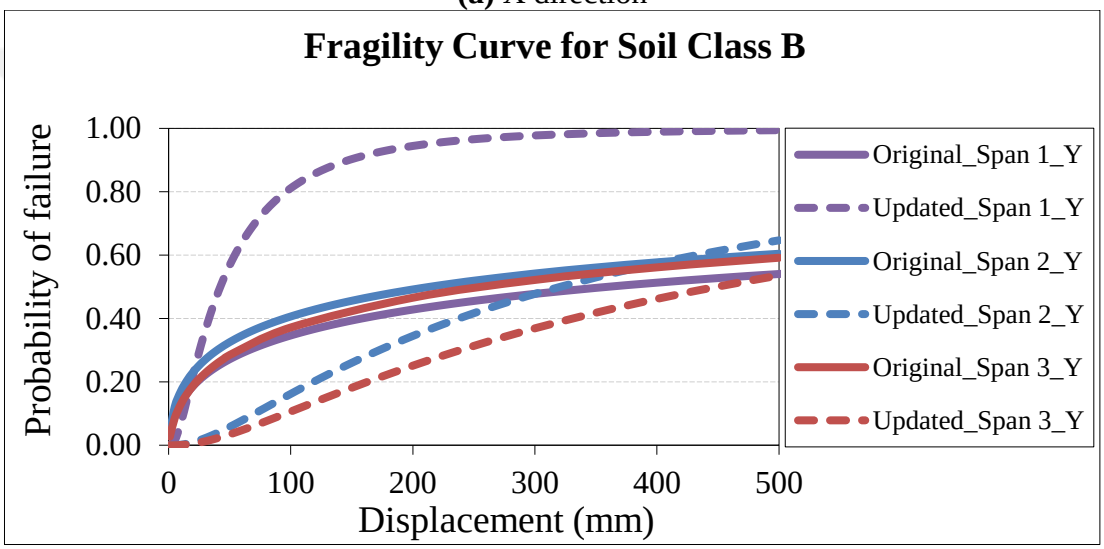


**(b)** Y direction

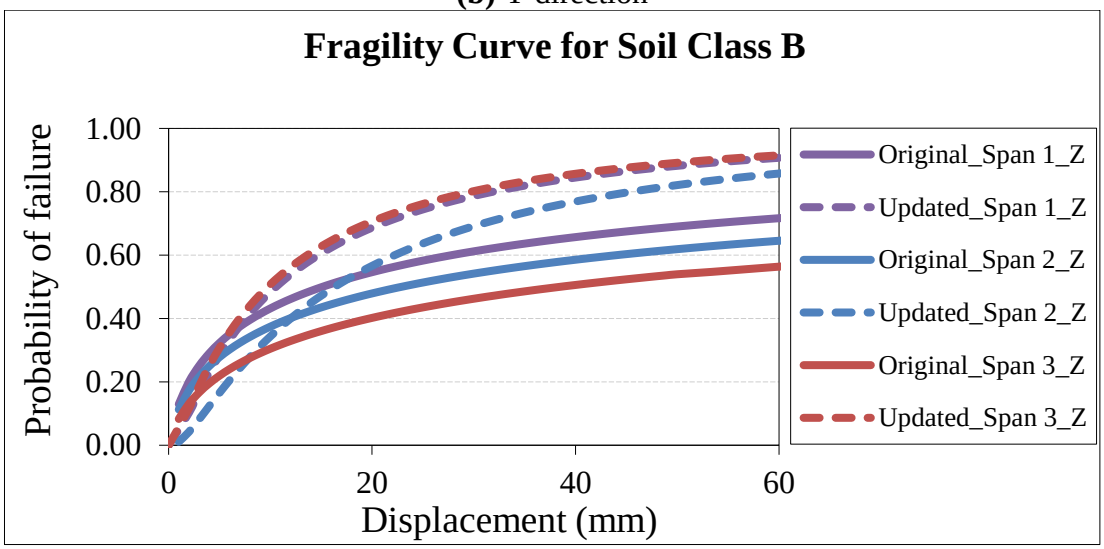


**(c)** Z direction

**Figure A.10 :** Comparison fragility curves of original and updated Karaçam bridge model for soil class B.

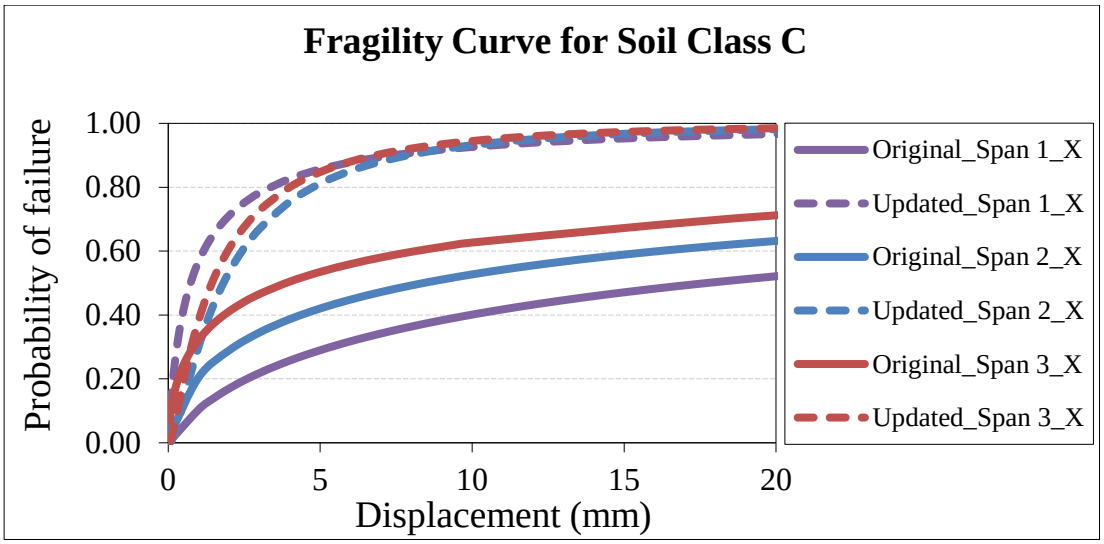


**(a)** X direction

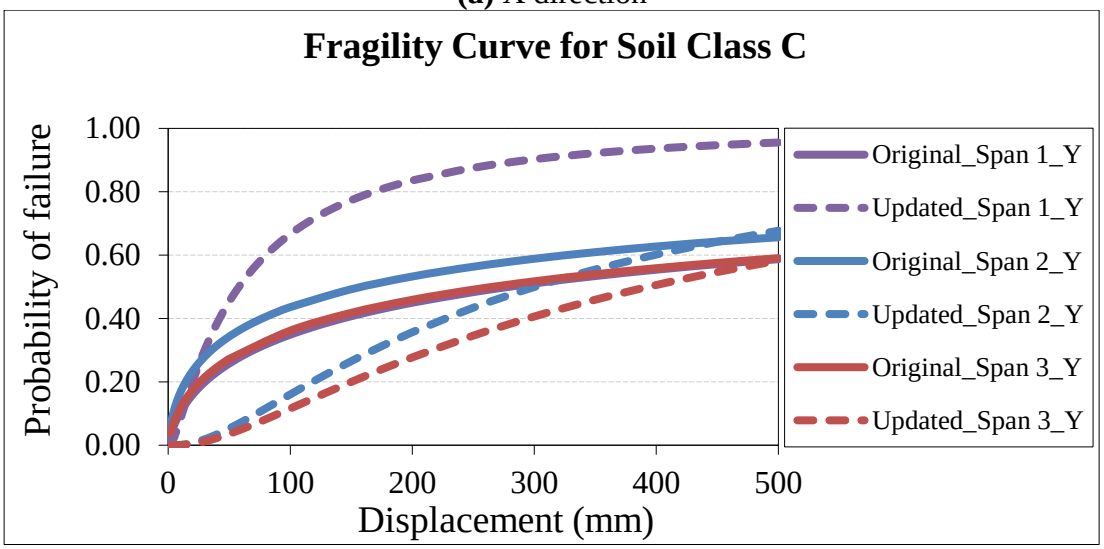


**(b)** Y direction

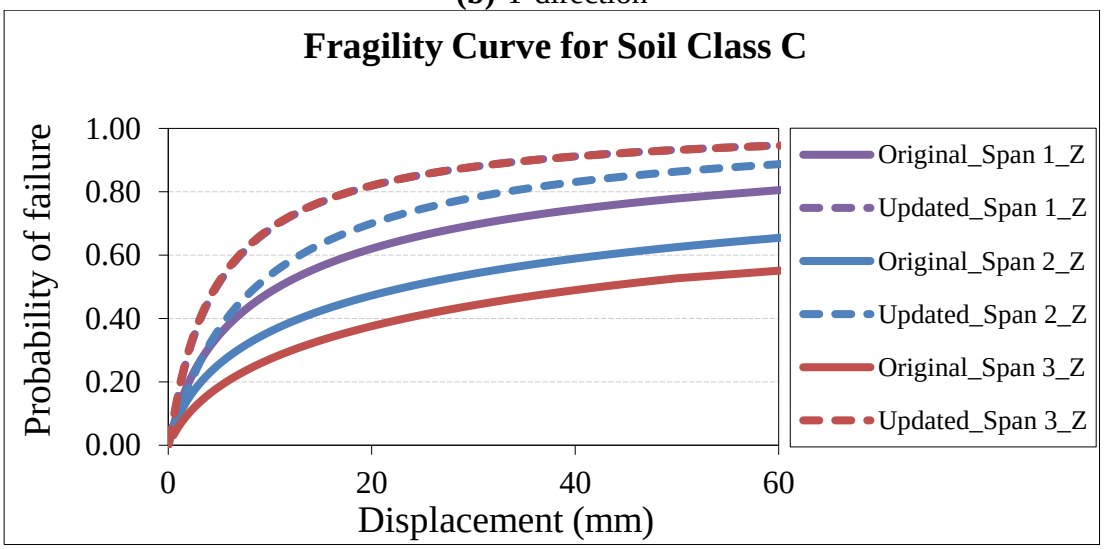


**(c)** Z direction

**Figure A.11 :** Comparison fragility curves of original and updated Karaçam bridge model for soil class C.

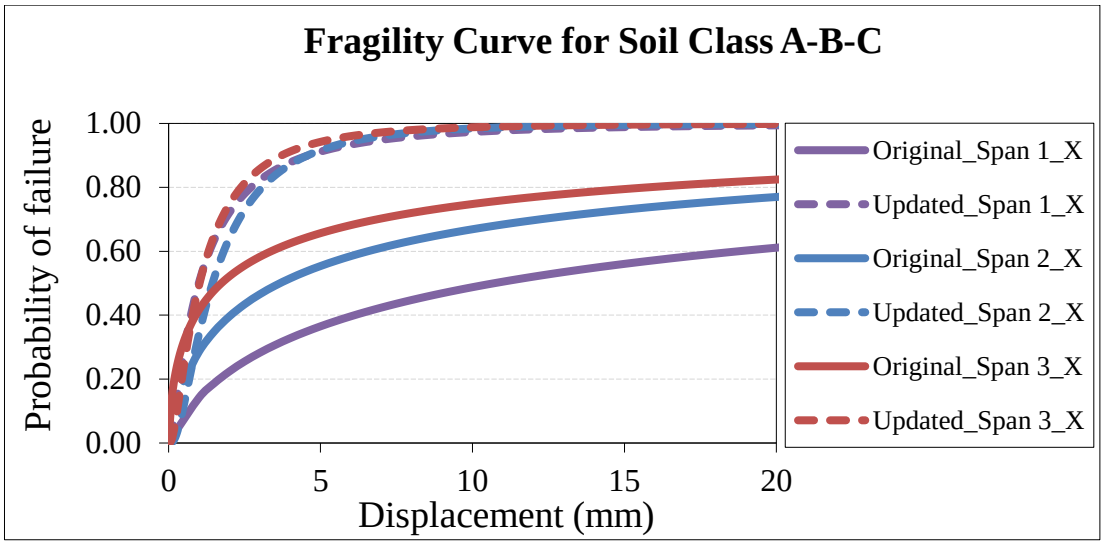


**(a)** X direction

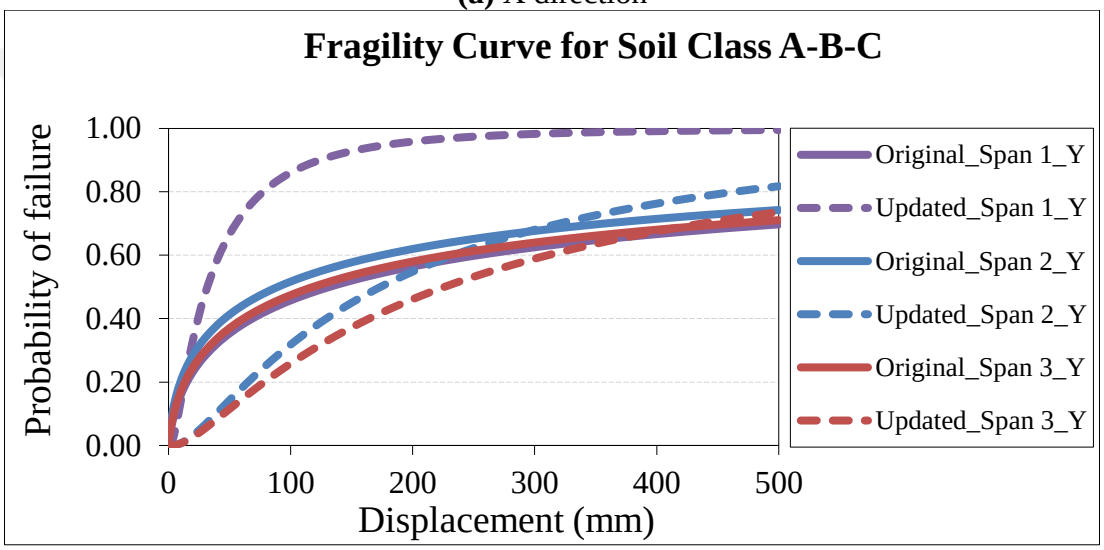


**(b)** Y direction

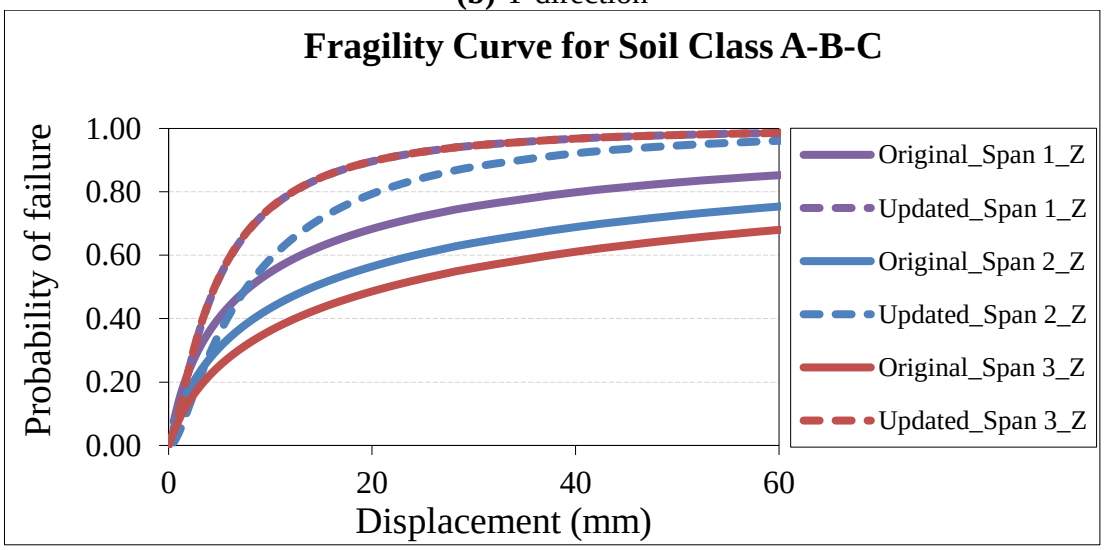


**(c)** Z direction

**Figure A.12 :** Comparison fragility curves of original and updated Karaçam bridge model for soil class A-B-C.

## APPENDIX B

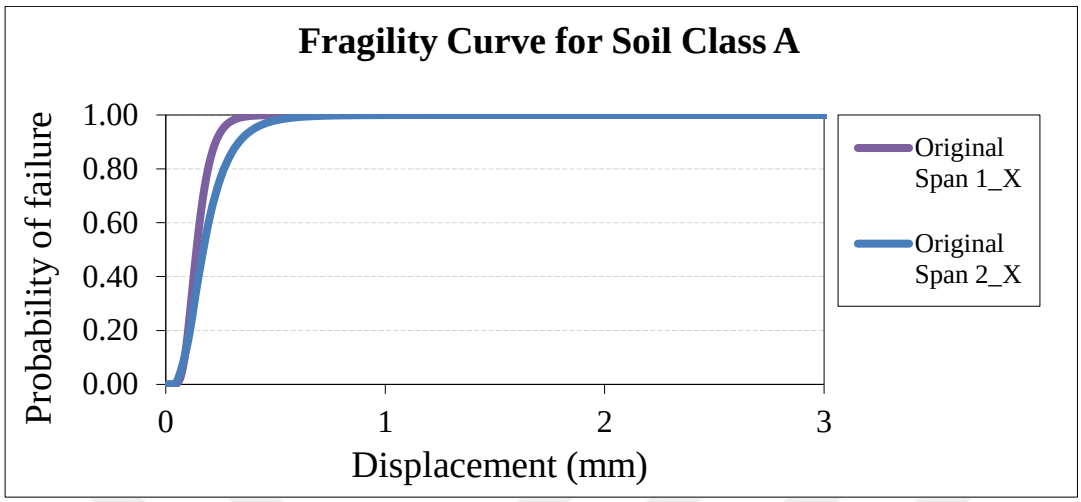


**(a)** X direction

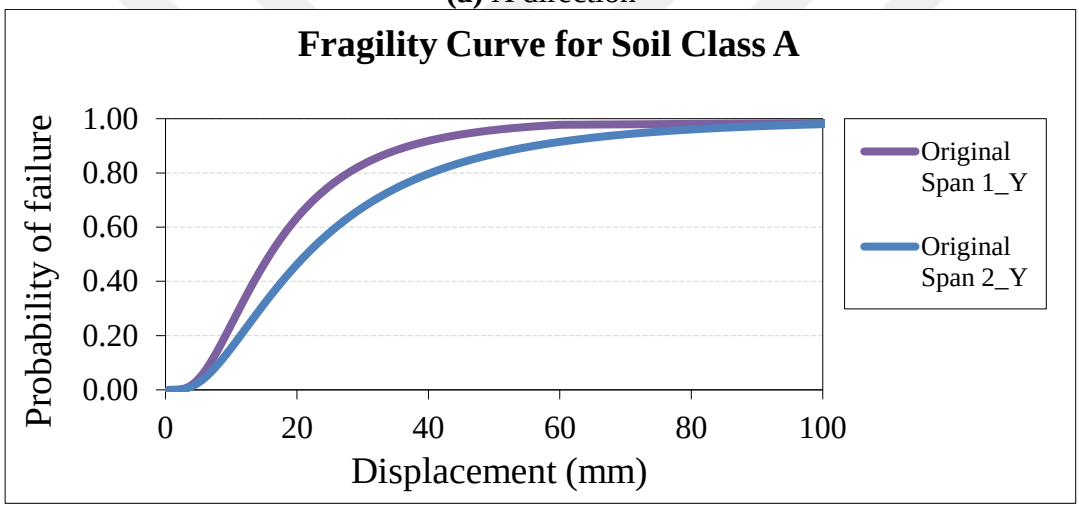


**(b)** Y direction

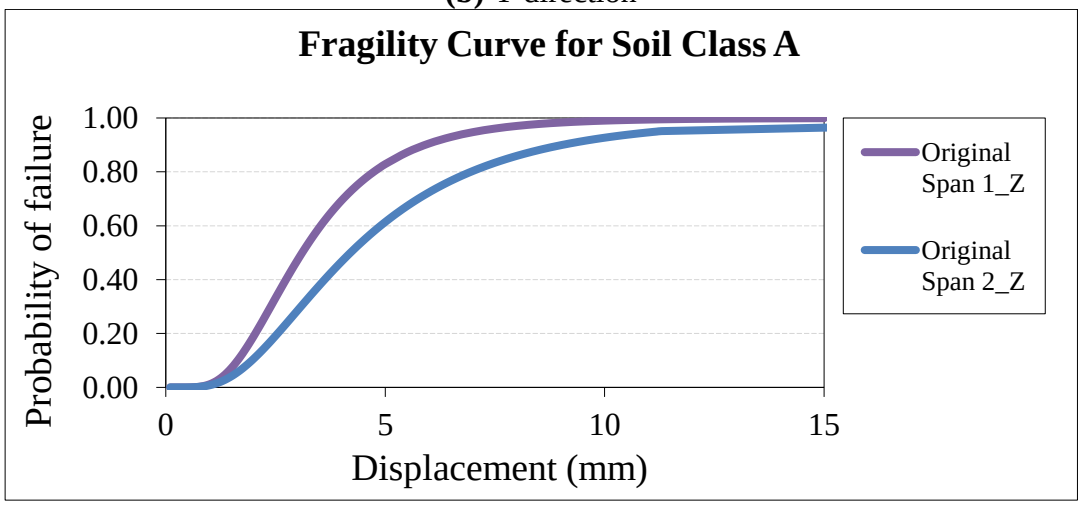


**(c)** Z direction

**Figure B.1 :** Fragility curves of original Cambazkaya bridge model for soil class A.

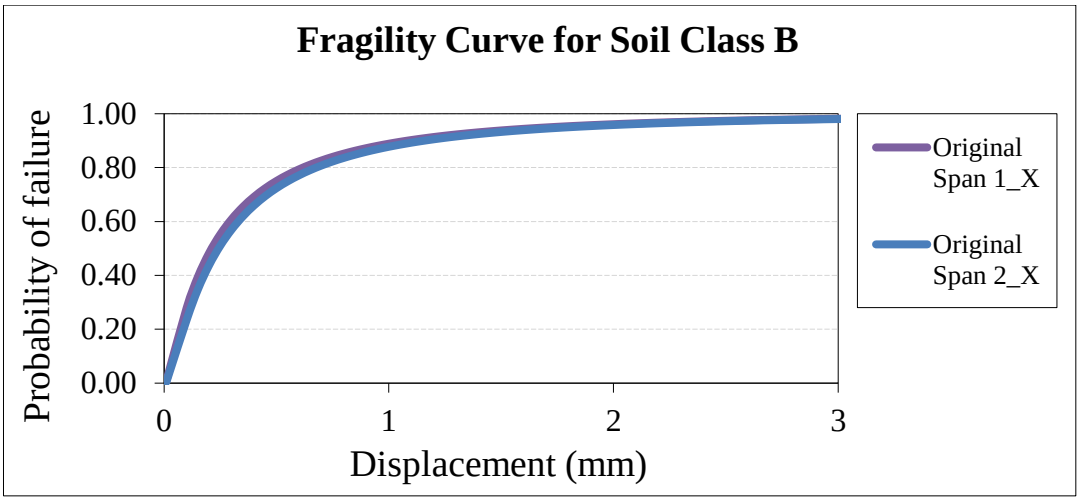


**(a)** X direction

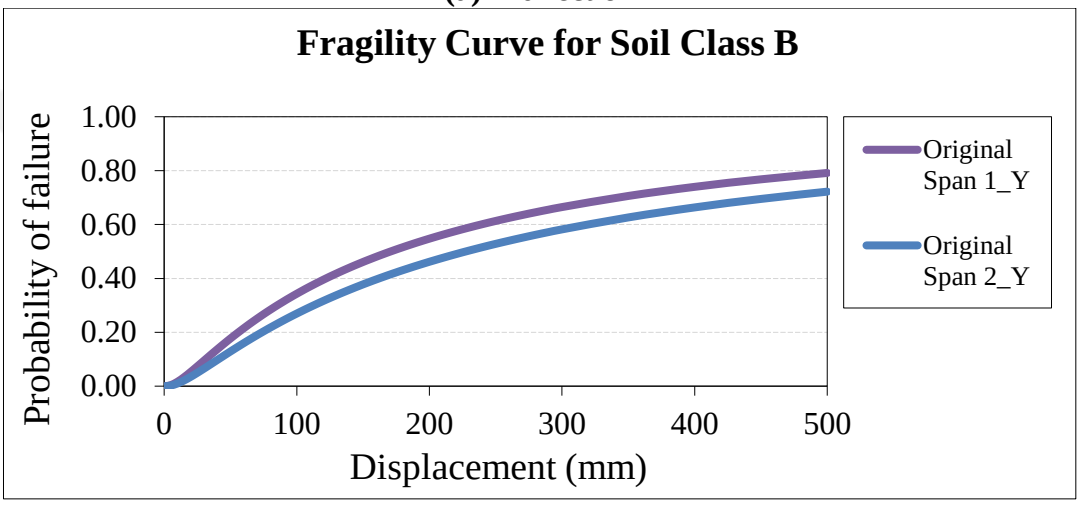


**(b)** Y direction

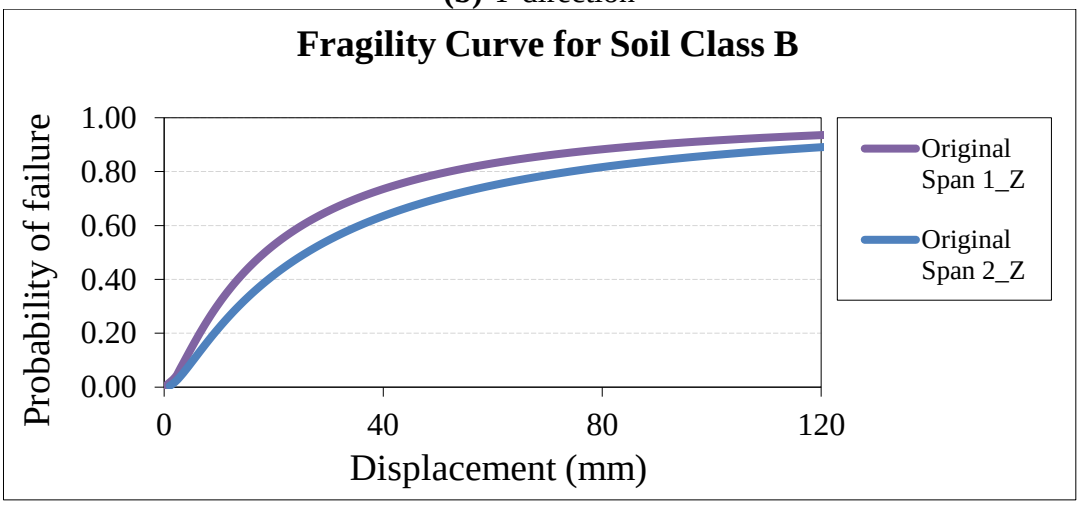


**(c)** Z direction

**Figure B.2 :** Fragility curves of original Cambazkaya bridge model for soil class B.

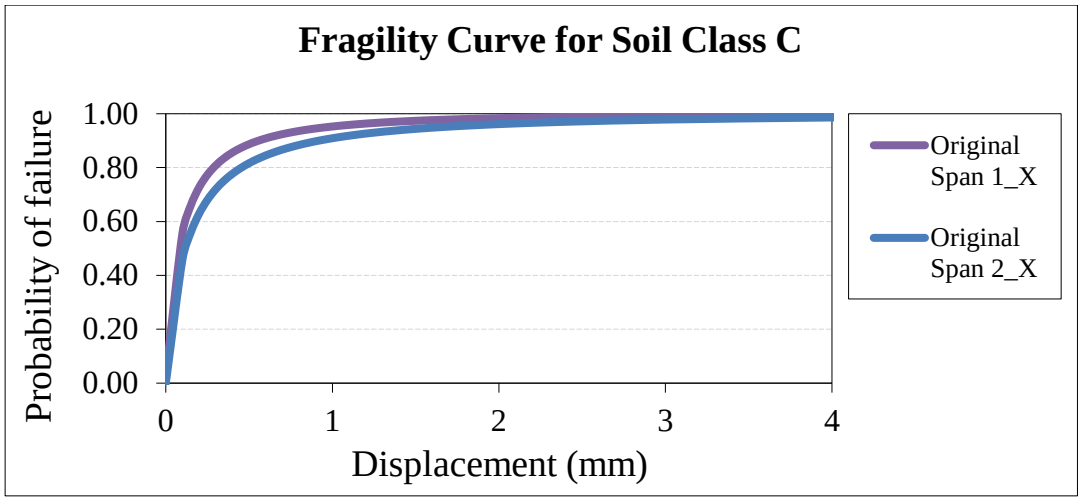


**(a)** X direction

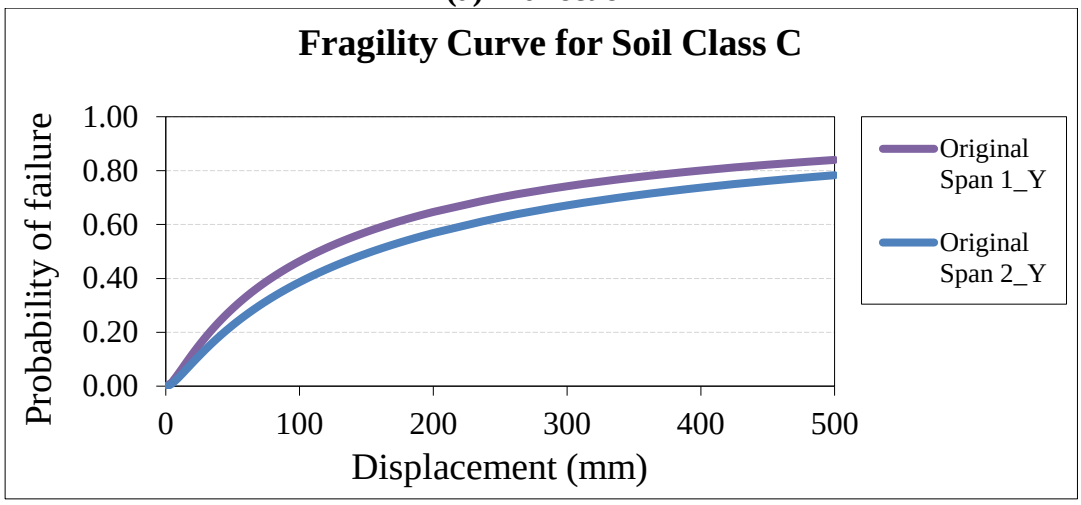


**(b)** Y direction

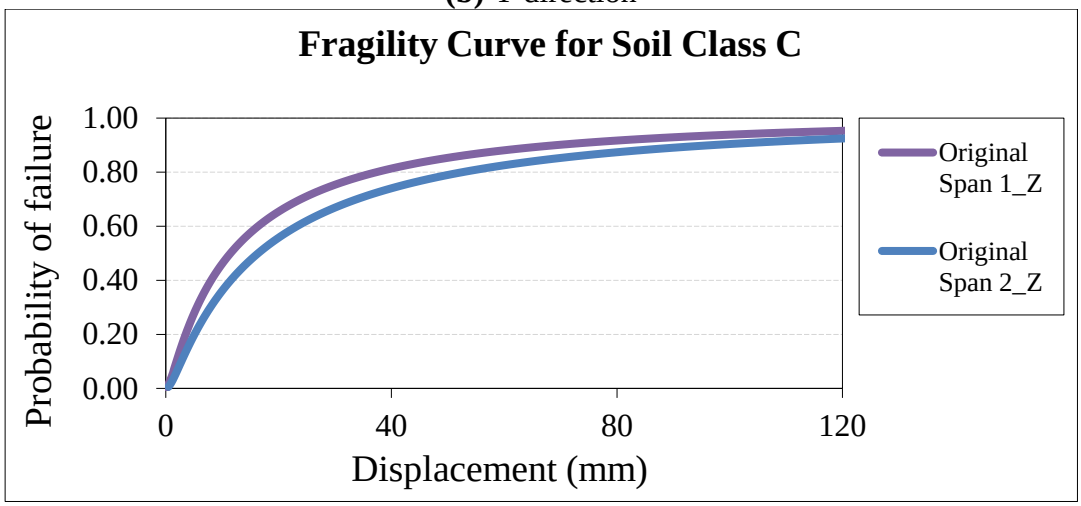


**(c)** Z direction

**Figure B.3 :** Fragility curves of original Cambazkaya bridge model for soil class C.

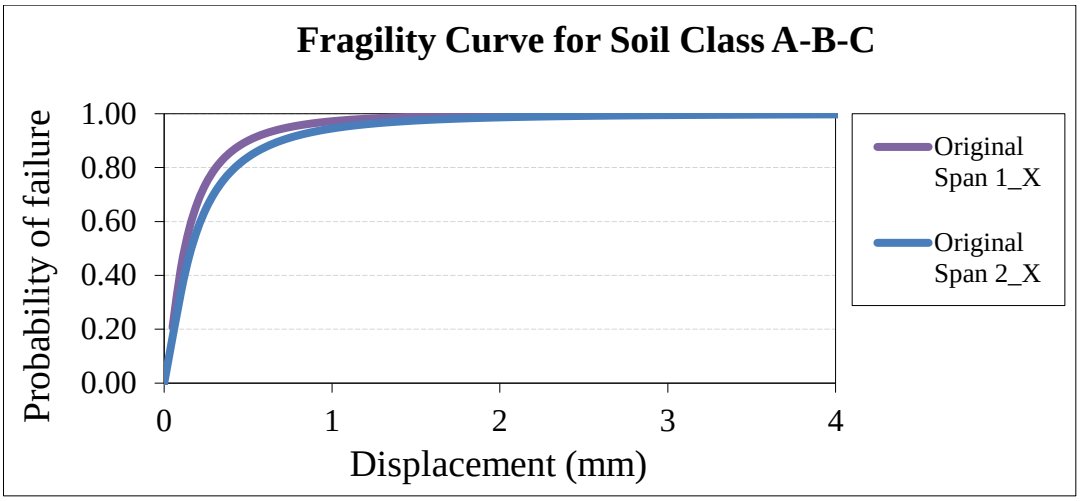


**(a)** X direction

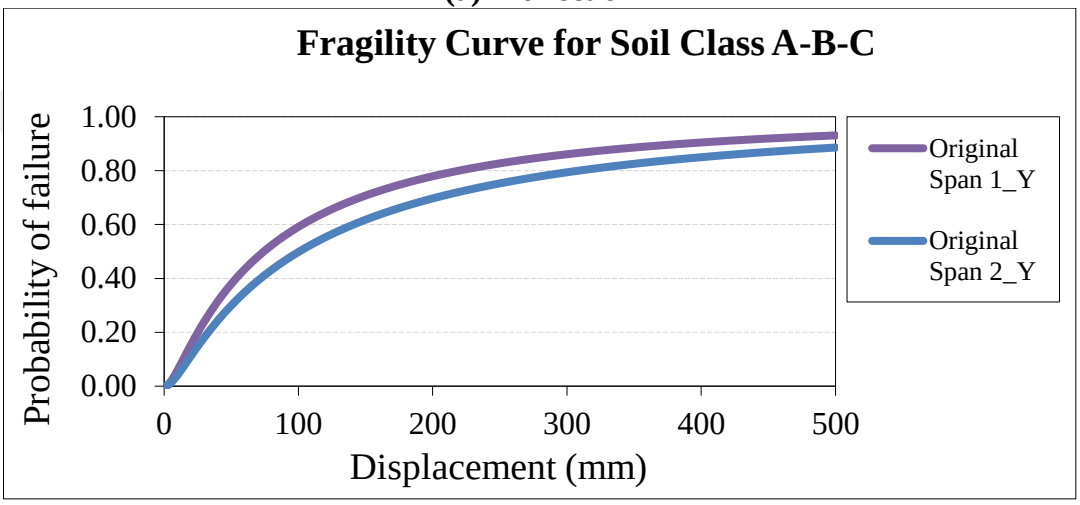


**(b)** Y direction

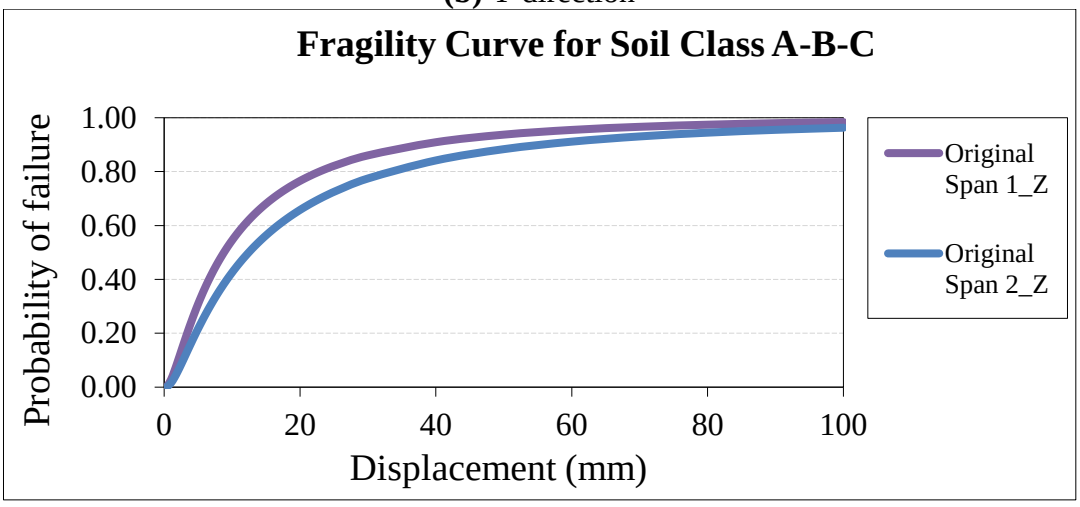


**(c)** Z direction

**Figure B.4 :** Fragility curves of original Cambazkaya bridge model for soil class A-B-C.

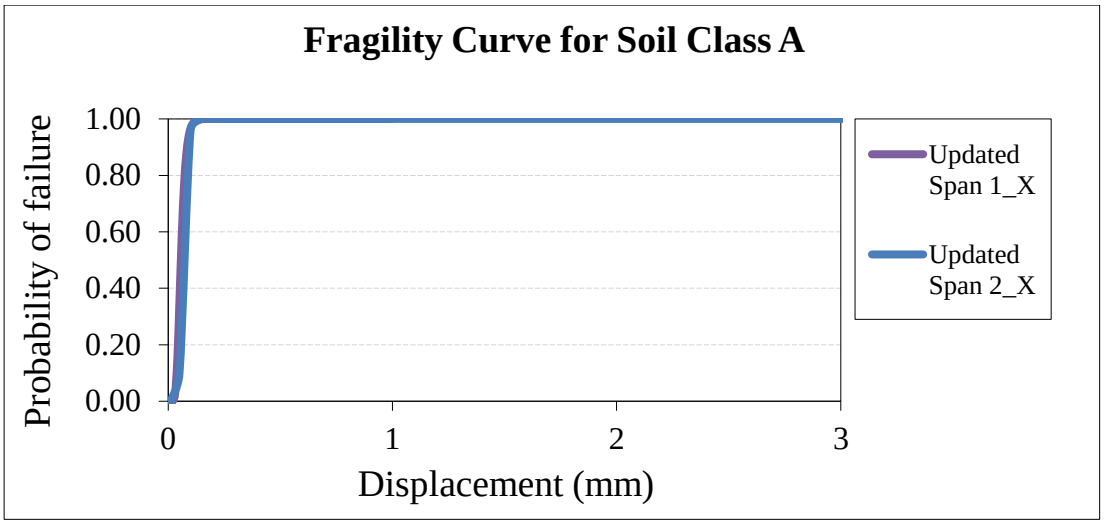


**(a)** X direction

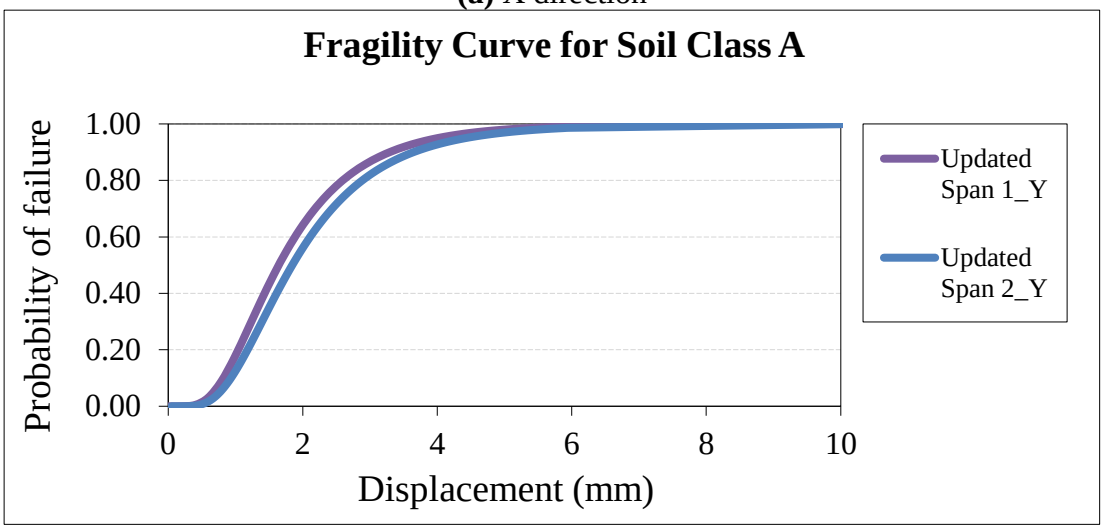


**(b)** Y direction

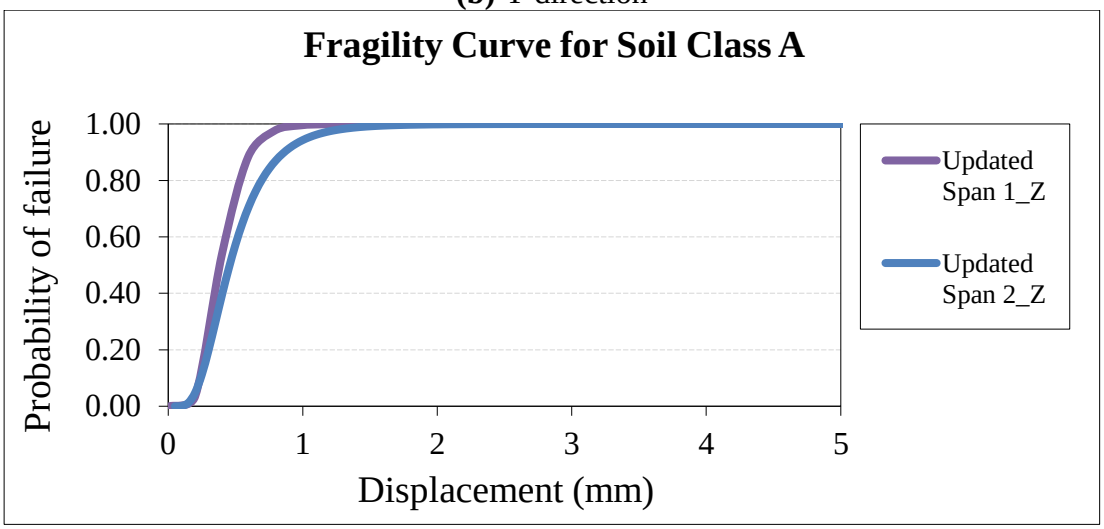


**(c)** Z direction

**Figure B.5 :** Fragility curves of updated Cambazkaya bridge model for soil class A.

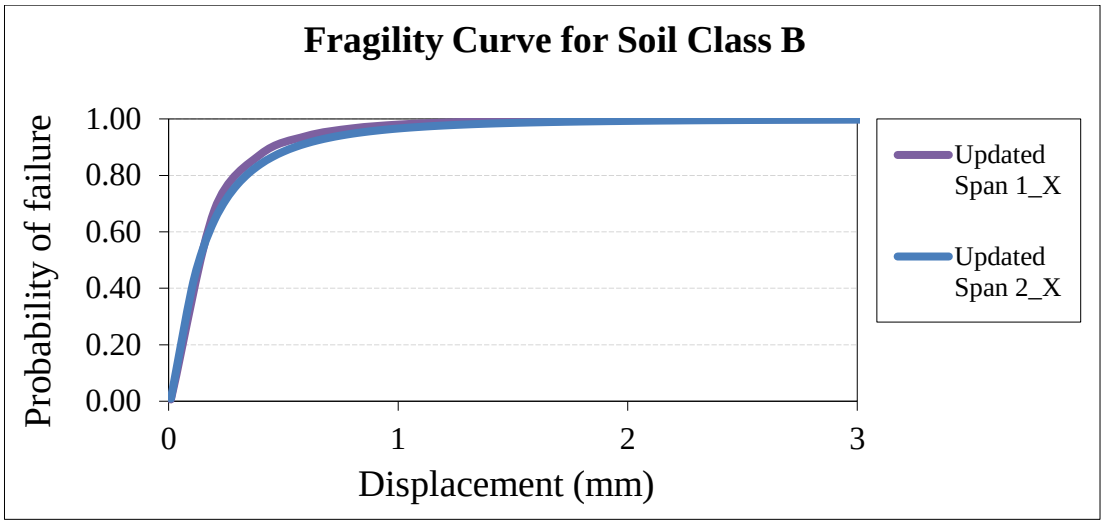


**(a)** X direction

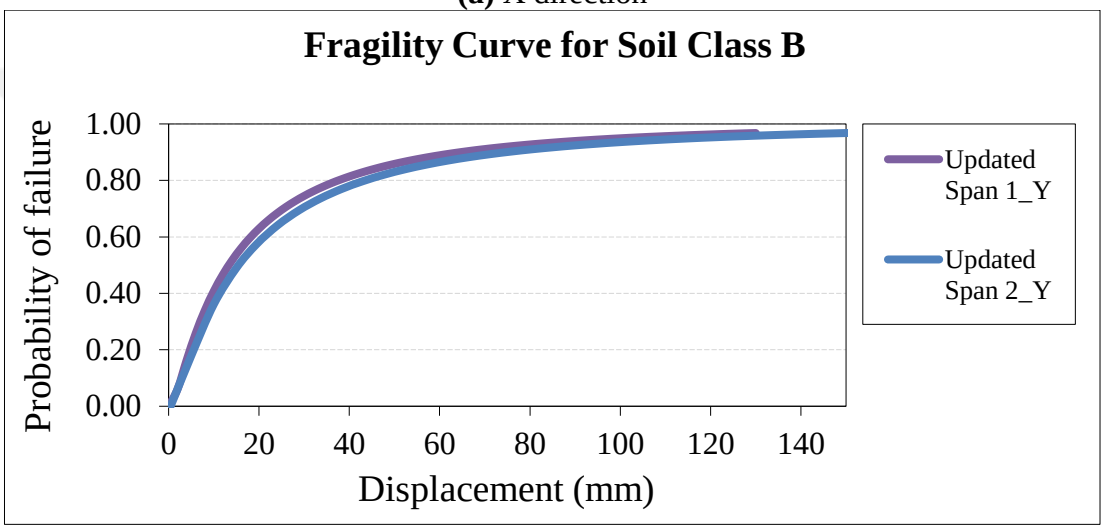


**(b)** Y direction

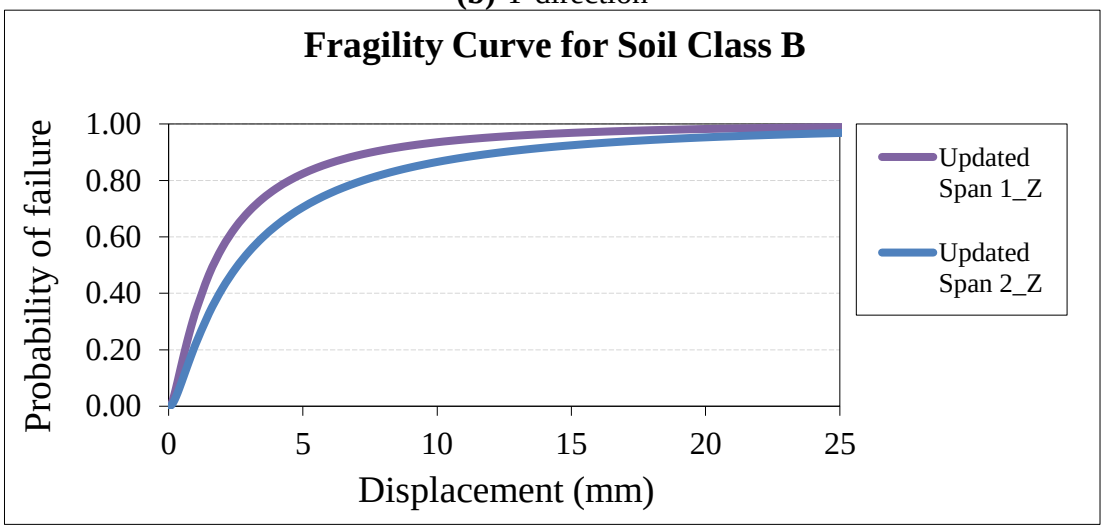


**(c)** Z direction

**Figure B.6 :** Fragility curves of updated Cambazkaya bridge model for soil class B.

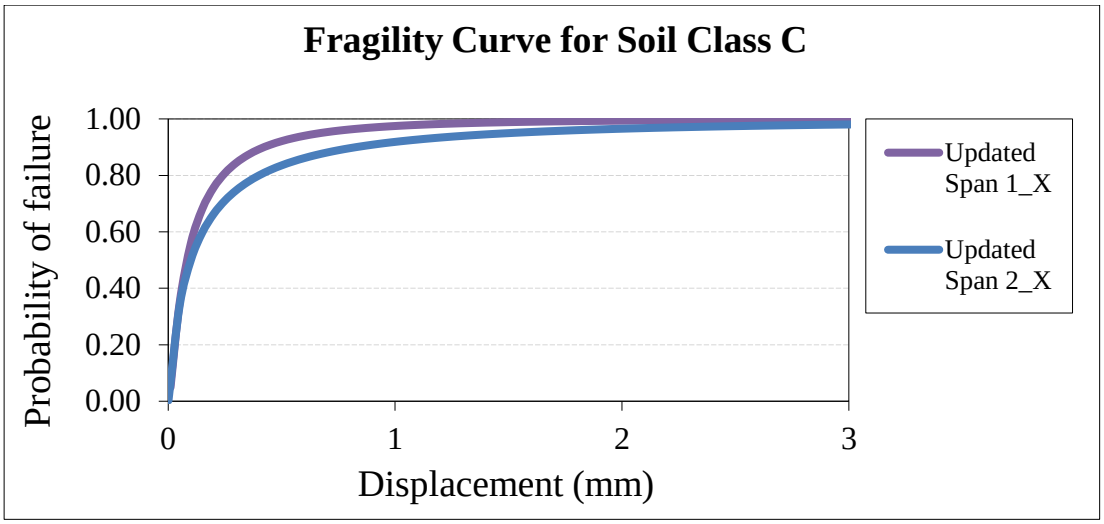


**(a)** X direction

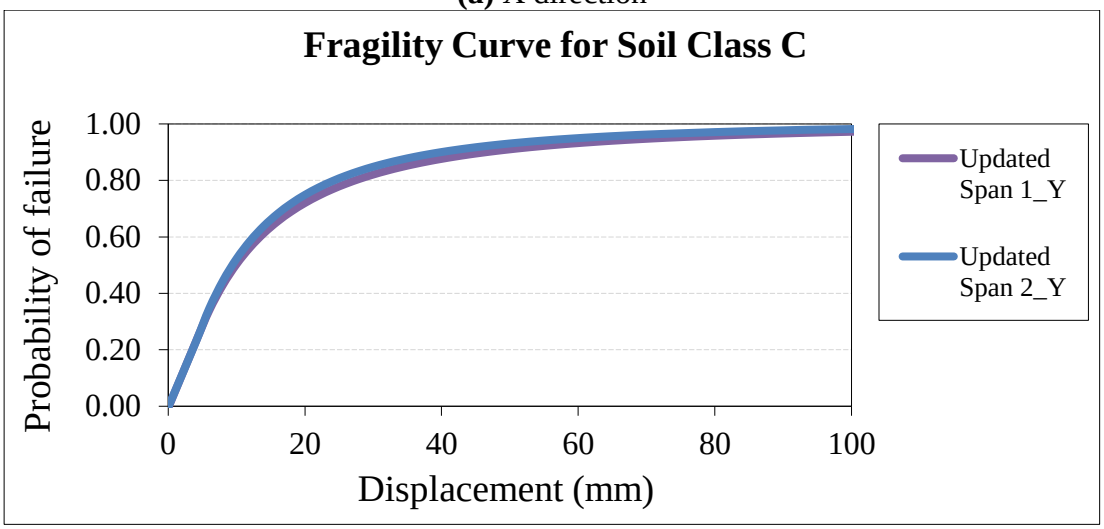


**(b)** Y direction

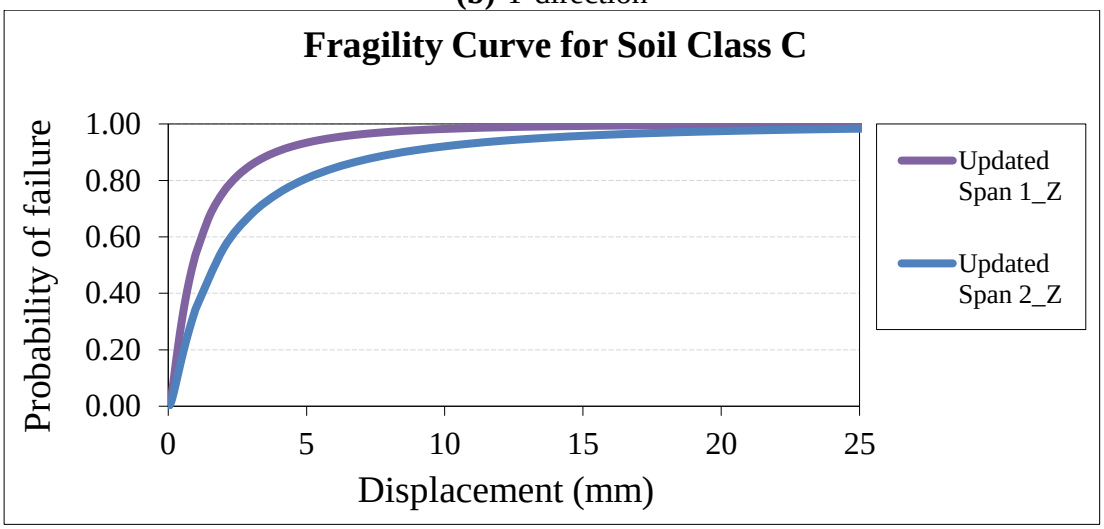


**(c)** Z direction

**Figure B.7 :** Fragility curves of updated Cambazkaya bridge model for soil class C.

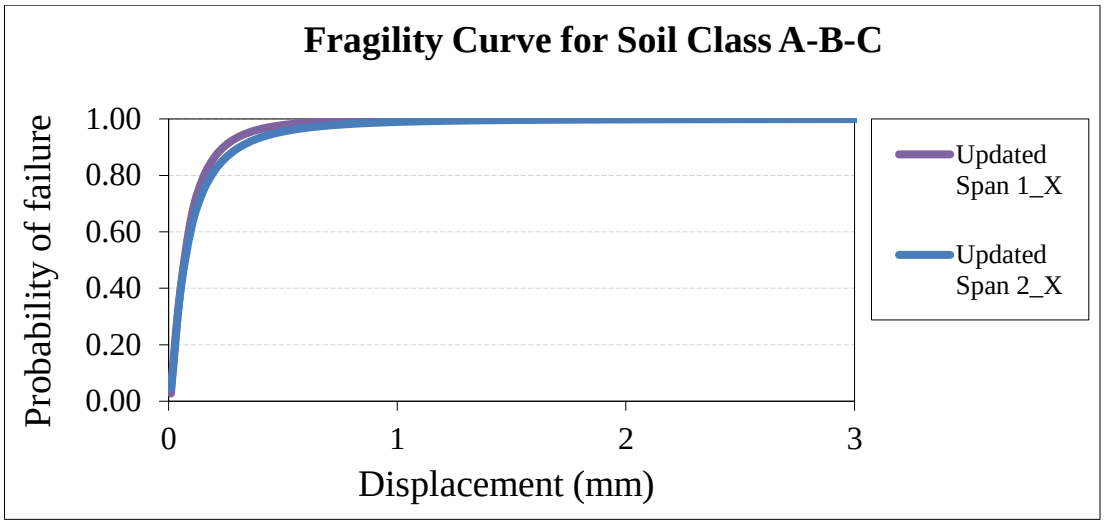


**(a)** X direction

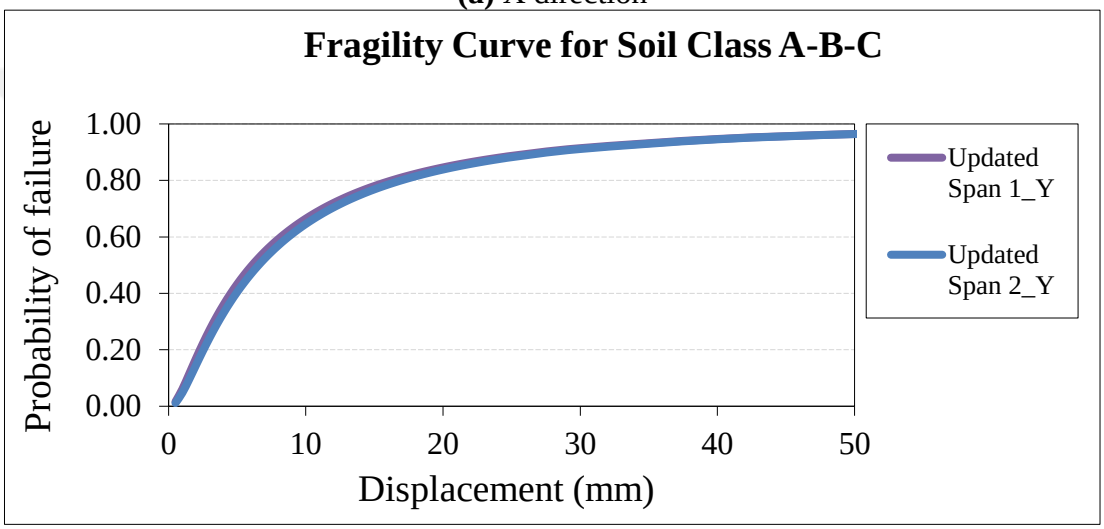


**(b)** Y direction

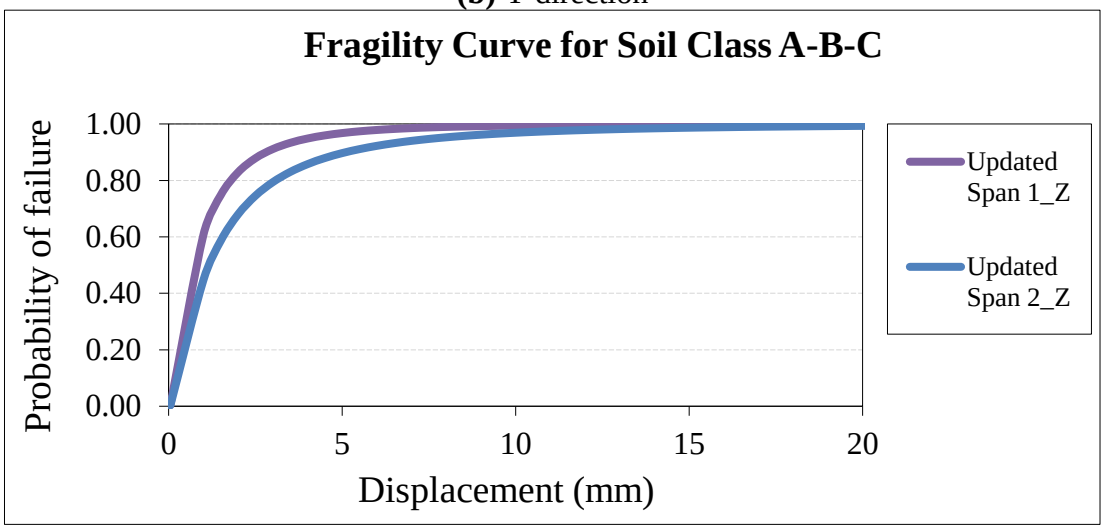


**(c)** Z direction

**Figure B.8 :** Fragility curves of updated Cambazkaya bridge model for soil class A-B-C.

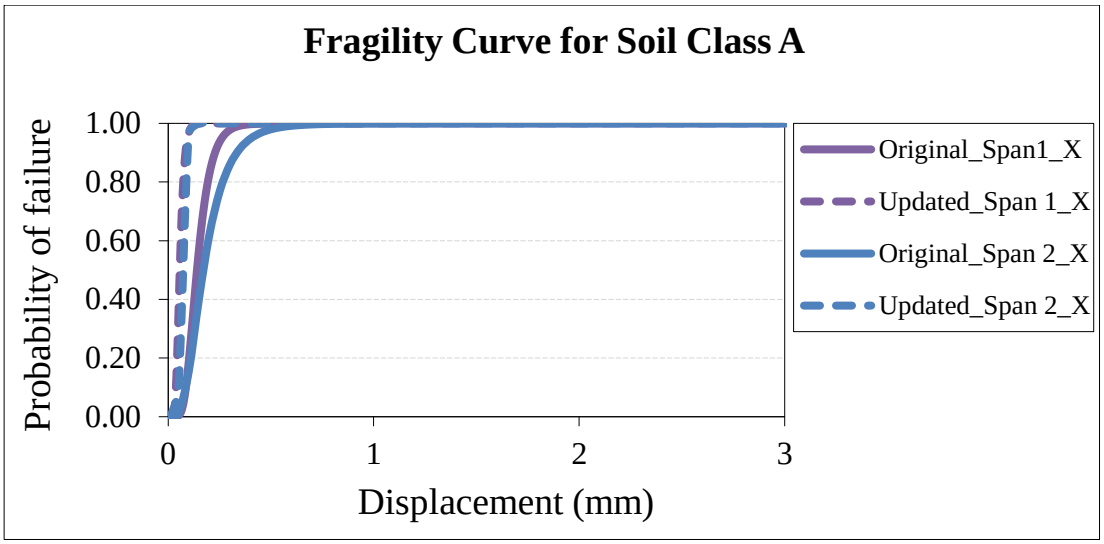


**(a)** X direction

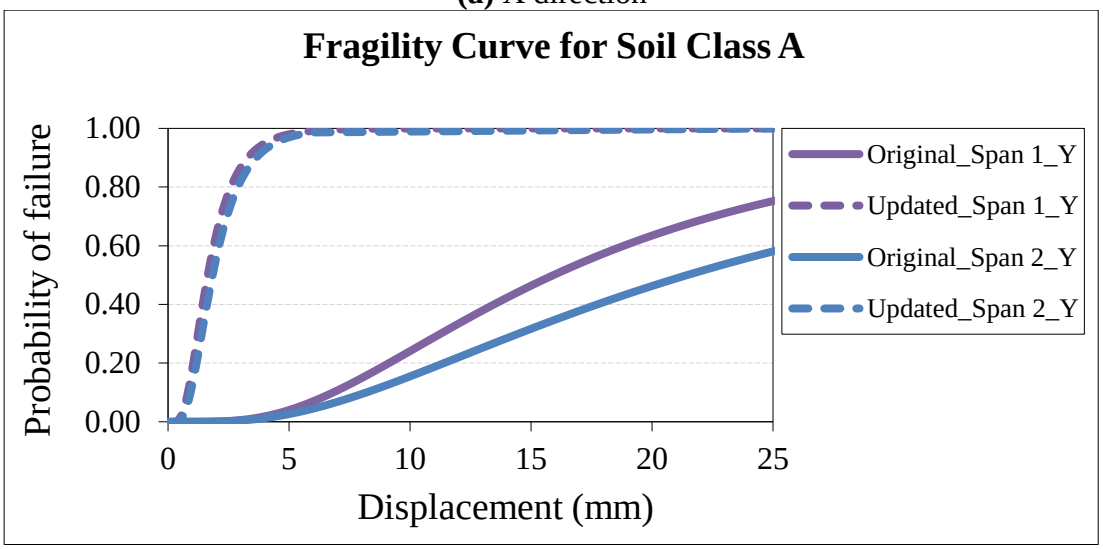


**(b)** Y direction

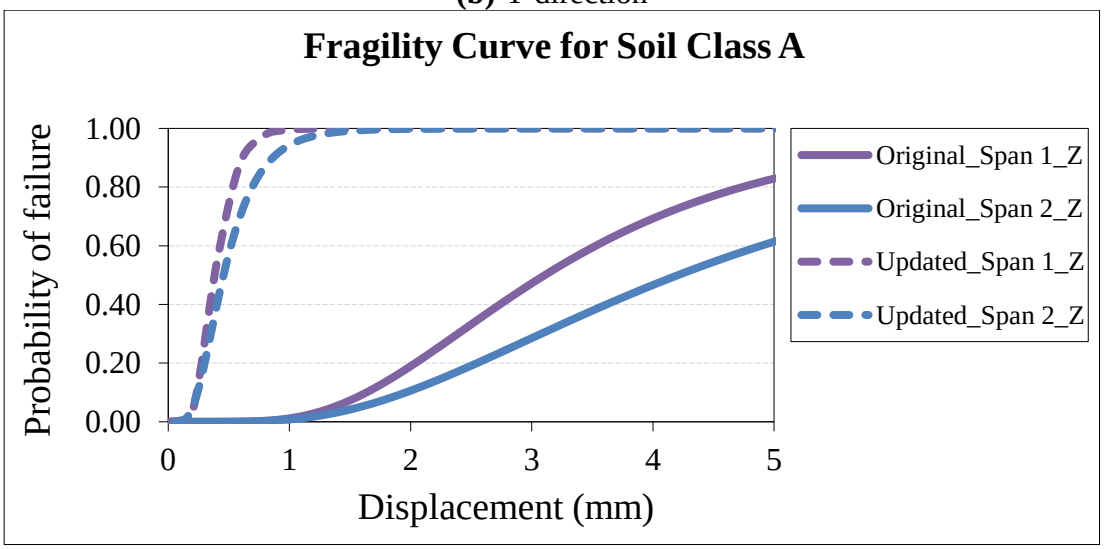


**(c)** Z direction

**Figure B.9 :** Comparison fragility curves of original and updated Cambazkaya bridge model for soil class A.

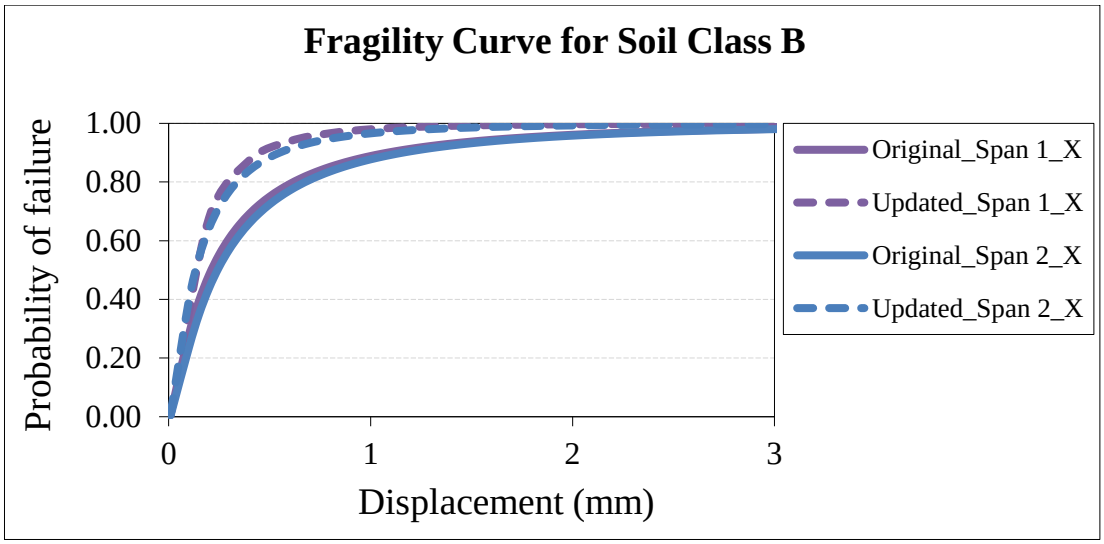


**(a)** X direction

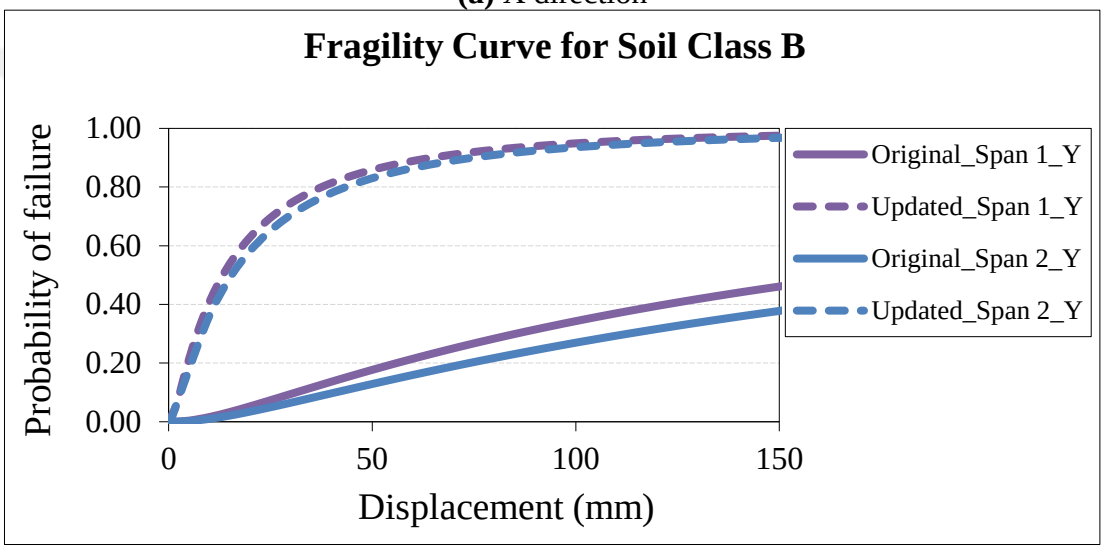


**(b)** Y direction

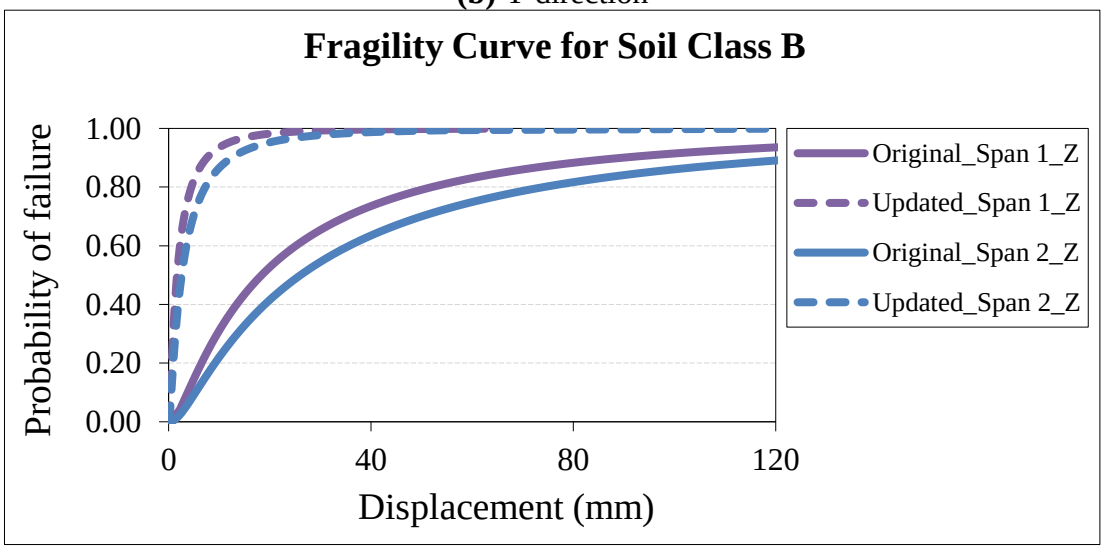


**(c)** Z direction

**Figure B.10 :** Comparison fragility curves of original and updated Cambazkaya bridge model for soil class B.

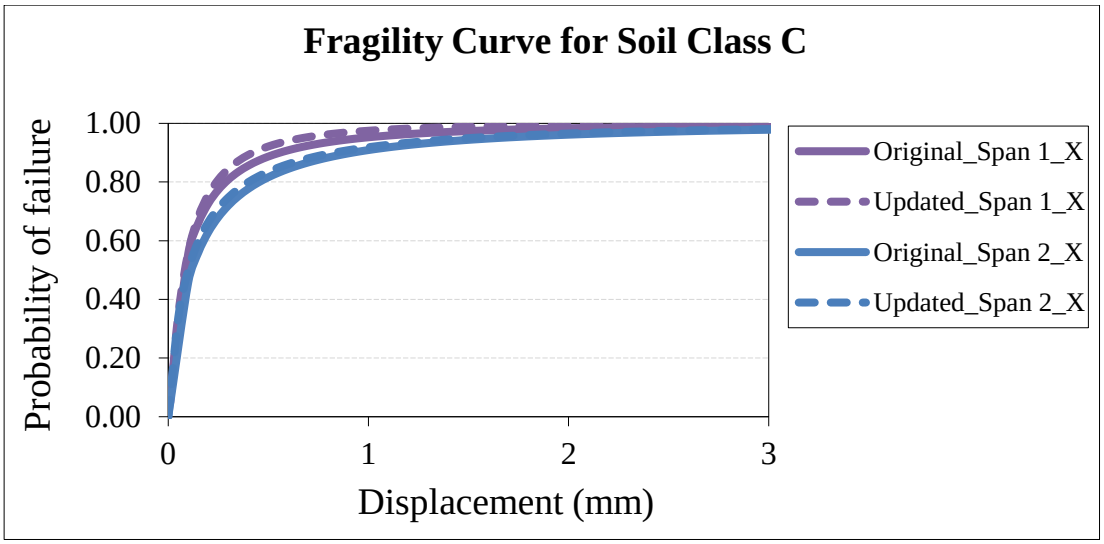


**(a)** X direction

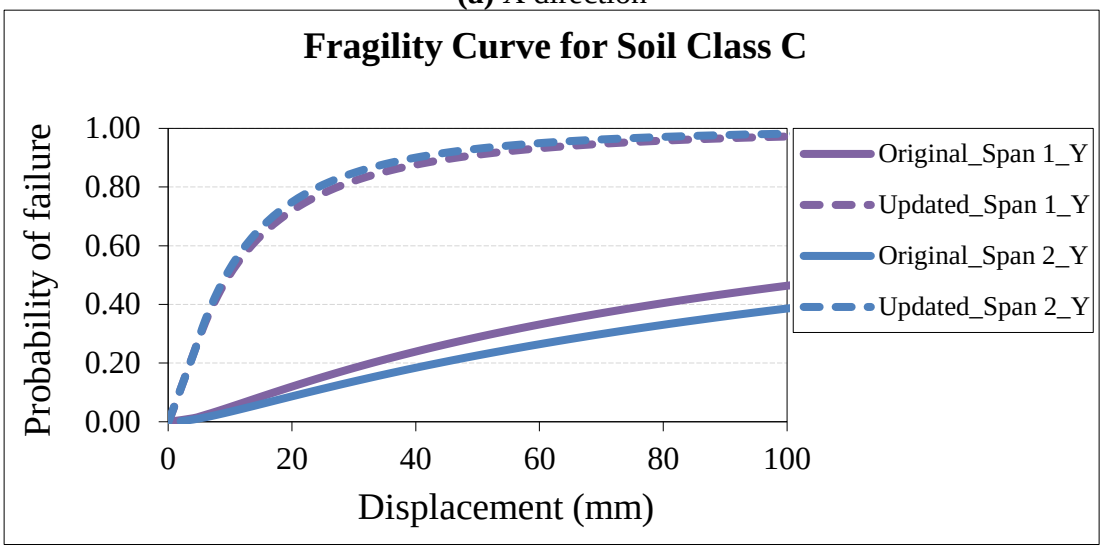


**(b)** Y direction

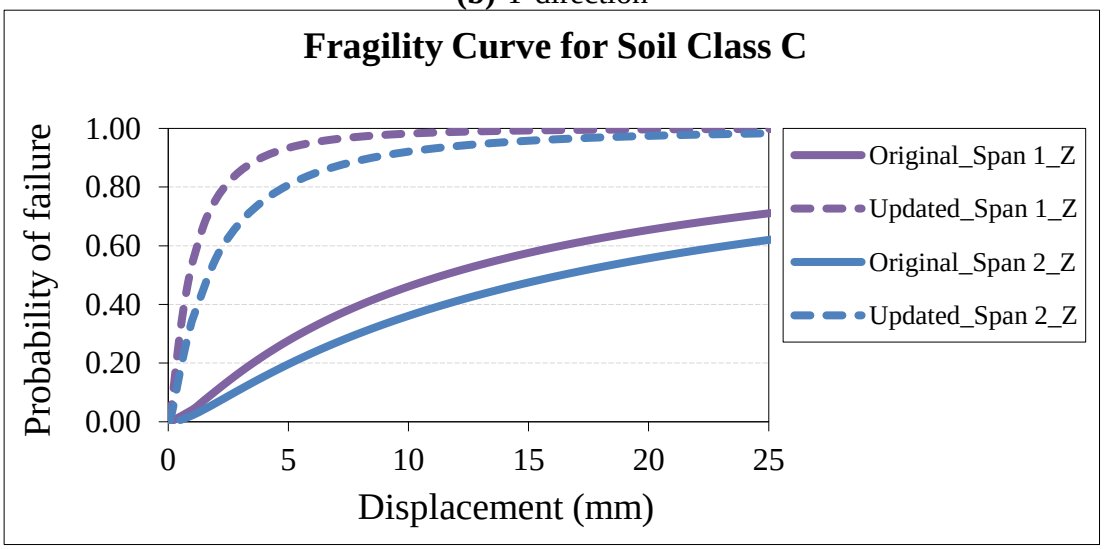


**(c)** Z direction

**Figure B.11 :** Comparison fragility curves of original and updated Cambazkaya bridge model for soil class C.

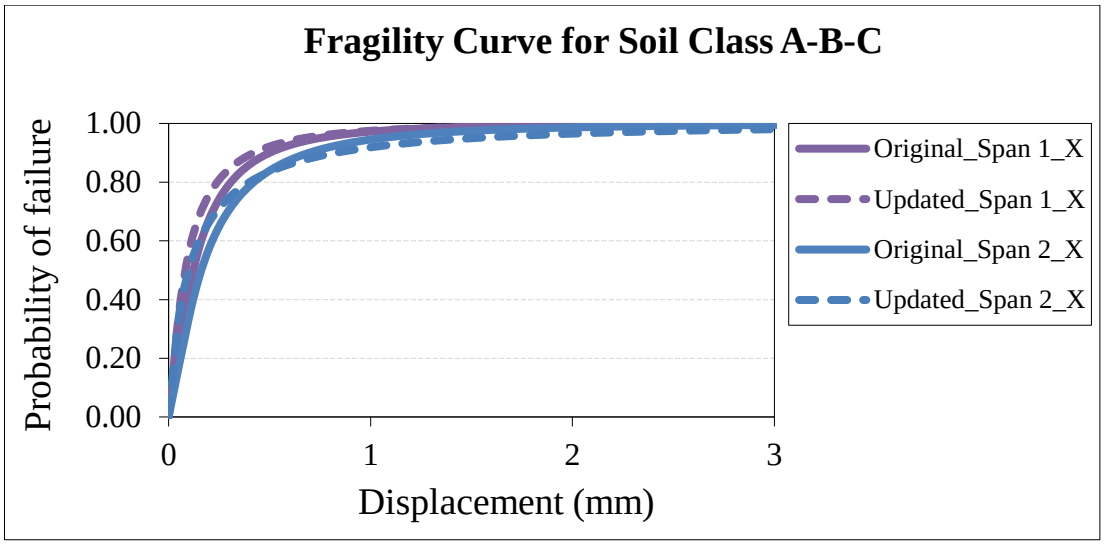


**(a)** X direction

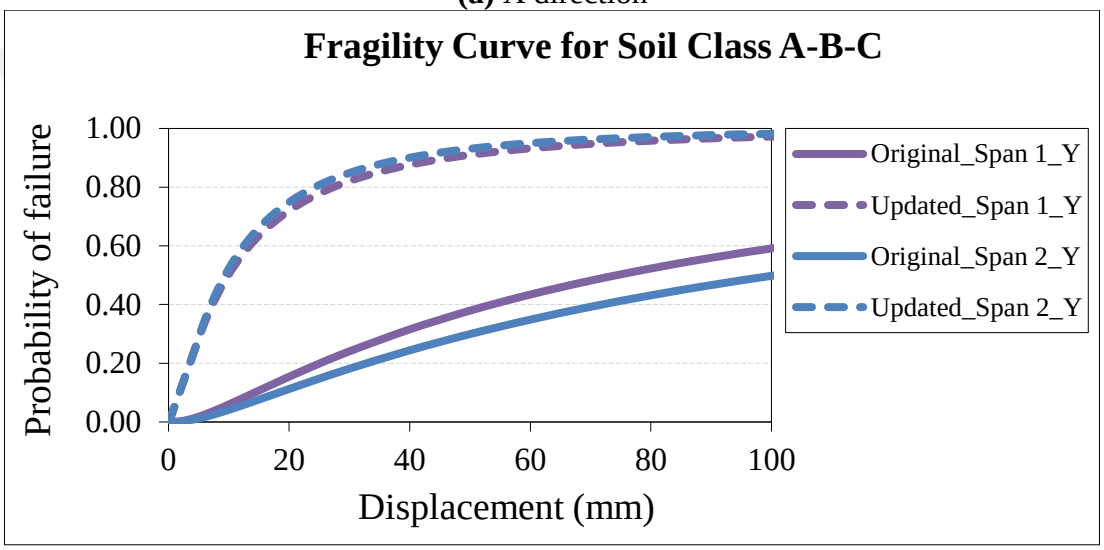


**(b)** Y direction

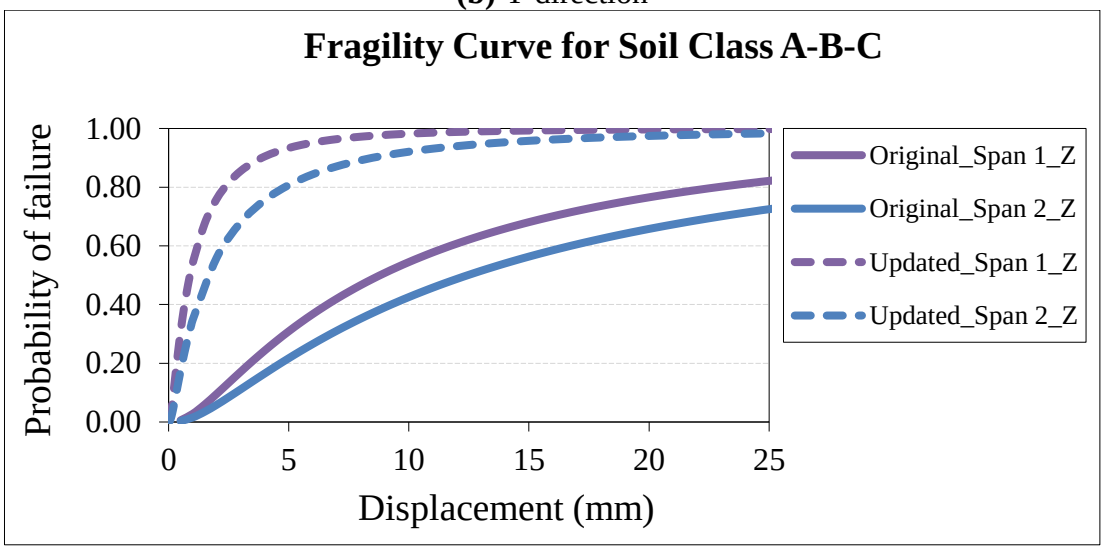


**(c)** Z direction

**Figure B.12 :** Comparison fragility curves of original and updated Cambazkaya bridge model for soil class A-B-C.

## APPENDIX C

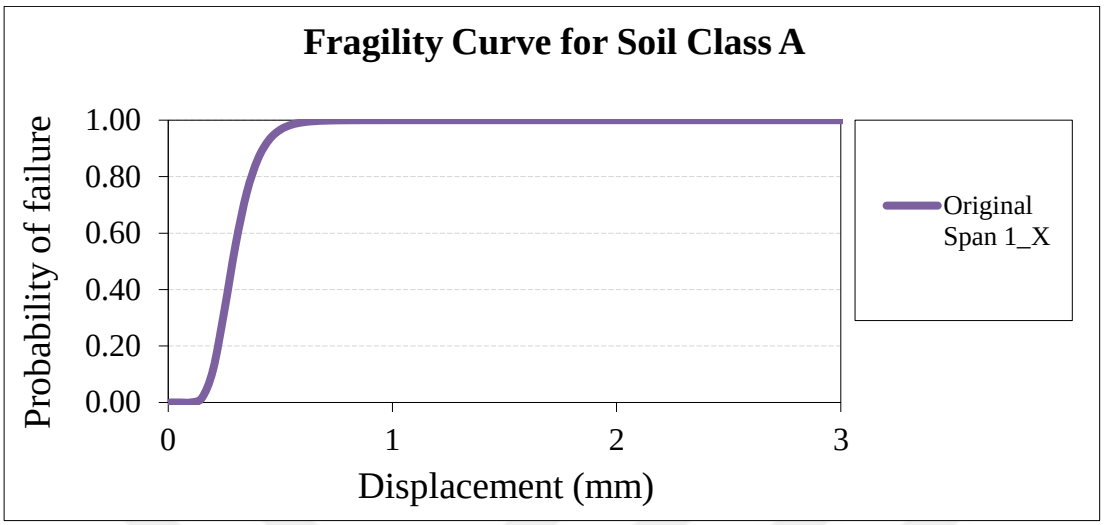


**(a)** X direction

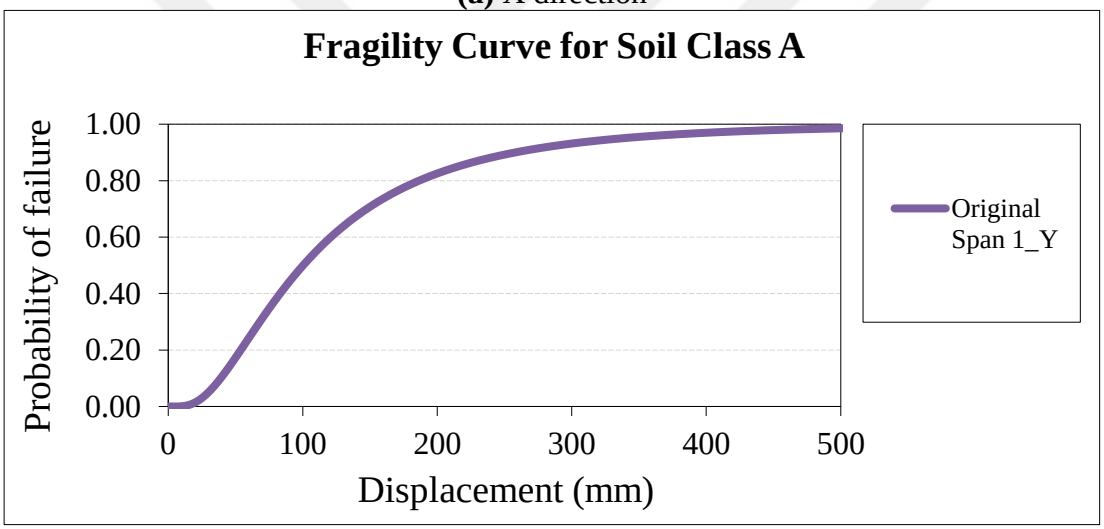


**(b)** Y direction

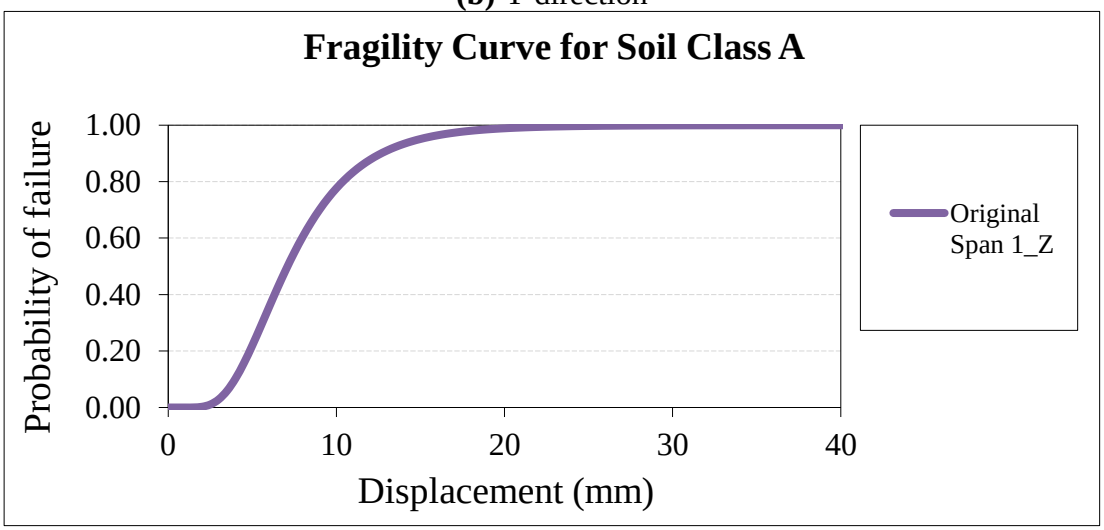


**(c)** Z direction

**Figure C.1 :** Fragility curves of original Ceyhan bridge model for soil class A.

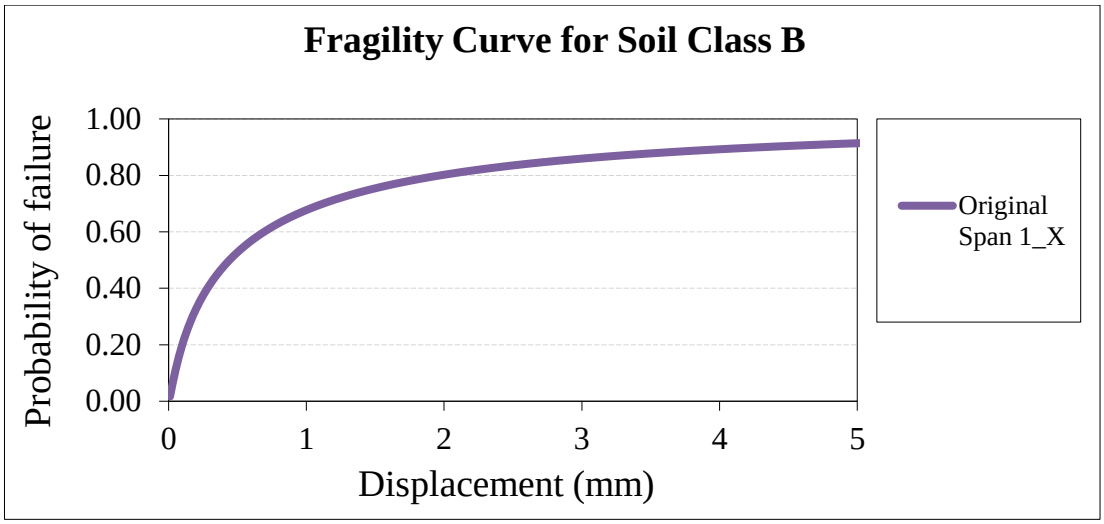


**(a)** X direction

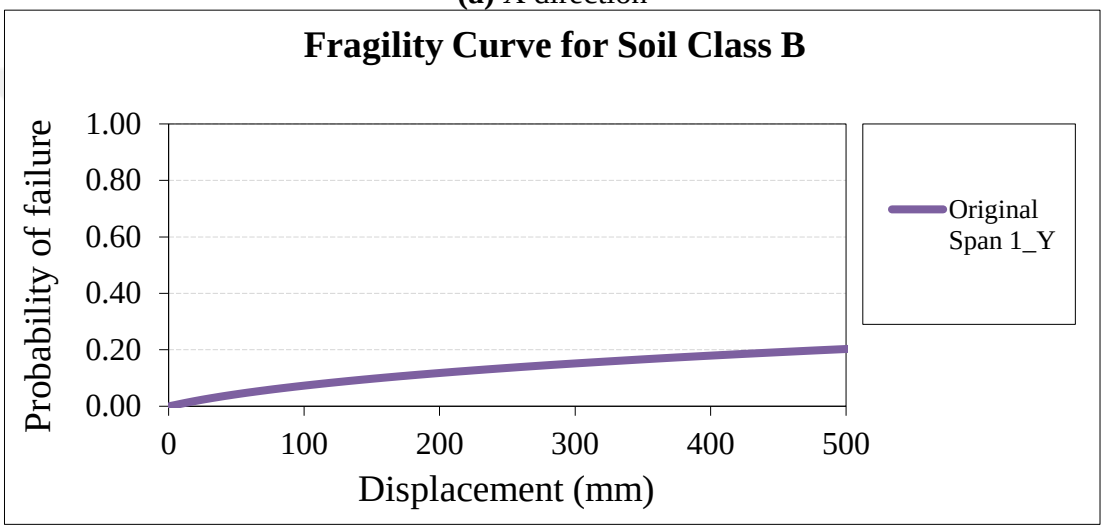


**(b)** Y direction

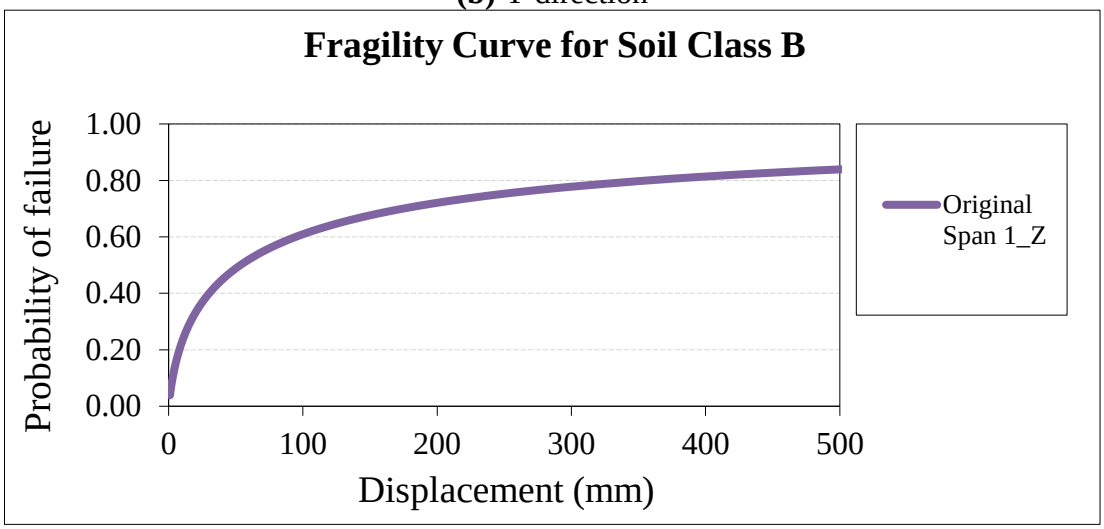


**(c)** Z direction

**Figure C.2 :** Fragility curves of original Ceyhan bridge model for soil class B.

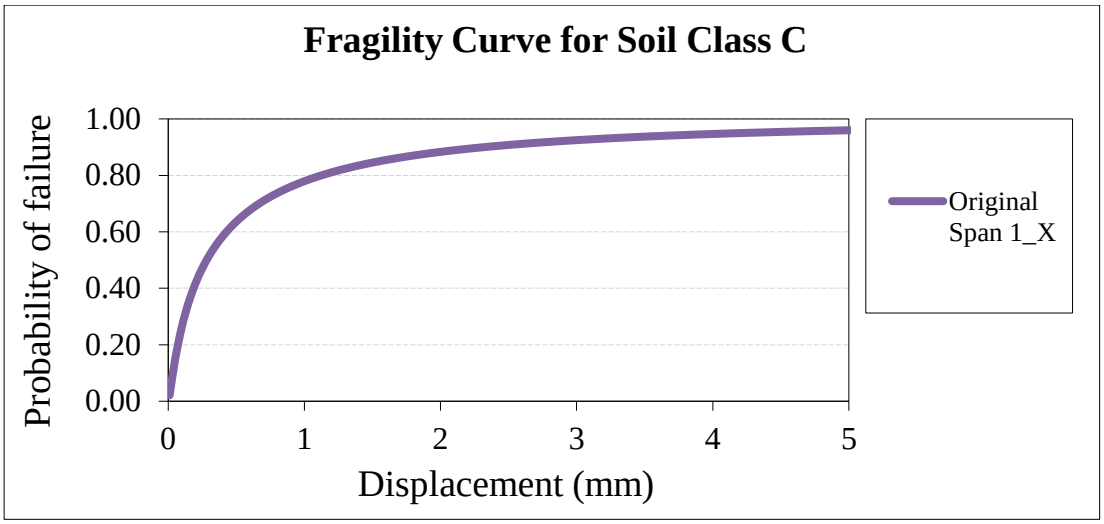


**(a)** X direction

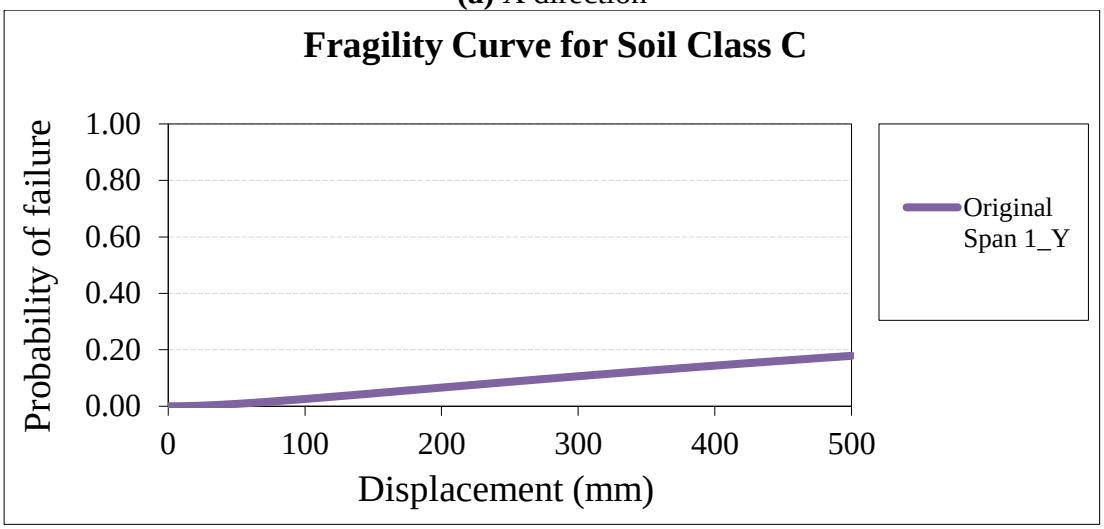


**(b)** Y direction

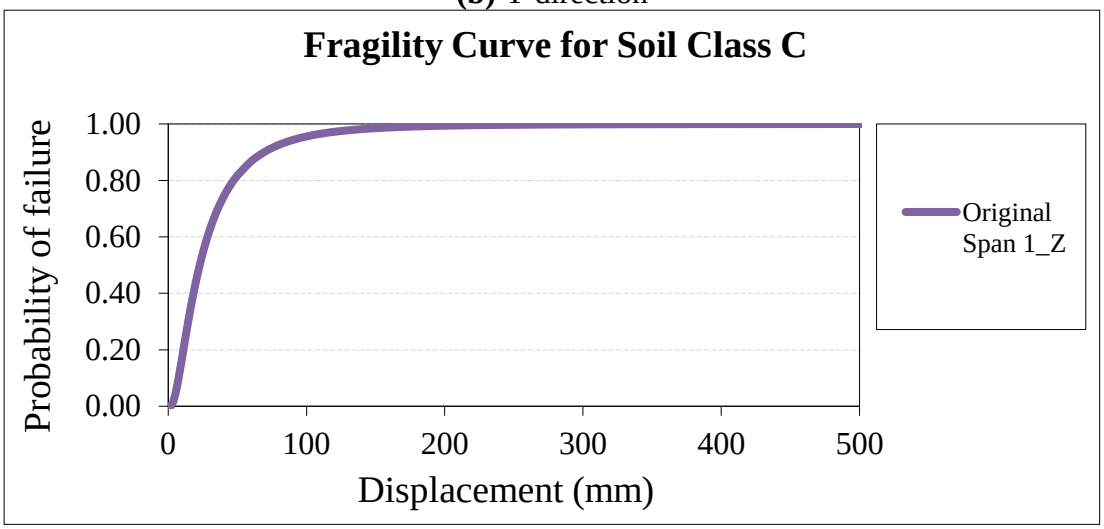


**(c)** Z direction

**Figure C.3 :** Fragility curves of original Ceyhan bridge model for soil class C.

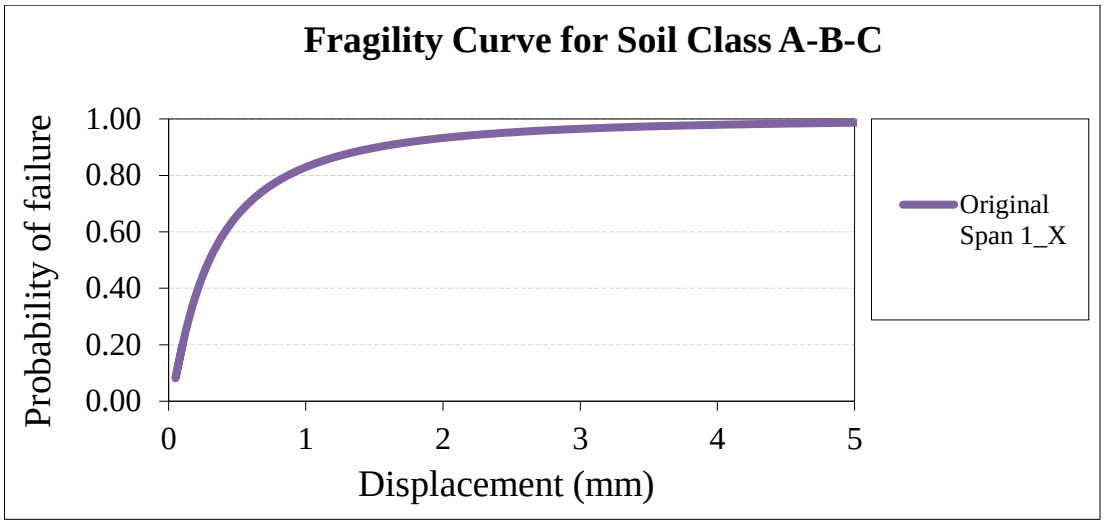


**(a)** X direction

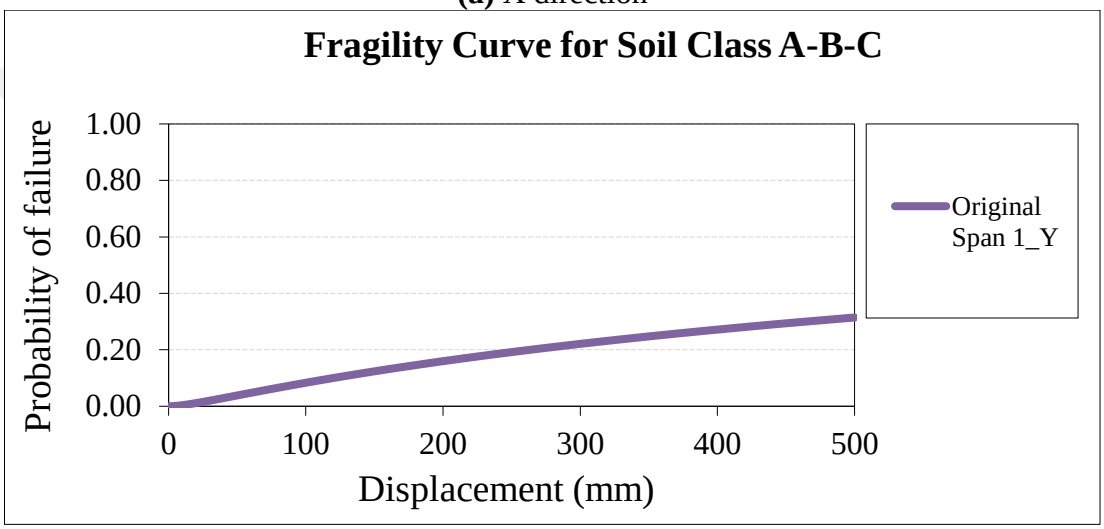


**(b)** Y direction

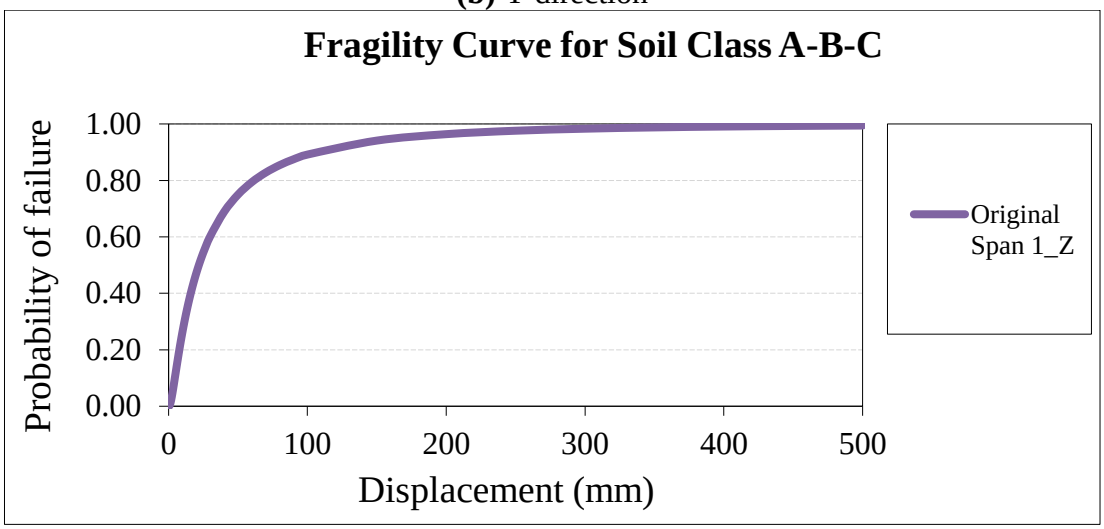


**(c)** Z direction

**Figure C.4 :** Fragility curves of original Ceyhan bridge model for soil class C.

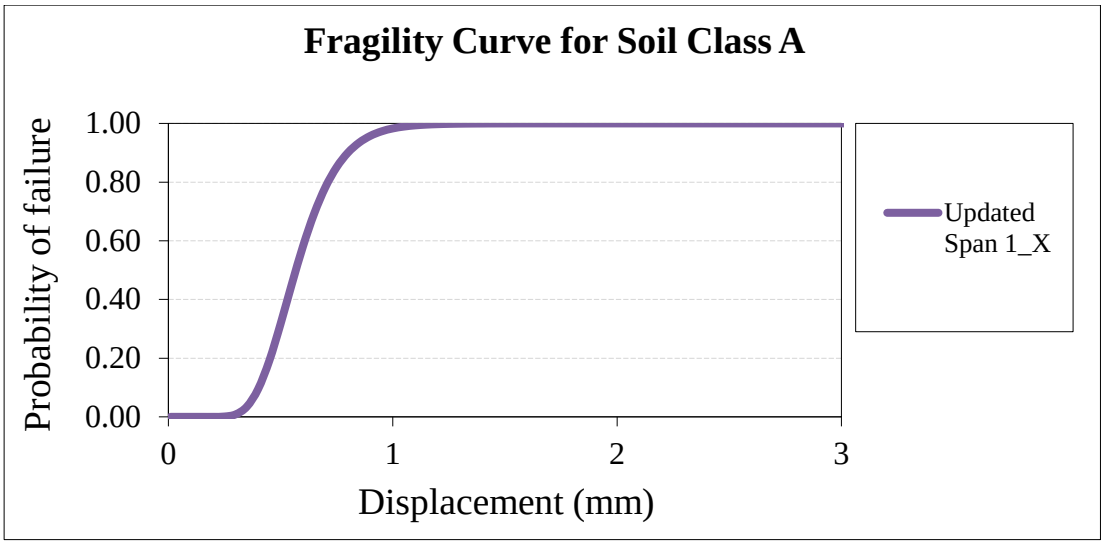


**(a)** X direction

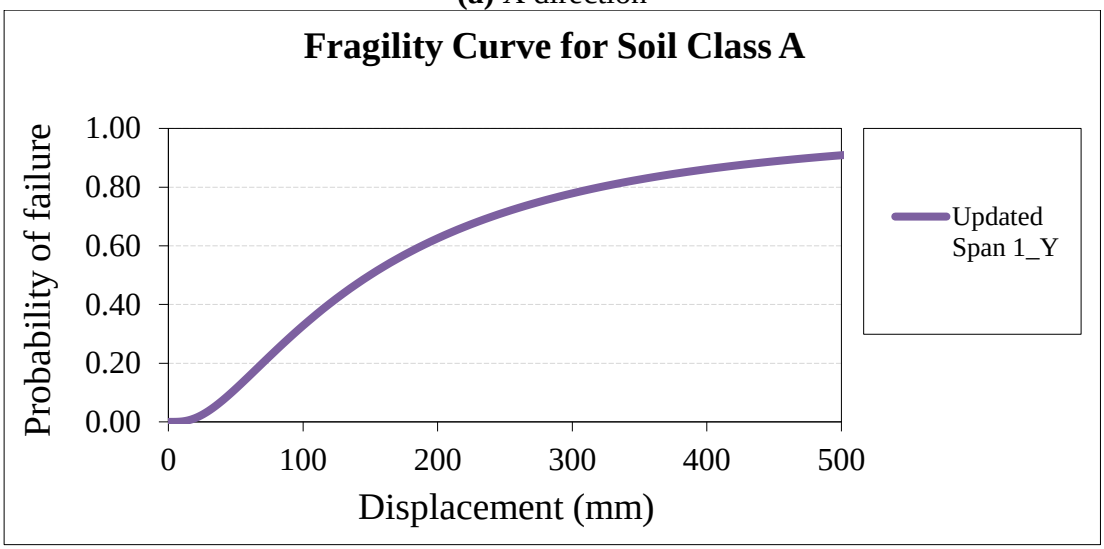


**(b)** Y direction

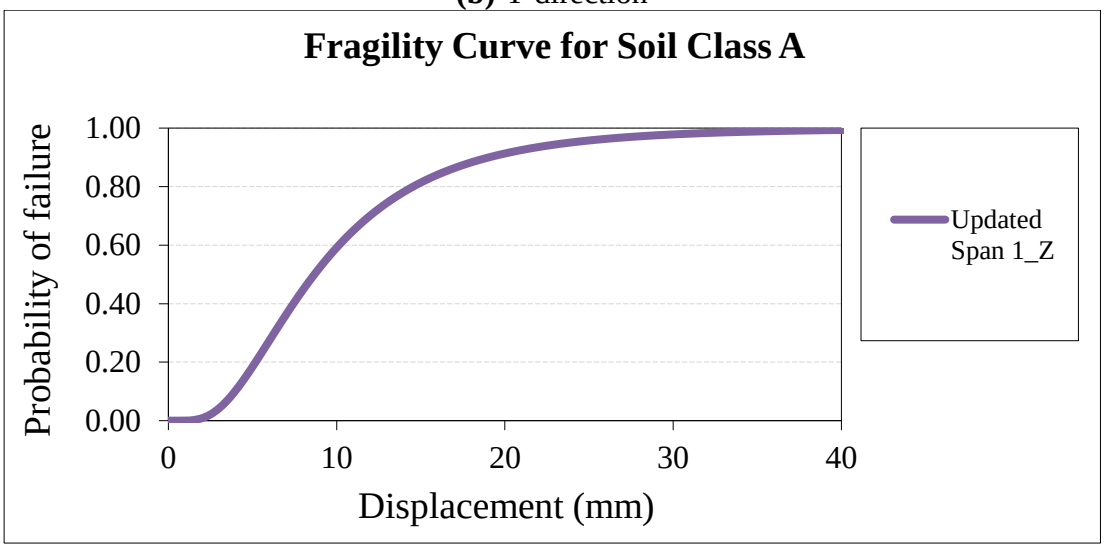


**(c)** Z direction

**Figure C.5 :** Fragility curves of updated Ceyhan bridge model for soil class A.

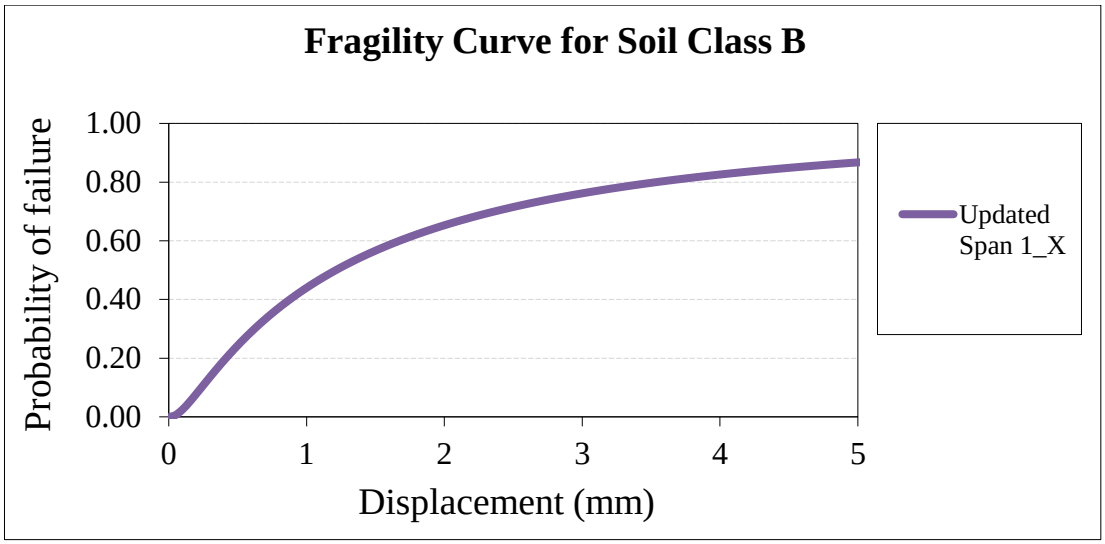


**(a)** X direction

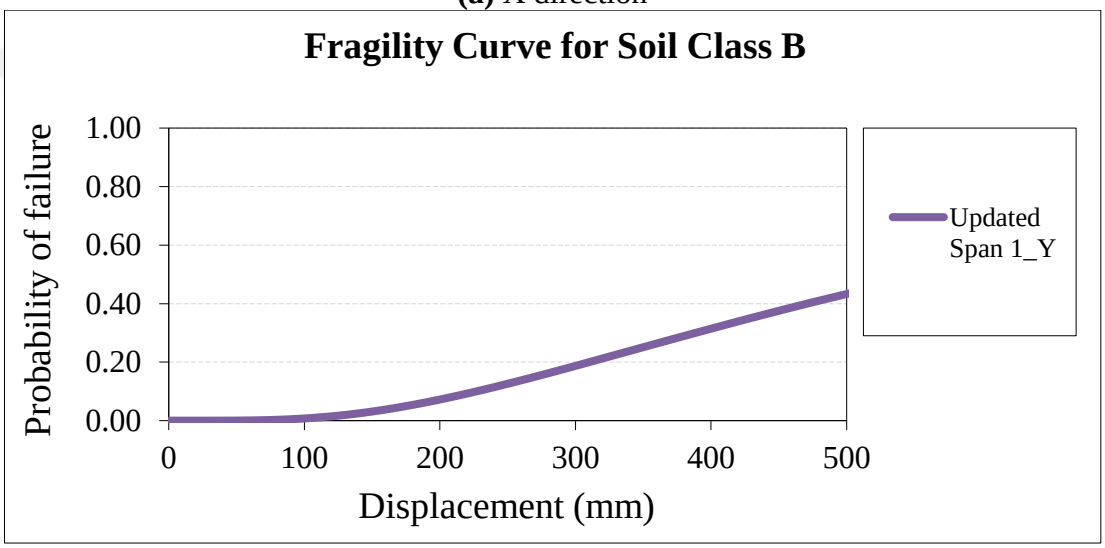


**(b)** Y direction

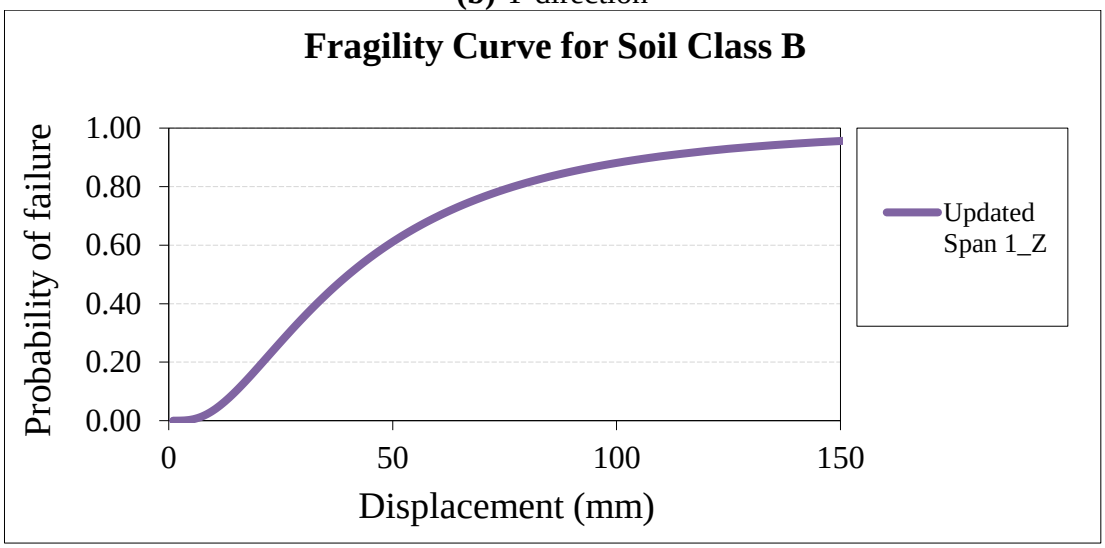


**(c)** Z direction

**Figure C.6 :** Fragility curves of updated Ceyhan bridge model for soil class B.

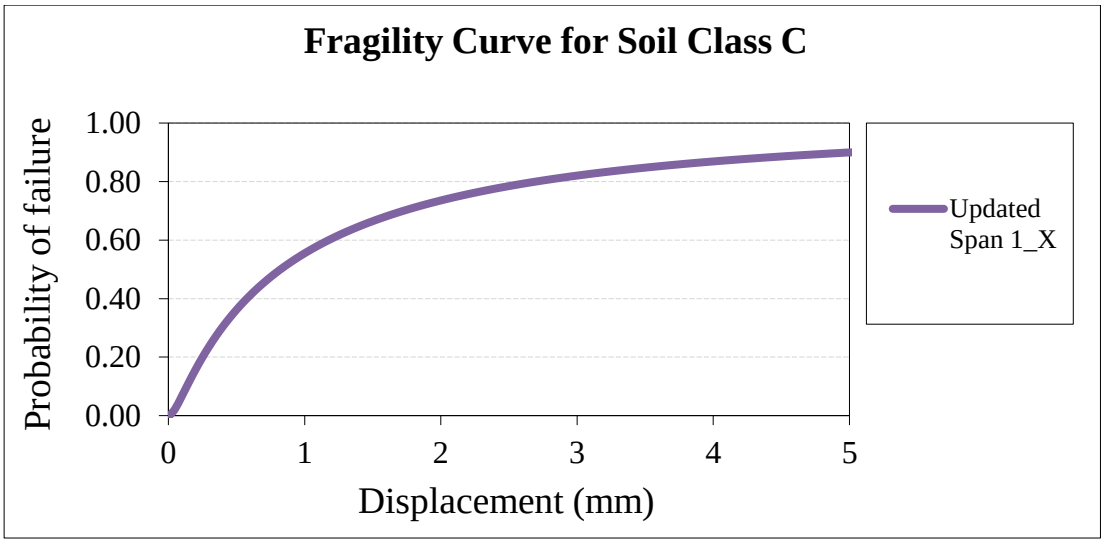


**(a)** X direction

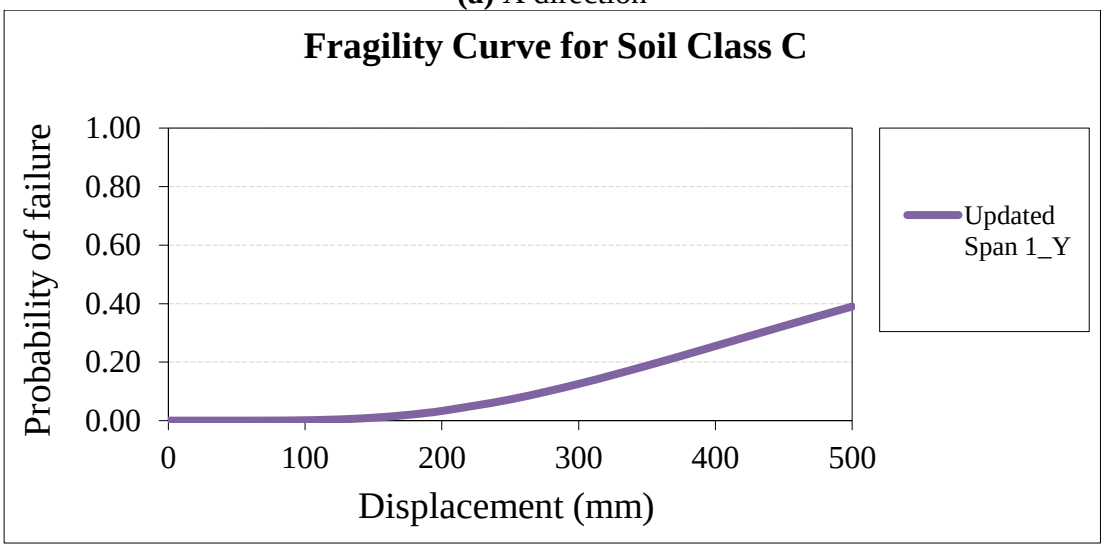


**(b)** Y direction

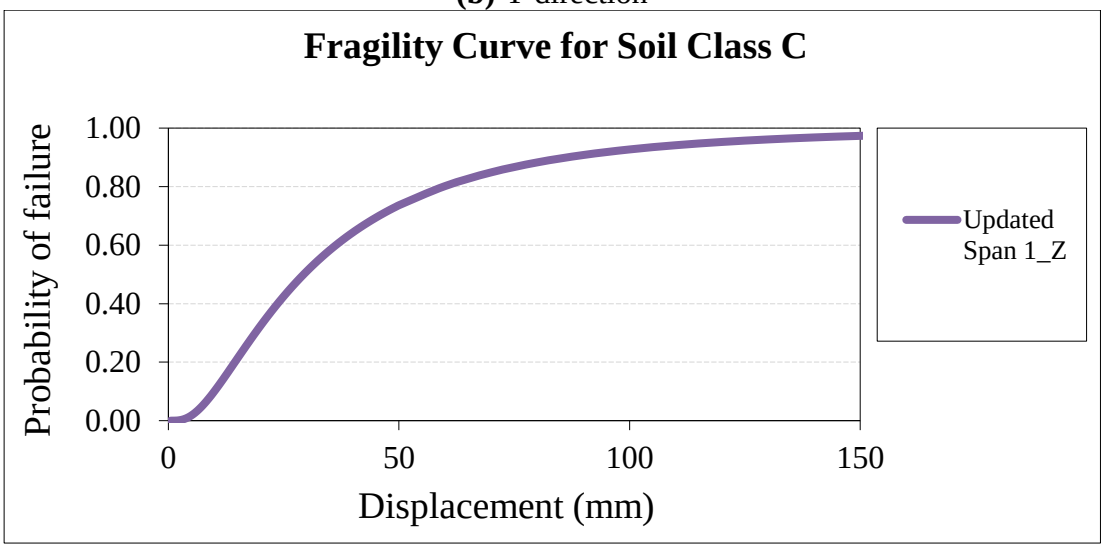


**(c)** Z direction

**Figure C.7 :** Fragility curves of updated Ceyhan bridge model for soil class C.

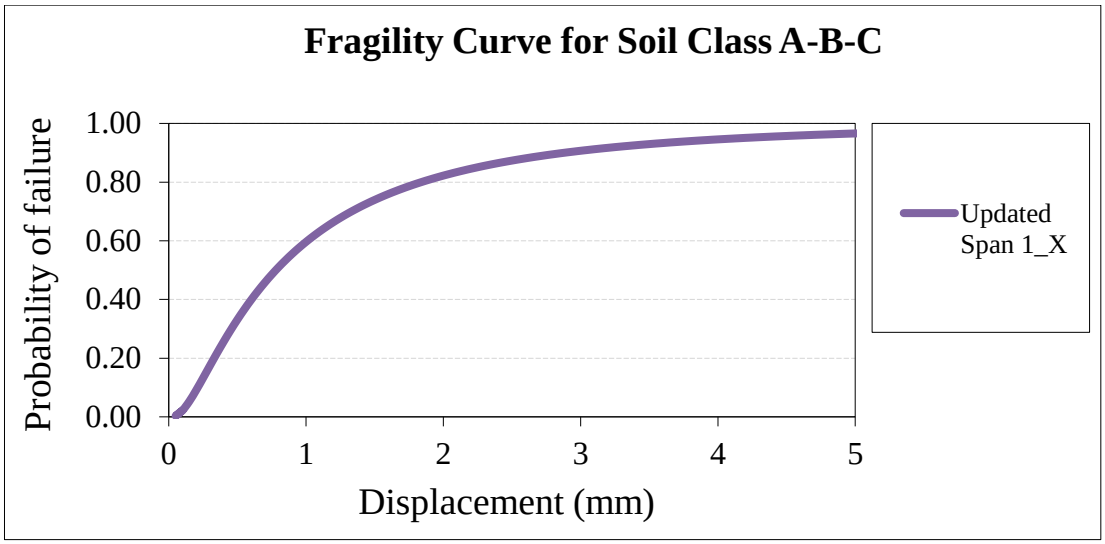


**(a)** X direction

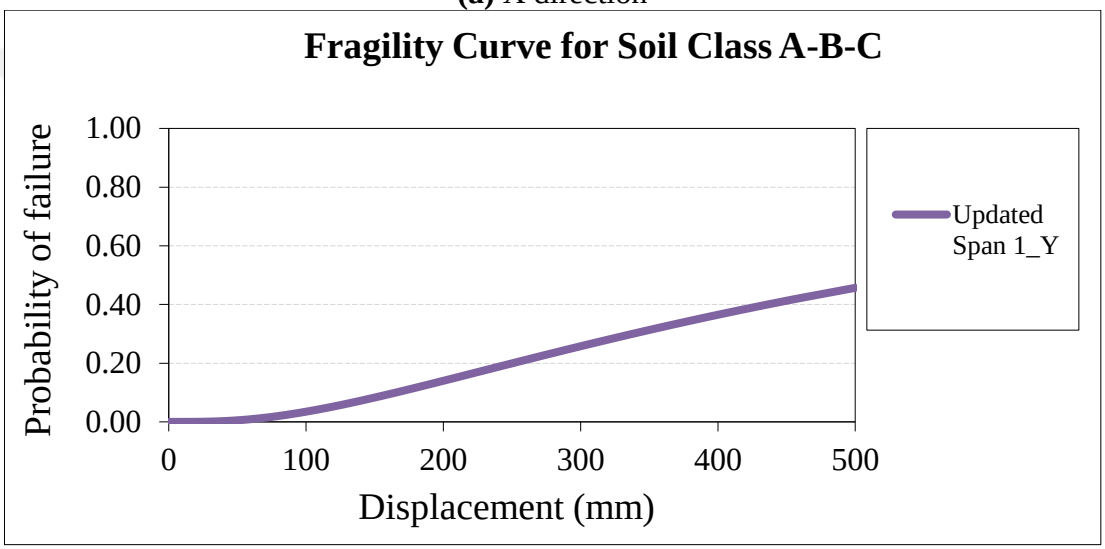


**(b)** Y direction

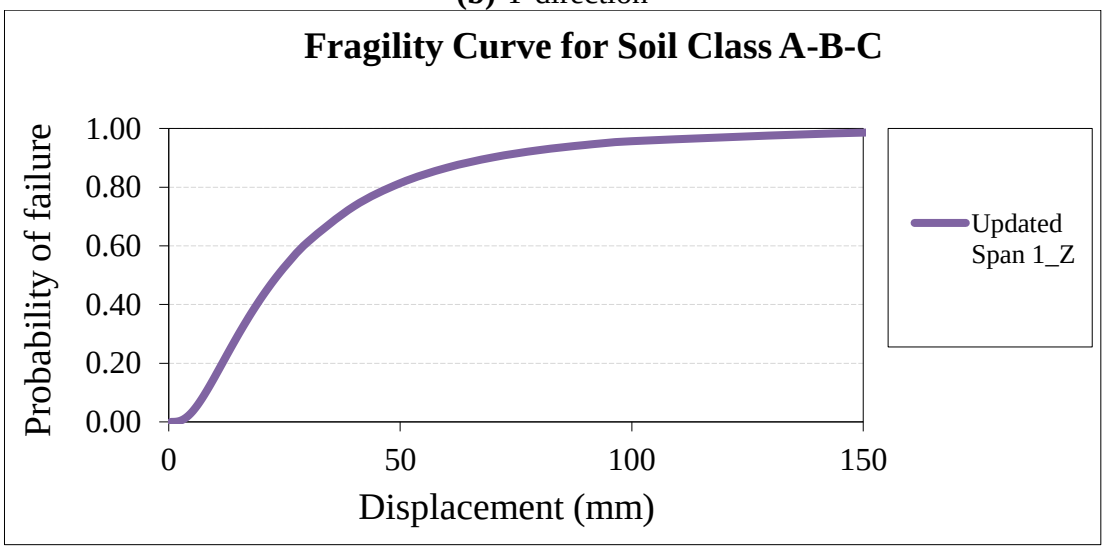


**(c)** Z direction

**Figure C.8 :** Fragility curves of updated Ceyhan bridge model for soil class A-B-C.

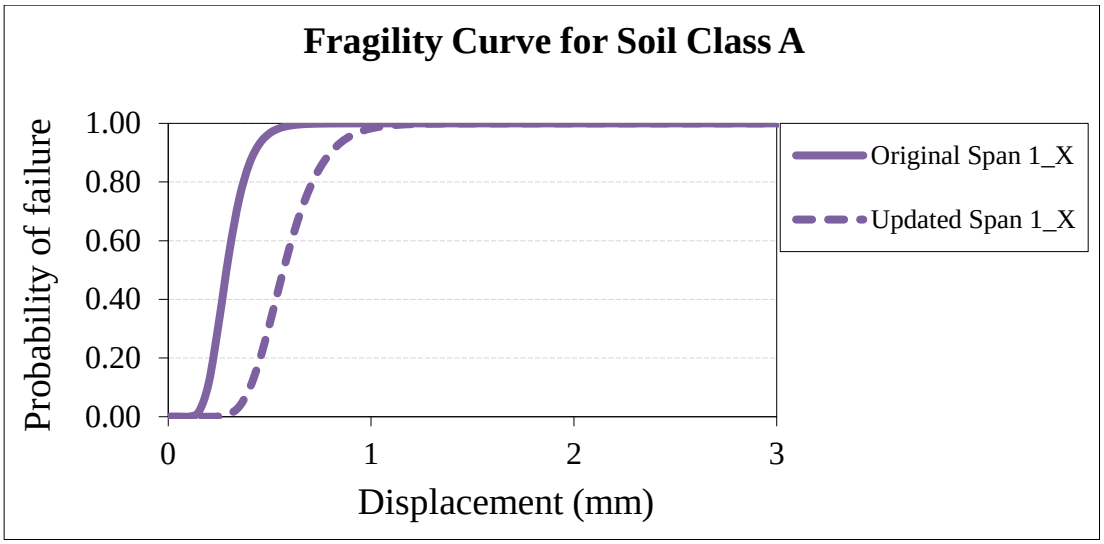


**(a)** X direction

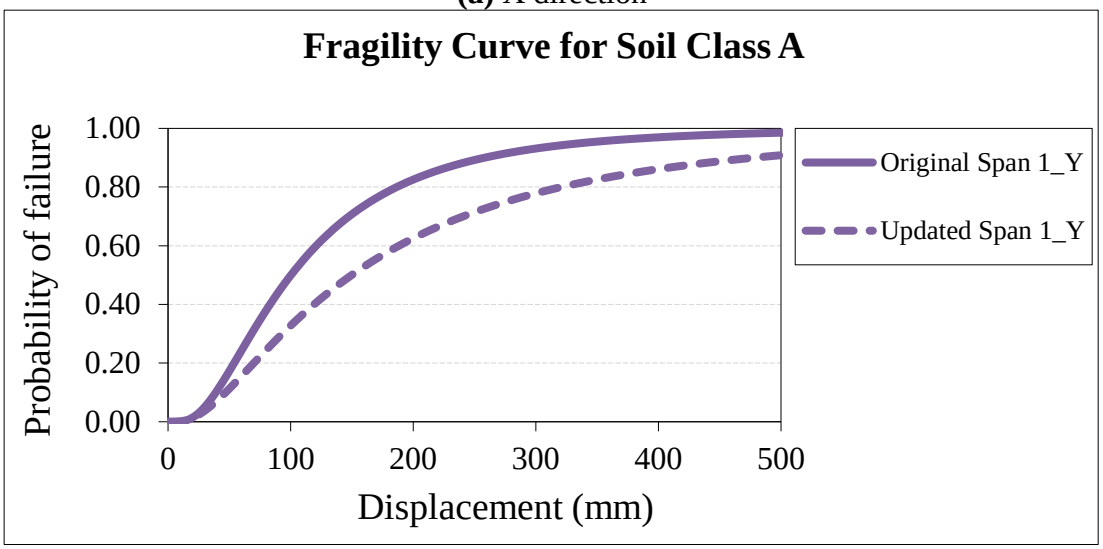


**(b)** Y direction

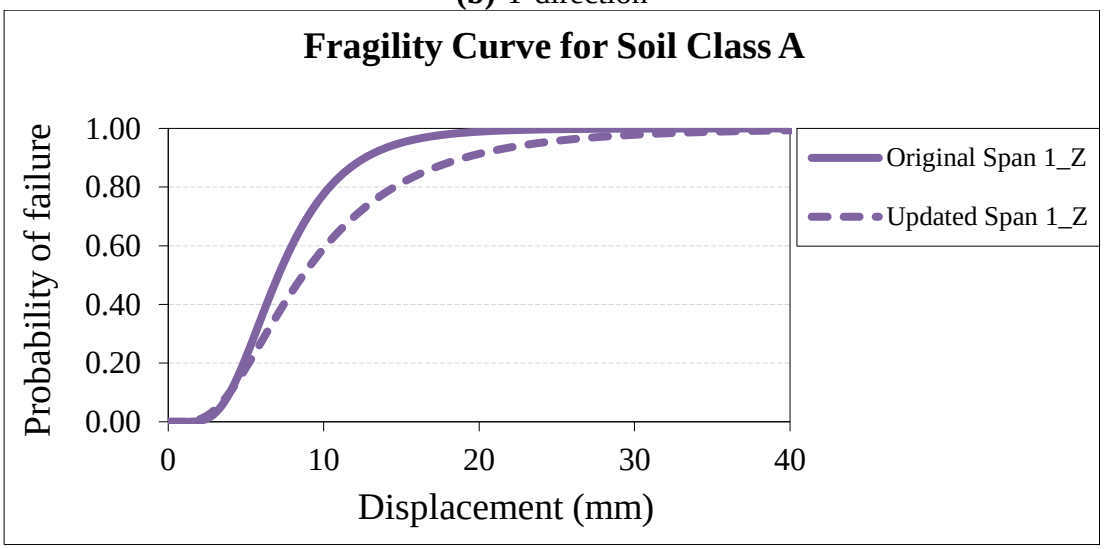


**(c)** Z direction

**Figure C.9 :** Comparison fragility curves of original and updated Ceyhan bridge model for soil class A.

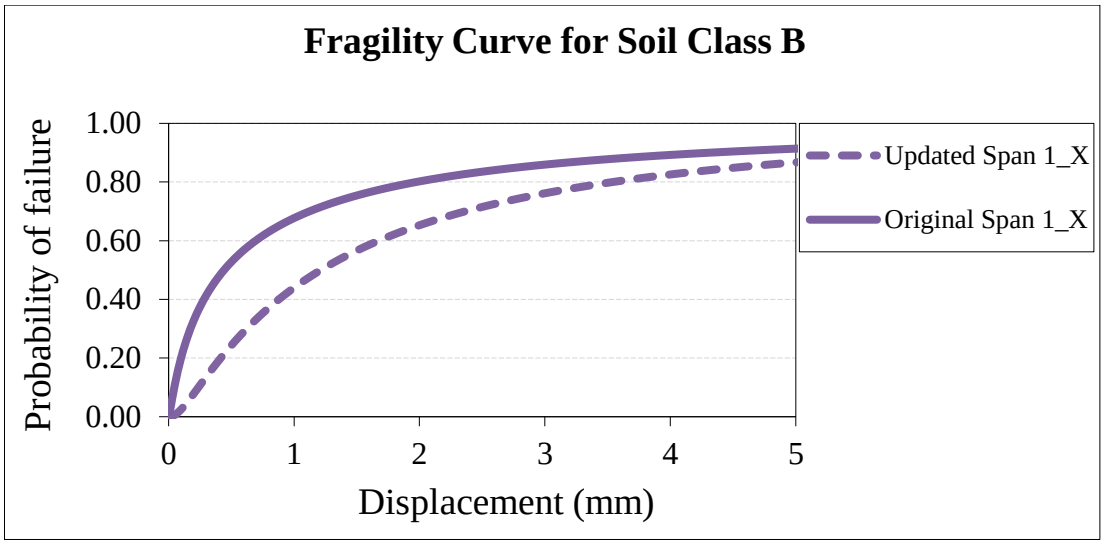


**(a)** X direction

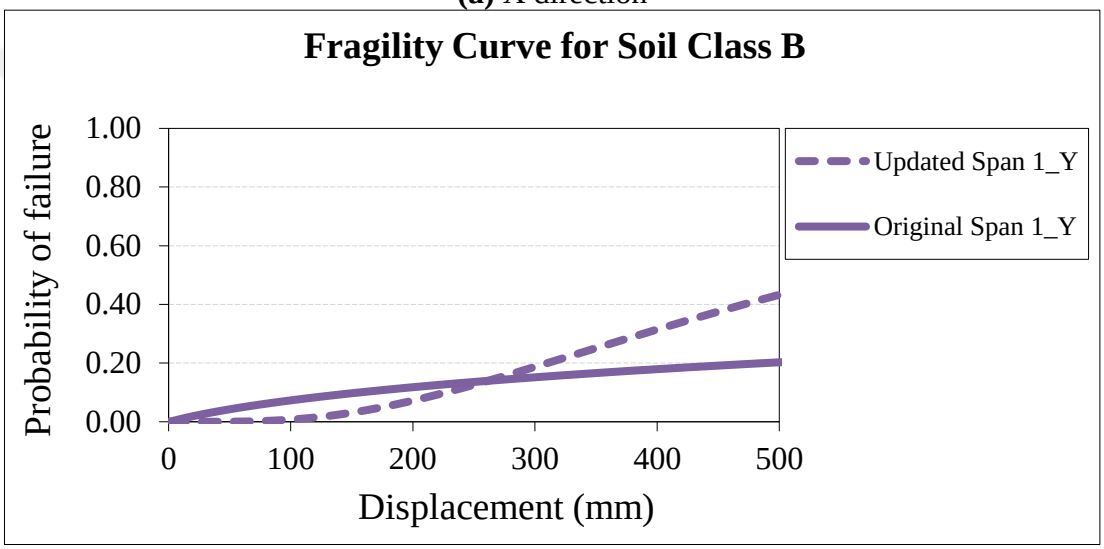


**(b)** Y direction

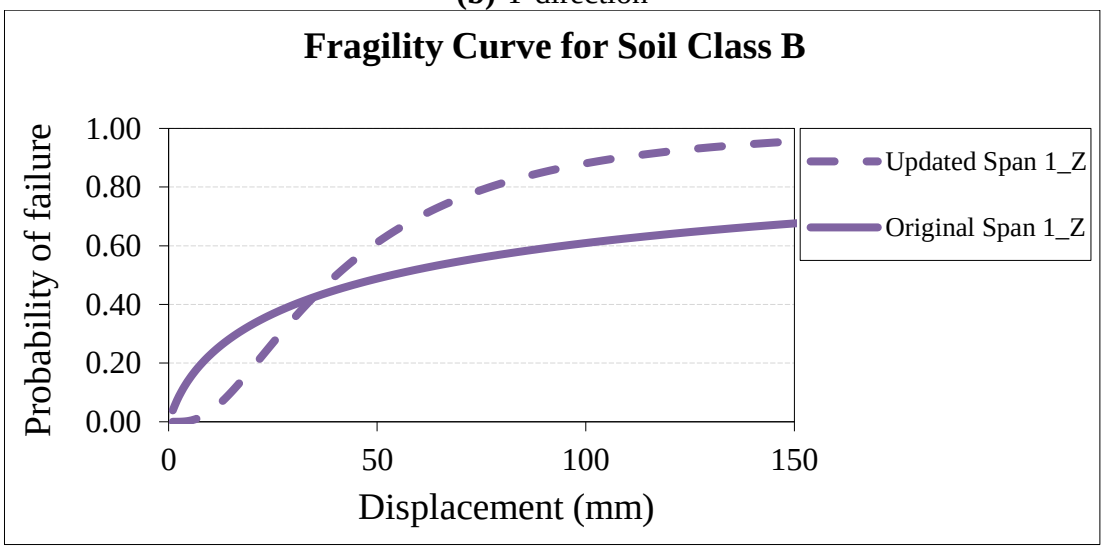


**(c)** Z direction

**Figure C.10 :** Comparison fragility curves of original and updated Ceyhan bridge model for soil class B.

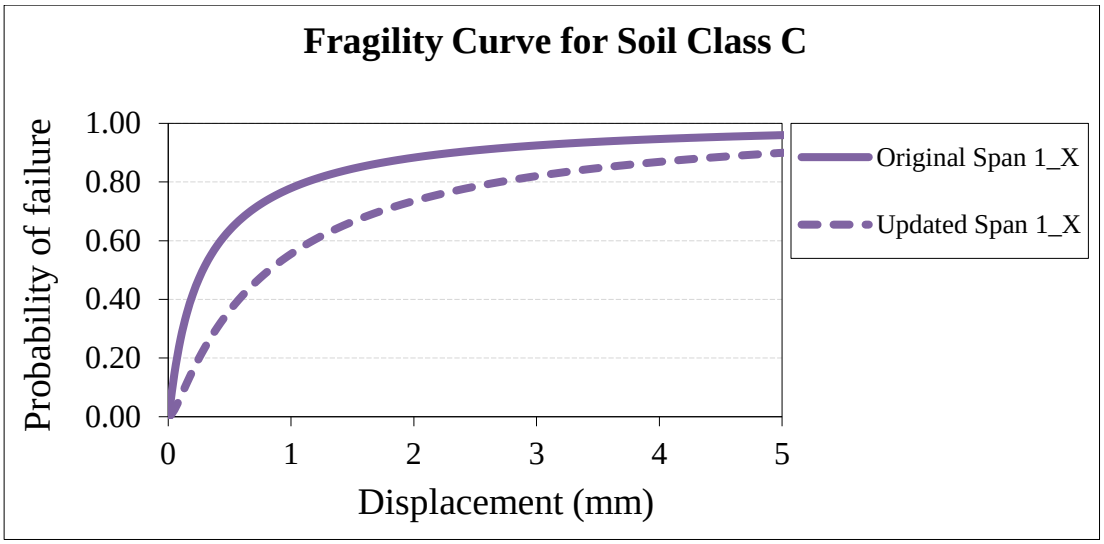


**(a)** X direction

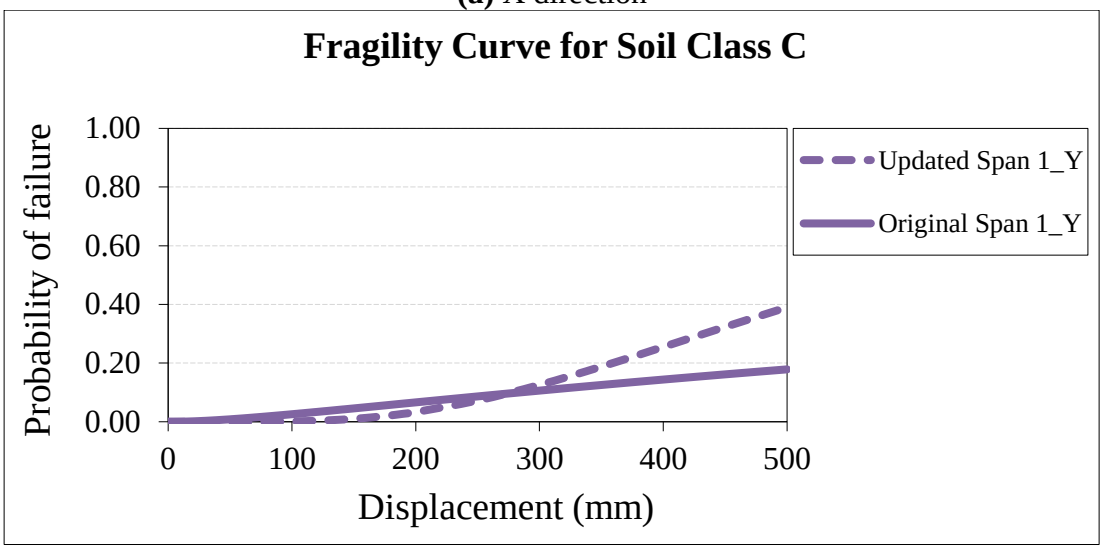


**(b)** Y direction

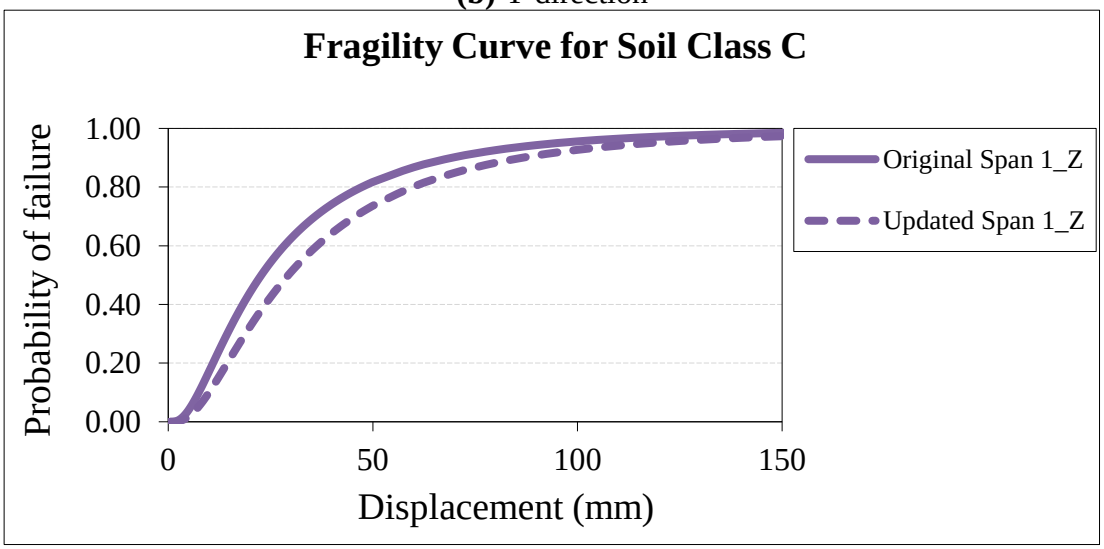


**(c)** Z direction

**Figure C.11 :** Comparison fragility curves of original and updated Ceyhan bridge model for soil class C.

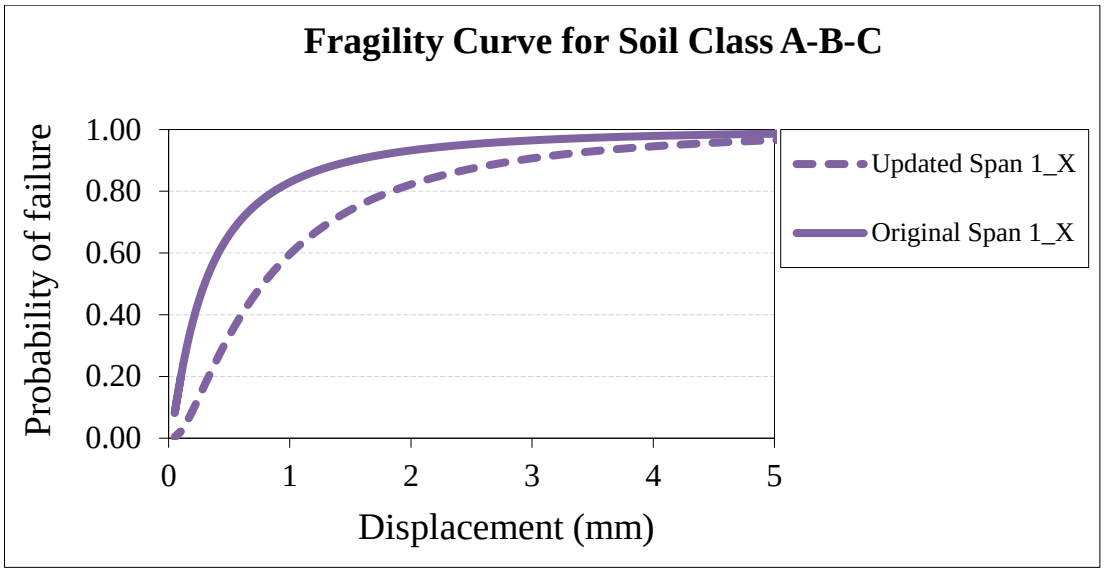


**(a)** X direction

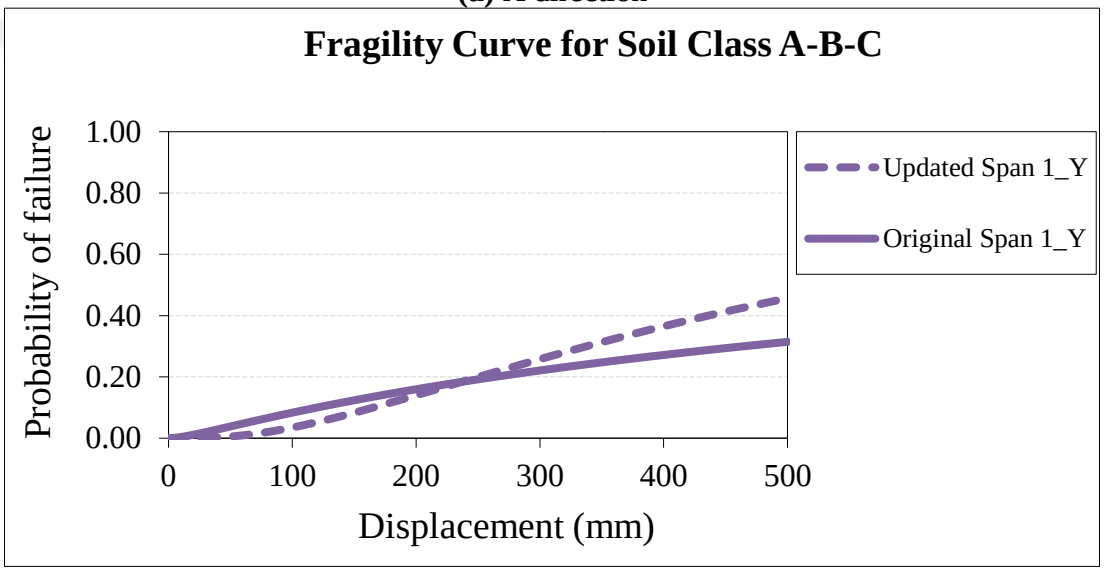


**(b)** Y direction

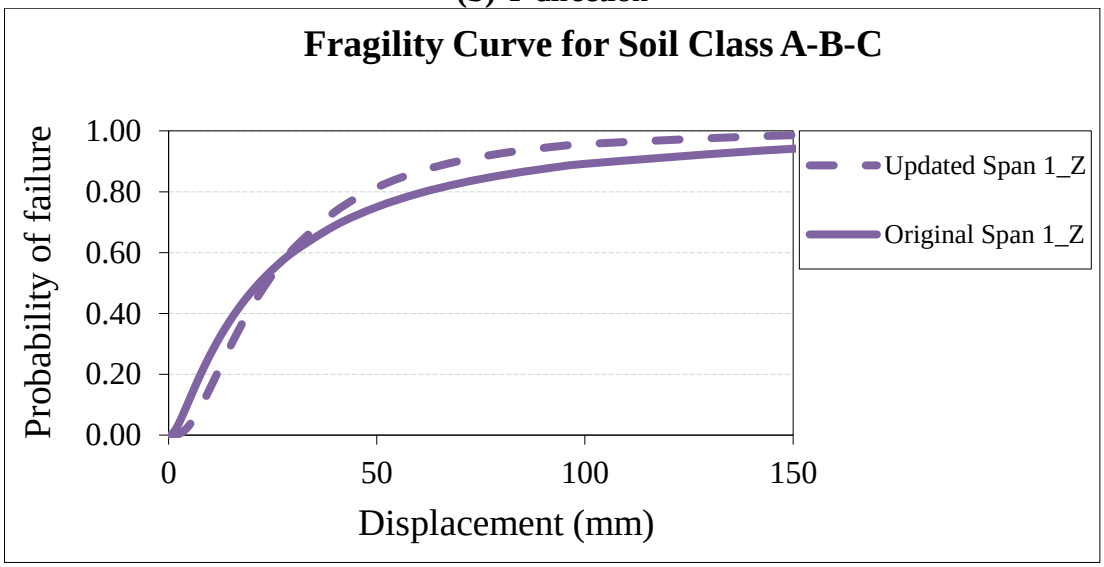


**(c)** Z direction

**Figure C.12 :** Comparison fragility curves of original and updated Ceyhan bridge model for soil class A-B-C.

**CURRICULUM VITAE**

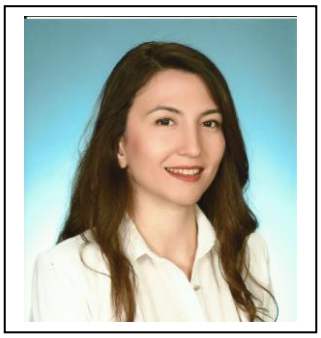

**Name Surname** **:Seda KONOR**

**Place and Date of Birth** **:Gölköy/ORDU – 28.12.1991**

**E-Mail** **:sedakonor@hotmail.com**

**EDUCATION** **:**

- **B.Sc.** **:** 2014, Dokuz Eylül University, Engineering Faculty, Department of Civil Engineering (3.74/4.00)

**PROFESSIONAL EXPERIENCE AND REWARDS:**

- Highest Ranked Student of Engineering Faculty at Dokuz Eylül University
- Highest Ranked Student of Deparment of Civil Engineering at Dokuz Eylül University
- Certificate of High Honor List at Dokuz Eylül University

**OTHER PUBLICATIONS, PRESENTATIONS AND PATENTS:**

- **Konor S., Korkmaz K. A.** "Structural Investigation R/C Residential Buildings Considering Soil-Structure Interaction", 04/2016, International Workshop on Natural Hazards-Soil characterization and site effects, Azores, Portugal, 23.04.2016
- **Yılmaz M. F., Konor S., Korkmaz K. A., Güler K.** "Structural Behavior Investigation of Turkish Highway Bridges Considering Soil-Structure Interaction", 08/2016, Istanbul Bridge Conference, 08.08.2016-10.08.2016
- **Konor S., Korkmaz K. A., Özakgül K., Gençoğlu M., Çağlayan B. Ö.** "Experimental and Analytical Investigations of Masonry Railway Arch Bridges" 09/2016, 12th International Congress on Advances in Civil Engineering, 21.09.2016-23.09.2016